

WALL CHARACTERIZATION AND AUTOFOCUSING TECHNIQUES FOR TWI SYSTEM

A DISSERTATION

*Submitted in partial fulfillment of the
requirements for the award of the degree
of*

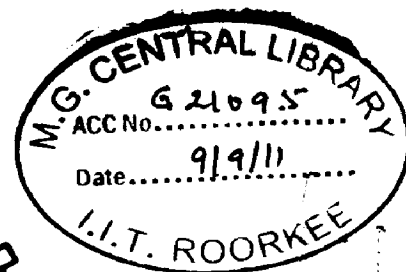
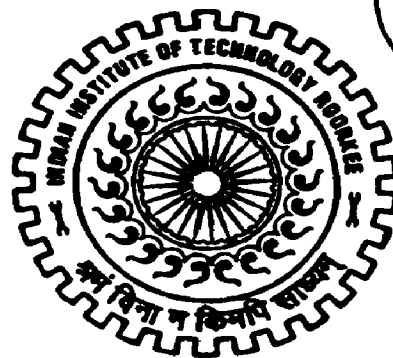
MASTER OF TECHNOLOGY

in

**ELECTRONICS AND COMMUNICATION ENGINEERING
(With Specialization in RF and Microwave Engineering)**

By

VISHAL NARAIN SAXENA



**DEPARTMENT OF ELECTRONICS AND COMPUTER ENGINEERING
INDIAN INSTITUTE OF TECHNOLOGY ROORKEE
ROORKEE-247 667 (INDIA)**

JUNE, 2011

CANDIDATE'S DECLARATION

I hereby declare that the work, which is presented in this dissertation report, entitled "**Wall Characterization and Autofocusing Techniques for TWI System**", being submitted in partial fulfillment of requirements for the award of degree of Master in Technology with specialization in RF and MW, in the Department of Electronics and Computer Engineering, Indian Institute of Technology, Roorkee is my original work. The results submitted in this dissertation report have not been submitted for the award of any other Degree or Diploma.

Date: 27-06-11

Place: Roorkee

Vishal Narain
(Vishal Narain Saxena)


M.Tech (RF and MW)
Enrolment #09533014
ECE Deptt.
IIT Roorkee

CERTIFICATE

This is to certify that the statement made by the candidate is correct to the best of my knowledge and belief. This is to certify that this dissertation entitled, "**Wall Characterization and Autofocusing Techniques for TWI System**", is an authentic record of candidate's own work carried out by him under my guidance and supervision. He has not submitted it for the award of any other degree.

Date: 27-06-11

Place: Roorkee


(Dr. Dharmendra Singh)

Associate Professor,
ECE Deptt., IIT Roorkee

ACKNOWLEDGEMENT

I would like to give sincere gratitude to my guide Dr. Dharmendra Singh for his inspiration, guidance, motivation and encouragement during the course of my dissertation work.

I would like to thank the whole team of Remote Sensing Lab. I have really enjoyed the time spent with them. Special thanks are extended to Mr. Abhay N. Gaikwad, Mr. Rishi Prakash Shrivastava, Prashant Chaturvedi and Shashi Kant Pandey. There were times when I was stuck and discussions with them paved solutions.

Thanks to all my friends esp. M.Tech, RF and MW students, for their moral support and valuable suggestions.

And above all my heartfelt gratitude is for my parents and my brother Vaibhav for their support and encouragement.

Vishal Narain

Vishal Narain Saxena

Roorkee

ABSTRACT

Investigation of the objects behind an opaque wall is very promising field for a rescue and security applications nowadays. The quality of through the wall radar image depends upon knowledge of the wall parameters. Ambiguities in parameters smear and blur the image and shift the targets from its true location. In this research first calculation of complex dielectric constant of low loss material has been done by means of real equations requiring only one dimensional root search techniques, in which data has been taken from both side of the wall. But it is not suitable in real time applications as other side come in danger zone. So a new method has been developed, which require measurement from one side of the wall for this purpose the magnitude and the time position of reflections from inner and outer surfaces of the wall are extracted from the data.

The effect of wall parameters on image has been shown by developing 2D- beam forming image. The wall causes wave refractions and change in propagation speed, this effect alters the time between transmitter to target, and target to receiver. Coherently combining all the signals at a same position can enhance image quality, but the calculated wall parameters are not exact so auto-focusing techniques based on higher order statics is presented which correct errors under ambiguities. All the techniques have been developed on real data and data has been taken in real time environments by interfacing the VNA to the laptop.

ACRONYMS

1D -	One dimensional
2D -	Two dimensional
3D -	Three dimensional
FFT -	Fast Fourier Transform
GPR -	Ground Penetrating Radar
IFFT -	Inverse Fast Fourier Transform
LOS-	Line of Sight
PC-	Personal Computer
RADAR -	Radio Detection and ranging system
RAW -	Unprocessed data
RX -	Receiver
SAR -	Synthetic Aperture Radar
TOA -	Time of Arrival
TWI	Through Wall Imaging
TWR -	Through Wall Radar
TX -	Transmitter
VNA-	Vector Network Analyzer
UWB -	Ultra Wide Band

TABLE OF CONTENTS

CANDIDATE'S DECLARATION.....	i
CERTIFICATE.....	i
ACKNOWLEDGEMENT.....	ii
ABSTRACT.....	iii
ACRONYMS.....	iv
TABLE OF CONTENTS.....	v
LIST OF FIGURE.....	viii
LIST OF TABLE.....	x
1. INTRODUCTION AND MOTIVATION.....	1
1.1 Introduction.....	1
1.2 Problems in TWI.....	3
1.3 Problem Statement.....	4
1.4 Dissertation overview.....	4
2. BASIC REVIEW.....	6
2.1 Introduction.....	6
2.2 Step-Frequency Waveform.....	7
2.3 Basic Radar target detection and measurement.....	8
2.4 Through Wall Radar Basic Model: Data collection.....	9
2.5 Data Processing.....	11
3. METHODOLOGY.....	15
3.1 Experimental Setup.....	15
3.2 TWI Components and Properties.....	16
3.2.1 Antenna.....	16
3.2.1.1 Antenna pattern.....	17
3.2.2 Vector Network Analyzer (VNA).....	19
3.2.2.1 Selection of frequency band:.....	19
3.2.2.2 VNA calibration.....	20
3.2.3 Scanner.....	22

3.2.4 Cables	22
3.2.5 Personal Computer	22
3.3 Data Collection	22
3.3.1 Wall characterization.....	23
3.3.2 Single Target	24
3.4 Data Processing.....	25
3.4.1 Properties of Wave Penetrating Through Wall	25
3.4.2 Measurement of wall Parameters	26
3.4.2.1 Measurement by Insertion Transfer Function.....	27
3.4.2.1.1 Analysis Technique:.....	28
3.4.2.1.2 Calculation of Dielectric Constant of the Wall:.....	30
3.4.2.2 Measurement by Reflection Method:	32
3.4.2.2.1 Clutter reduction	34
3.4.2.2.2 Wall Parameters calculation.....	35
3.4.3 Through-Wall TOA Estimation.....	36
3.4.3.1 Calculation of TOA between Antenna and target.....	36
3.4.4 Imaging: Beamforming	37
3.4.4.1 Beam forming Concept.....	38
3.4.4.2 Effect of Dielectric Wall on Beam forming	40
3.4.4.3 Effect of Wall Parameters Ambiguities on Beam forming image	41
3.4.5 Auto focusing Approach	42
3.4.5.1 Image quality measurement:.....	43
4. RESULTS AND DISCUSSION	46
4.1 Wall parameters Calculation by using insertion transfer function.....	46
4.2 Reflection Method.....	53
4.3 Imaging: Beam forming	62
4.4 Auto focusing Approach	66
5. CONCLUSION AND FUTURE SCOPE.....	79
5.1 Conclusion	79
5.2 Future Work	79
REFERENCES.....	81

APPENDIX.....	87
I. Experimental Setup, delay calculation of antenna and A-Scan algorithm	87
II. MATLAB Code.....	89

LIST OF FIGURE

Figure 2.1: Radar operation scenarios	6
Figure 2.2: Stepped-frequency CW waveform with frequencies	7
Figure 2.3: Reflection and Scattering from the targets.....	9
Figure 2.4: Attenuation of radio signals through various materials as a function of frequency	12
Figure 3.1: Experimental setup.....	15
Figure 3.2: (a) HF 906 antenna (b) VSWR of antenna.....	17
Figure 3.3: Diagram indicating H-plane (Vertical Polarization) and E-plane (Horizontal Polarization) cuts for Horn antenna	18
Figure 3.4: Antenna Pattern (a) E Plane (b) H-Plane	18
Figure 3.5: Front view of R&S ZVL3 vector network analyzer.....	19
Figure 3.6: One port calibration menu in VNA	21
Figure 3.7: Model for characterizing wall parameters.....	28
Figure 3.8: EM wave propagation through the wall	30
Figure 3.9: Model of wave propagation through the wall	33
Figure 3.10: Model for calculation of True TOA	37
Figure 3.11: Layout representing the free space and block diagram of time domain beam former	38
Figure 3.12: 2-D beamformer flow chart.....	39
Figure 3.13: Image quality measurement feedback systems	42
Figure 3.14: Flow chart for adaptive autofocusing algorithm	45
Figure 4.1: Transmission Coefficient; magnitude vs frequency.....	47
Figure 4.2: Variation of Dielectric Constant with frequency	48
Figure 4.3: Variation of Attenuation Constant with frequency	49
Figure 4.4: Variation of Loss Tangent with frequency.....	49
Figure 4.5: Variation of Dielectric Constant with frequency	50
Figure 4.6: Variation of Attenuation Constant with frequency	51
Figure 4.7: Variation of Loss Tangent with frequency	51
Figure 4.8: Variation of Dielectric Constant with frequency	52
Figure 4.9: variation of Attenuation Constant with frequency	53
Figure 4.10: Variation of Loss tangent with frequency4. 2 Reflection Method.....	53
Figure 4.11: Range profile of wall (clearly showing the reflections).....	55
Figure 4.12: Range profile of metal (peak due to metal).....	55
Figure 4.13: Reflection at air wall interface clear view.....	55
Figure 4.14: Reflection at wall air interface clear view.....	56
Figure 4.15: Calculation of parameter	56
Figure 4.16: Experimental set up (front and side view)	57
Figure 4.17: Range profile of plywood wall(clearly showing the reflections).....	58

Figure 4.18: Range profile of metal (peak due to metal).....	58
Figure 4.19: Reflection at air wall interface clear view.....	58
Figure 4.20: Reflection at air metal interface clear view.....	59
Figure 4.21: Calculation of parameter	59
Figure 4.22:Range profile of Asbestos wall (clearly showing the reflections)	60
Figure 4.23: Range profile of metal (peak due to metal).....	60
Figure 4.24: Reflection at air wall interface clear view.....	60
Figure 4.25: Reflection at air metal interface clear view.....	61
Figure 4.26: Calculation of parameter	61
Figure 4.27: Beam forming image at different dielectric value (a) 3.9 (b) 4.1 (c) 4.3 (d) 4.6 (e) 4.9 (f) 5.2 (g) 5.5 (h) 5.9 keeping wall thicknesses value 12.5 cm.	64
Figure 4.28: Beam forming image at different wall thickness value (a) 8.5 (b) 9.5 (c) 10.5 (d) 11.5 (e) 12.5 (f) 13.5 (g) 14.5 cm, keeping dielectric constant value constant 5.2	65
Figure 4.29: Plot of quality indices values (a) normalize sum of image intensity (b) Negative of image entropy (c) Ratio of Standered deviation to mean (d) Standardized moment at different values of n.	67
Figure 4.30: Plot of quality indices values (a) normalize sum of image intensity (b) Negative of image entropy (c) Ratio of Standered deviation to mean (d) Standardized moment at different values of n.	68
Figure 4.31: nth standardized moment for unknown dielectric and thickness value where n is equal to (a) 5 (b) 10 (c) 15 (d) 20.....	69
Figure 4.32: Quality indices plot at constant dielectric value and, varying thickness around 12.0cm by an amount of 0.2, (a) Normalize Sum of image intensity (b) Ration of standardizes deviation to mean (c) 20th moment.	70
Figure 4.33: Quality indices plot at constant dielectric value and ,varying thickness around 12.0cm by an amount of 0.2.	71
Figure 4.34: Quality indices plot at constant thickness value and, varying dielectric around 5.0by an amount of 0.2.	73
Figure 4.35: Quality indices plot at constant thickness value and, varying dielectric around 5.0by an amount of 0.1.	74
Figure 4.36: Beamforming image for dielectric value 5.4 and thickness 12.8cm.	78

LIST OF TABLE

Table 3.1: Antenna Specification	17
Table 3.2: Data collection for wall characterization.....	23
Table 3.3: Data collection for single Target	24
Table 4.1: System parameter	46
Table 4.2: Variation of Dielectric Constant with frequency.....	48
Table 4.3: Variation of Dielectric Constant with frequency.....	50
Table 4.4: Variation of Dielectric Constant with frequency.....	52
Table 4.5: System parameter	54
Table 4.6: Dielectric constant with distance.....	57
Table 4.7: Dielectric constant with distance.....	59
Table 4.8: Dielectric constant with distance.....	61
Table 4.9: System Parameters.....	62
Table 4.10: Constant terms value for equation (4.1).	71
Table 4.11: Constant values for equation 4.2	72
Table 4.12: Values of constant for equation 4.3	72
Table 4.13: Values of constant for equation 4.4	73
Table 4.14: Obatin values of constant by using curve fitting method for equation (4.5)..	75
Table 4.15: Average value	76
Table 4.16: Obatain values of constant for eq (4.6)	77
Table 4.17: Average value	77

1. INTRODUCTION AND MOTIVATION

1.1 Introduction

Detection and imaging of objects behind walls, i.e., through wall and other visually opaque materials, using microwave signals has become a major area of interest in a variety of applications such as rescue mission, in collapsed buildings or avalanches, surveillance and reconnaissance, detection of human maneuvering, police search operations, hostage situations.

- **Rescue Mission:** In the process of police investigation with terrorists and hostages are inside the room. The police can get real time information about the interior state of the room, before getting inside. Also in hazardous environment full of smoke with zero visibility, it is useful for the fireman to get information about the position of the object.
- **Security:** investigating objects through plastic, rubber, dress or other nonmetallic material could be highly useful as an additional tool to the existing X-rays scanners.

The technology is either active or passive imaging. In active imaging, RF, acoustic, optical or X ray energy are used to estimate the reflectivity distribution of a remote scene and in passive imaging millimeter wave imaging radiometer are used which uses energies that is radiated by the bodies of persons within a building for detection [1].

Any object can be visualized by the reflection of light. However, wavelength of visible light is such that we can only see the transparent view. On the other hand UWB signals are able to penetrate through the opaque material. So by applying some techniques on these signals we can investigate behind the opaque material. According to FCC UWB signals must have bandwidths of greater than 500 MHz or a fractional bandwidth larger than 20 percent at all times of transmission [55]. Fractional bandwidth is a factor used to classify signals as narrowband, wideband, or ultra-wideband and is defined by the ratio of bandwidth at -10 dB points to center frequency [42]. So

$$B_f = \frac{BW}{f_c} \times 100\% = \frac{2(f_h - f_l)}{(f_h + f_l)} \times 100\% \quad (1.1)$$

Where, f_h and f_l are the highest and lowest cutoff frequencies of a UWB pulse spectrum, respectively. UWB based radar system have become more popular since it provide both the requirements resolution and penetration, to a large extent without much compromise i.e. with low center frequency high bandwidth is achieved. The advantages of UWB signal are

- a. It improves the resolution that improves detected target range measurement accuracy.
- b. Identification of target class and type.
- c. Reduce the radar passive interference from rain, must and interfering object.
- d. Decrease the radar dead zone.

To achieve high resolution image is the measure aspect in TWI, the wall parameters have major effects on the target imaging and location estimation. The composition and thickness of the wall, its dielectric constant, and the angle of incidence all affect the characteristics of the signal propagating through the wall. The propagating wave slows down, encounters refraction, and is attenuated as it passes through the wall. In practical situation these parameters are not known. Ambiguities in these parameters smear and blur the image and shift the image of the target from its true position. These effects increase significantly when multiple walls separate the target from the radar, which typically is the case in urban sensing applications [10].

Electromagnetic characterization of materials is essential to many applications like transmission line, microwave devices, and optical components and for wave propagation in indoor environment [8-10]. Various techniques have been developed for the characterization of materials, the techniques using insertion transfer function [11] dielectric constant, attenuation constant and loss tangent can be calculated for a material.

It is assume that material should be homogenous (ϵ and μ are constant), isotropic (ϵ and μ are scalar), and linear. But in practical situation, we have no information behind the wall so it is meaningless to measure the wall from both the side. A further approach uses different standoff distances to locate the position of the object behind the wall under unknown parameters [12-13]. For this method a small object, behind the wall, has to be

visible at least from two antenna position which is also impractical. Approach using Fresnel equation at the wall interface and by concept of reflectometry [14]. However, the piece of wall has been placed in anechoic chamber; it's a challenging aspect to use it in real time environment.

For accurate measurement high resolution sensor is the primary requirement. TWI radar system requires very wide bandwidth to achieve high resolution. The attenuation due to building materials increases rapidly with frequency so the radar should have the transmitted signal at a frequency low enough to be able to penetrate walls. Due to resolution problem the wall thickness cannot measure accurately so some error has been remained in location estimation of target. Although blurring of images is in practice very small and mostly lost in noise [16].

An auto focusing system for through-the-wall applications that focuses the image and corrects for shifts in imaged locations of stationary targets is presented [17]. The analysis shows that at correct wall parameters all signals has been conserved at a signal points and focused image has been obtained, for the focused image the intensity values should be high so by calculation of intensities values wall parameters error can be nullified. For the processing of these techniques large amount of data, in future work data size can be reduce by using some preprocessing techniques. The work has been more effective if use in real time environment.

1.2 Problems in TWI

The major goal for TWI is detecting and identifying target enclosed in building structures. An Electromagnetic wave is transmitted via antenna system, penetrates through the wall, it is reflected by the investigated object, penetrates again through the wall, and is received back via receiver antenna, and by applying some signal processing techniques on receive signal, we can detect and identify the target. This whole process contains some complexities and difficulties in which some of them are listed below:

1. The signal, reflected from the target is very complex signal, full of noise and clutters, which is very difficult to interpret.
2. Every time the wave passes through the wall, the reflection, refraction, diffraction, and absorption on the boundaries of these materials occurs [16]. Also

multiple reflections between antennas, walls, and all the objects in the scanned area arise.

3. Due to wall target get displaced and defocused.
4. For high precision imaging, high resolution radar is required. The basic rule for good recognition ability is that, the resolving power of radar system must be 1/10 times of the maximum dimension of objects. TWI radar system requires very wide bandwidth to achieve high resolution. On the other hand the radar should have the transmitted signal at a frequency low enough to be able to penetrate walls. Since resolution also increases with frequency there is a tradeoff between power and resolution.

1.3 Problem Statement

This dissertation is based upon characterization of wall for TWI system in real time of different material, as dielectric constant and thickness and then applies Auto focusing techniques to nullify the wall ambiguities to achieve focused image behind the wall. To achieve this goal following problems have been attempted:

1. Critical study of characterization of wall parameters like dielectric constant, attenuation constant and loss tangent.
2. Develop B scan image of the target by beam forming technique.
3. Applying focusing techniques to achieve accurate wall parameters.
4. Calculate the quality index value of image at different wall parameters.
5. Development of adaptive Statistical model for calculating the wall parameters and get focused image that can be used for identification and classification of targets.

This dissertation work focused on implementing a real time through wall imaging system which addresses these issues. Therefore, a Vector Network Analyzer was interfaced with a PC to enable processing in real time.

1.4 Dissertation overview

For fulfilling the dissertation task this report is structured in the following sections. First chapter is the introductory chapter showing the work going on TWI and brief introduction of TWI and UWB. Second chapter gives brief introduction of SFCW Radar, Basic Radar operations which are used in the experimental case which basically consist

of VNA and working in frequency domain. Radar data collection and data processing techniques have been describes in subsequent sections.

Chapter 3 describe about experimental setup and properties of components used in the experiment which will be useful for deciding whether these components can be used in the experiment or not and also from their characterization system performance can be found. Data collection process and collected data have been showed also in this chapter. Further calculations of actual time of arrival, detailed description of technique used in characterization of different walls is described next. The technique is applied from which dielectric constant and attenuation variation with respect to frequency is calculated. Other method used to calculate walls dielectric constant and thickness in time domain. Description about beam forming image technique, affected of wall errors on the image quality and auto focusing approach used to neglect wall errors have been describes in next sections of chapter 3.

Chapter 4 first discussed results of wall characterization process by different techniques and compare. Then beam forming image at different wall parameters have been shown, and then by applying quality indices parameters focused image have been developed. Finally a contribution of this thesis and possible extensions of the research are proposed in Chapter 5.

2. BASIC REVIEW

2.1 Introduction

To achieve high resolution image is challenging task in TWI. For this purpose high resolution radar is require. Radar is electromagnetic instrument that is use for detection and location estimation of targets. Basic operation of radar is shown in fig (2.1). It transmitted electromagnetic wave towards the target and receives reflected signals from the target and clutters. The unwanted signals that interfere with desire target signal is a clutter signal. So by analyzing received signal and reducing the clutter, information about the target can be achieved. Compare to optical and infrared sensors the radar can perform at large range with high accuracy under the weather condition. Therefore it has been widely used for civilian and military operation [21].

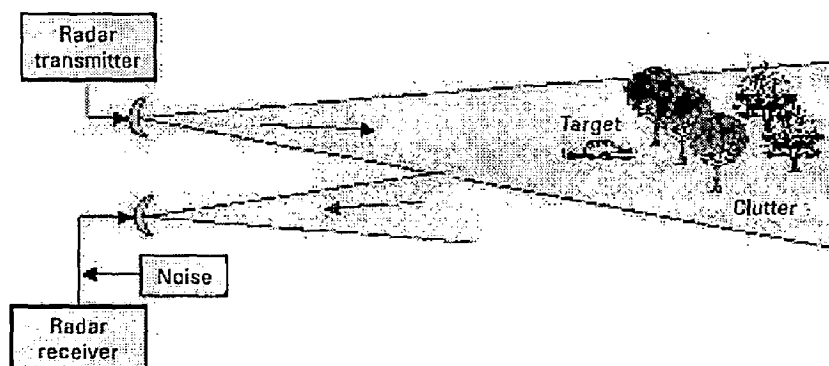


Figure 2.1: Radar operation scenarios [25]

Stepped frequency radar and short pulse radar represent two different techniques that are used to generate wide band of frequencies for detection of hidden objects. Stepped frequency radar is frequency domain system whereas pulse radar is time domain. SFCW radar system possesses several advantages over time domain systems. The main advantage of the stepped frequency technique is that it is relatively easy with current technologies to efficiently sample ultra wideband signals with low speed analog to digital converters. The other advantages are high dynamic range, low power consumption and high signal to noise ratio [2].

2.2 Step-Frequency Waveform

The waveform for step-frequency radar consists of a group of N coherent pulses with constant frequency increment of Δf . The frequency for n th pulse can be written as:

$$f_n = f_0 + n\Delta f \quad (2.1)$$

Where f_0 is the starting carrier frequency and Δf is the step frequency size. In SFCW radar frequency is constant within the individual pulse; its bandwidth is approximately equal to the inverse of pulse width. The effective bandwidth is determined by the total frequency excursion, i.e., $N\Delta f$ over the duration of N pulses. The downrange range resolution of step-frequency radar is given by [47]

$$\Delta R = \frac{c}{2B_{eff}} = \frac{c}{2N\Delta f} \quad (2.2)$$

The Cross Range Resolution is the resolution of the radar system in the cross-range direction. The Cross Range Resolution is given by [47]

$$\Delta CR = \frac{\lambda}{D} R \quad (2.3)$$

This implies that the system will be able to indentify two objects separated by a distance greater than ΔCR in the cross range as two distinct objects.

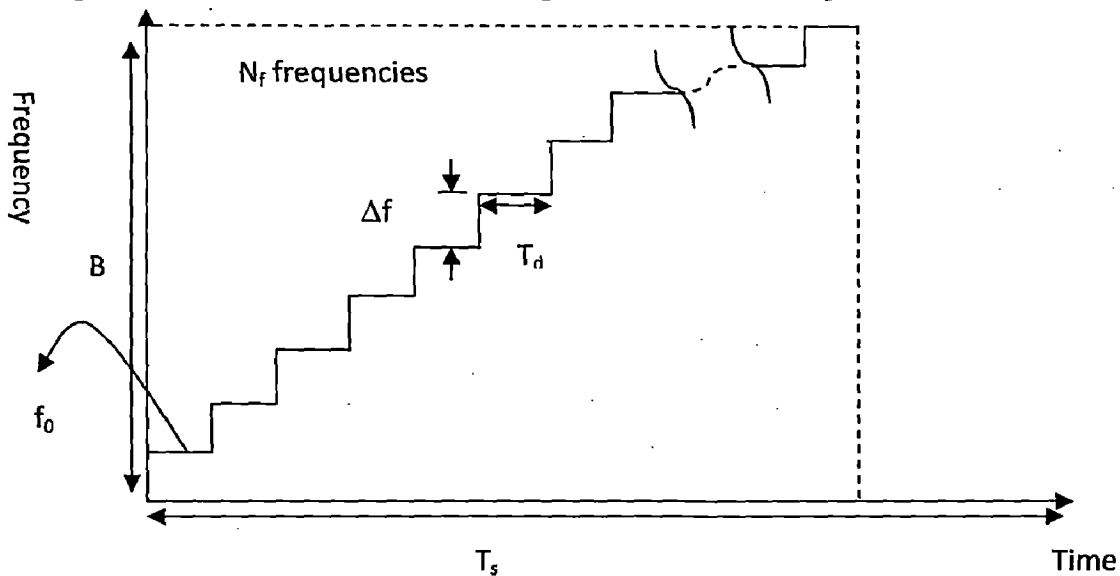


Figure 2.2: Stepped-frequency CW waveform with frequencies

The fact that step-frequency radar resolution does not depend on the instantaneous bandwidth, and that resolution can be increased arbitrarily by increasing $N\Delta f$, are

significant advantages. A step-frequency waveform achieves wide bandwidth ($N\Delta f$) sequentially (over a burst of many pulses) but has a narrow instantaneous bandwidth of $1/\tau$. It provides the high range resolution of wideband radar systems with some of the advantages of narrowband radar systems. Step-frequency radar achieves range resolution of $c/2N\Delta f$ (equivalent to a bandwidth of $N\Delta f$) as compared with range resolution of $c\tau/2$ for constant-frequency waveforms [2]. The main advantage of the stepped frequency technique is that it is relatively easy with current technologies to efficiently sample ultra wideband signals with low speed analog to digital converters. The other advantages are high dynamic range, low power consumption and high signal to noise ratio [2]. Because of these advantages SFCW radar has been preferred over pulse radar.

2.3 Basic Radar target detection and measurement

In the operation of radar, radar transmitted the signals towards the target. In the reflected signal, there is also an additive noise. The signal to noise ratio (SNR) at the receiver is determined by the intensity of the received signal, the noise figure, and bandwidth of the receiver. Any improvement in SNR increases the probability of target detection and accuracy in its measurement.

Target information contained in the returned signals may be extracted directly from the radar range profile or from its frequency spectrum by applying the Fourier transform [22-23]. The target's range measured along the radar LOS can be estimated by the time-delay between the transmitted signal and the received signal. For a moving target, its velocity is measured based on the well-known Doppler Effect. If the radar transmits a signal at a frequency f_0 , the reflected signal from the moving target is subjected to a Doppler frequency shift f_D from its transmitted frequency f_0 induced by the relative motion between the radar and the target [25].

The radar targets are considered as a collection of point-scatters. They have different types of reflecting and back-scattering behaviors [24]. They can be surfaces, edges, corners, dihedrals, trihedral, and cavities (see Figure 2.3). Each type of scatter has a different back-scattering behavior. An important factor of image quality is its resolution. It is the ability to separate closely related scattered in range and cross range.

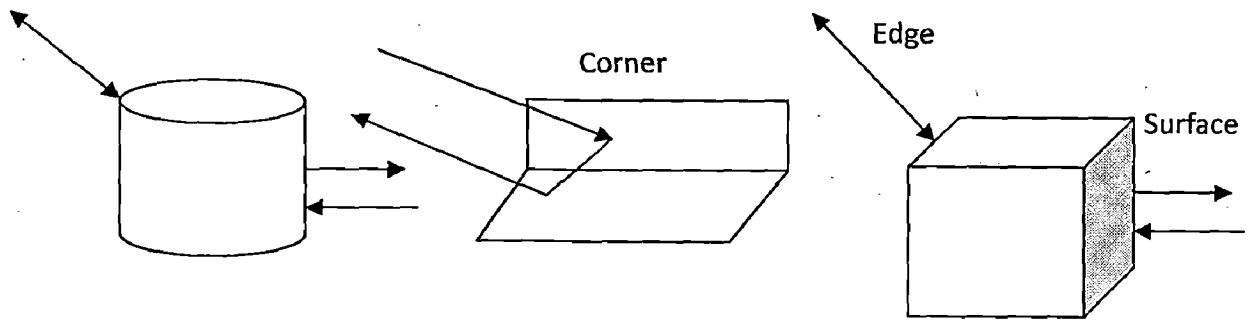


Figure 2.3: Reflection and Scattering from the targets.

The minimum distance in the range Δr_r , and in the cross range Δr_{cr} , by which two point-scatters can be separated, is the resolution of the image. High band-width is requiring for high down range resolution. For high cross range resolution, large antenna aperture is required. Usually a synthetic aperture is utilized to synthesize a large antenna aperture. Synthetic aperture processing coherently combines signals obtained from sequences of small apertures at different aspect angles of a target to emulate the result that would be obtained from a large antenna aperture [25].

Coherent processing maintains the relative phases of successive pulses. Thus, the phase from pulse to pulse is preserved and a phase correction can be applied to the returned signals to make them coherent for successive inter-pulse periods. If radar returns are processed coherently, the processed data retains both the amplitude and the phase information about the target. The amplitude is related to the radar cross section (a measure of the ability to reflect electromagnetic waves) of the target and the phase is related to the radial velocity of the target [25].

2.4 Through Wall Radar Basic Model: Data collection

There are two major components in through wall imaging system. First is how data will be collected and second is image formation. The sequence of data collection and image formation is referred as the imaging system. In data collection the transmitter T_x generates a microwave signal and radiates it to generate the illuminating field. The illuminating field is scattered by the object. The scattered field is measured by the receiver R_x . The radar can operate in monostatic, bistatic or multistatic mode. The target detection/identification process requires additional processing to form enhanced images.

This additional processing is achieved by preprocessing or by post processing [26]. The electric field which is generated by the T_X antenna is called E^{rad} and could be modeled by [28].

$$E^{rad}(r, \theta, \phi, n) = \frac{1}{2\pi r c} h_{TX}(\theta, \phi, n) * \frac{\sqrt{z_0} \Delta V_S(n)}{\sqrt{z_c} \Delta n} \quad (2.4)$$

Where r, θ, ϕ are spatial coordinates and n is a discrete time, Z_c and Z_0 impedances of the feed cable and free space respectively, and c is the speed of light in vacuum. The voltage time evolution applied to the T_X antenna is denoted $V_S(n)$, h_{TX} is the transfer function for the emitting antenna. The receive voltage at R_X is V_R then

$$V_R(n) = \frac{\sqrt{z_c}}{\sqrt{z_0}} h_{RX}(\theta, \phi, n) * E^{meas}(n) \quad (2.5)$$

Where h_{RX} is the transfer function of the receiving antenna, and $E^{meas}(n)$ is the field at the R_X antenna. The transformation of field from T_X to R_X depends upon travel signal path and shown by unknown impulse response $X(r, \theta, \phi, n)$ then

$$V_R(n) = \frac{\sqrt{z_c}}{\sqrt{z_0}} h_{RX}(\theta, \phi, n) * X(r, \theta, \phi, n) * E^{rad}(r, \theta, \phi, n) \quad (2.6)$$

If the $1/r$ dependency is taken out of the definition of E^{rad} all antenna terms could be combined into one term h_A

$$V_R(n) = \frac{1}{r} h_A(\theta, \phi, n) * X(r, \theta, \phi, n) \quad (2.7)$$

Antenna cross talk also effect between and receiver, it depend upon distance and impulse response of direct path, C_A between transmitting and receiving antenna then $V_R(n)$ become [28]

$$V_R(n) = \frac{1}{d_{TXRX}} h_A(\theta, \phi, n) * C_A + \frac{1}{r} h_A(\theta, \phi, n) * X_I \quad (2.8)$$

The first term can be measured by pointing the antenna system to the anechoic chamber room, so that X_I becomes zero. The second term contain information about target but the reflected signal also contain clutter signal means X_I contains target signal h_T and clutter signal h_c . clutter signal is undesired signal that interfere with desired target signal which is due to multiple reflections of the wall, multiple reflection of the wall and target

reflection from the environment, apart from that a noise signal also present at the receiver that is due to measurement system itself. Then model of receive signal become

$$V_R(n) = \frac{1}{d_{TXRX}} h_A(\theta, \phi, n) * C_A + \frac{1}{r} h_A(\theta, \phi, n) * (h_T(n) + h_C(n)) + noise \quad (2.9)$$

So the measured signal $V_R(n)$ is the combination of all these variable. By processing of these signals we can extract the information about the target. In data collection single antenna can be used as transmit and receive antenna simultaneously, two separate antenna or multiple antenna can be used. When scanning is used two approaches has been used, Synthetic aperture radar and real aperture synthetically organized radar.

2.5 Data Processing

After Data collection, challenging task in TWI is to process and extract information form collected data. Radar imaging is a well known field for ground penetrating radar (GPR) application [29]. Where through- wall- imaging (TWI) has been developed only few years before [30]. Nowadays most of the research has been going on to produce high quality of image and extract the information from the image. Different imaging and non-imaging sensor with these imaging capabilities are described in [3]. Several studies have been carried out to detect the target behind the wall with known and unknown wall parameters. For that purpose UWB radar system is used for scanning the object behind the wall. As UWB signal are able to penetrate through the wall and by using some sophisticated method object can be investigated behind the wall. The wall cannot be too thick and not form to attenuating material in the used frequency band. Figure (2.4) shows a comparison of measured one way losses versus frequency for a variety of different common wall and building materials. The one way attenuation for concrete block around 3 GHz appears to be less than 5 dB. Signal attenuation rises with frequency, so that at frequency of 10 GHz, the concrete block will introduce a two way attenuation of about 30 dB. These estimates are based on concrete blocks of thickness 6" [1].

Hence considering all these aspects there is a tradeoff between the system complexity, data collection time and image quality.

The building material like wooden, dry wall has small dispersion and loss effect on the other hand material like brick wall and blocks have significant dispersion and loss effect.

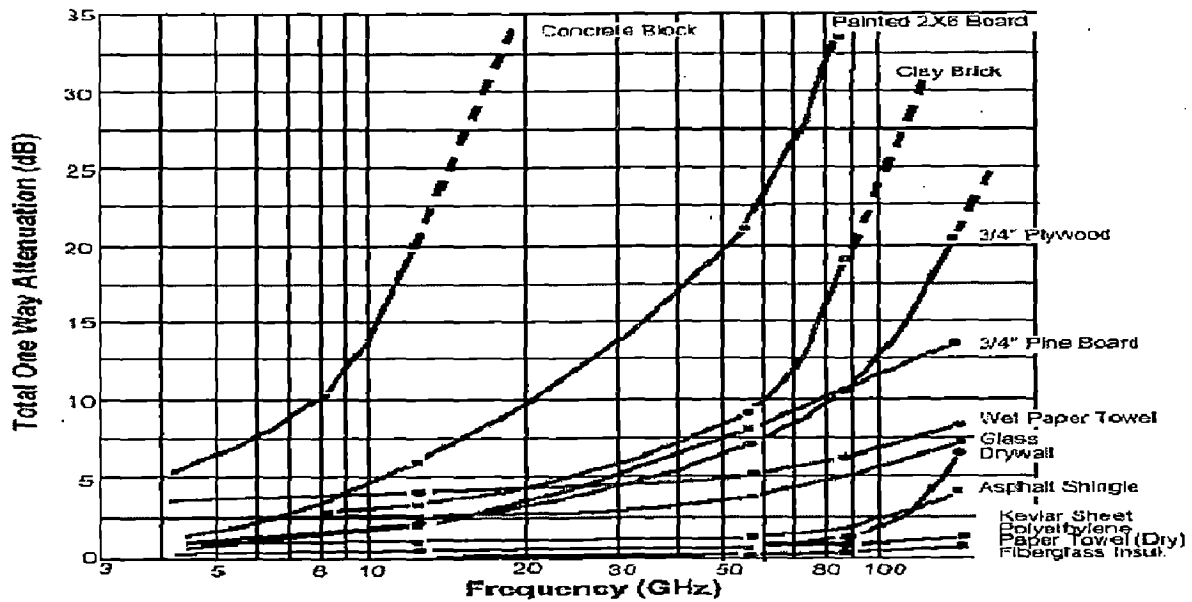


Figure 2.4: Attenuation of radio signals through various materials as a function of frequency [1].

In [32] a preliminary study on using ultra wide band synthetic aperture for through wall detection was conducted with focused on detection of human body without considering wall effect on detection. The blending of ultra wide band short pulse radar and synthetic aperture processing for through wall imaging application is described. The broadband content of a radiated pulse provides fine range resolution, while synthetic processing enhances cross range resolution.

In [13], the potentials and limitations of through wall human body detection are carried out experimentally. For target detection simple data processing technique is used to extract the data pertaining to reflected fields by target.

There are two different techniques used for imaging, coherent and non-coherent imaging. Coherent imaging require wide band beam forming using transmitter and receiver antenna array [3, 33, 34, 36]. Non-coherent approach mainly based upon trilateration technique [36-38]. In [39] a technique has been described to calculate correct target location without knowledge of wall parameters, this [39] method require data to be calculated using at least two different positions against the wall, at each positions imaging is performed for different assumed values of wall parameters, the displacement in target position because of incorrect parameters form a trajectory which shows highest

peak of the target image as a shift. The trajectory with different transmitter position will intersect at true positions.

Some methods are used to characterize wall parameters. They can be used more precisely when wall is placed between two antennas [40, 50]. But it has no use in real life as we are working in dangerous environment.

In [12, 43] estimation of wall parameters have been done by using different standoff distances. In this method target should be visible at least two antenna positions. The wall parameters that estimated are totally wrong if position of the object is calculated even with small inaccuracy. In [44], Prony's method is use to calculate the wall parameters, in this [44] reflections have been represented in Laplace domain and pole positions is use to find out these parameters. A method by using green [45] function that solve wave equations by iteration, it is computationally complex and require huge number of calculations.

Ahmad and Amin [46] generated images using wideband synthetic aperture data beam forming. The full-polarization, two dimensional synthetic aperture data measurements were taken using an Agilent network analyzer, implementing a stepped-frequency waveform over a 2-3 GHz frequency range with a step size of 5 MHz. The data is processed using post-data acquisition beam forming. The analysis in [46] did not address a key problem of practical importance in TWI systems, namely, the wave refraction due to the presence of the wall. The composition and thickness of the wall, its dielectric constant, and the angle of incidence all affect the characteristics of the signal propagating through the wall. The propagating wave slows down, encounters refraction, and is attenuated as it passes through the wall.

In [12] shows the effects of thickness and dielectric error on target locations. Effect on incident angle at air-wall interface, refraction angle on wall- air interface and focusing delay because of these errors all the signals are not converge at a single point that causes smearing and blurriness on the image quality.

Farris and Currie [1] developed a system, which can detect the person behind the wall and trace their movement, for this purpose the radar resolution should be high so that

system can detect the person behind the wall and trace their movement, if it is in small step. However, most of the systems have very low spatial resolution.

Dehanmollaian and Sarabandi [17] proposed auto focusing approach using synthetic aperture radar (SAR), in which the values of wall parameters have to be derived by solving non-linear optimization problem. In [49], auto focusing approach by using time reversal techniques has been developed, in this process First, radar transmits time domain fields to illuminate the unknown target; Second the signal scattered from the target received by the array of receiver and measure the data; Third, the receive signal is phase conjugate in frequency domain by sent to the same media for it receiver. The main aim of the works that have been done so far to obtain high quality of image and applying feature extraction techniques for classification purpose. 3D measurements capabilities significantly enhance the capability to discriminate the targets. One of the major thrusts for the near future will be investigating ways to reduce data throughput, possibly by some type of preprocessing, and develop more efficient imaging algorithms.

3. METHODOLOGY

The main aim of Through Wall Imaging is to obtain high quality of images. The quality of images is based upon wall parameters. Unknown parameters smear and blur the image and shift the targets from its true location [51]. So the aim of this dissertation is to calculate wall parameters that can be use to obtain high quality of images.

Techniques based upon transmission and reflection [16, 40, 50] coefficient have been applied on experimental data to characterize wall parameters, ambiguities in parameters have been nullify by using autofocusing [49, 51] approach.

For the implementation purpose first data has been collected then data processing techniques have been developed on collected data. In this chapter first three sections describe experimental setup, components used in experiment, collection, and then theoretical review of processing techniques have been described in fourth sections. Implementation of these techniques on real data and results has been described in later chapter.

3.1 Experimental Setup

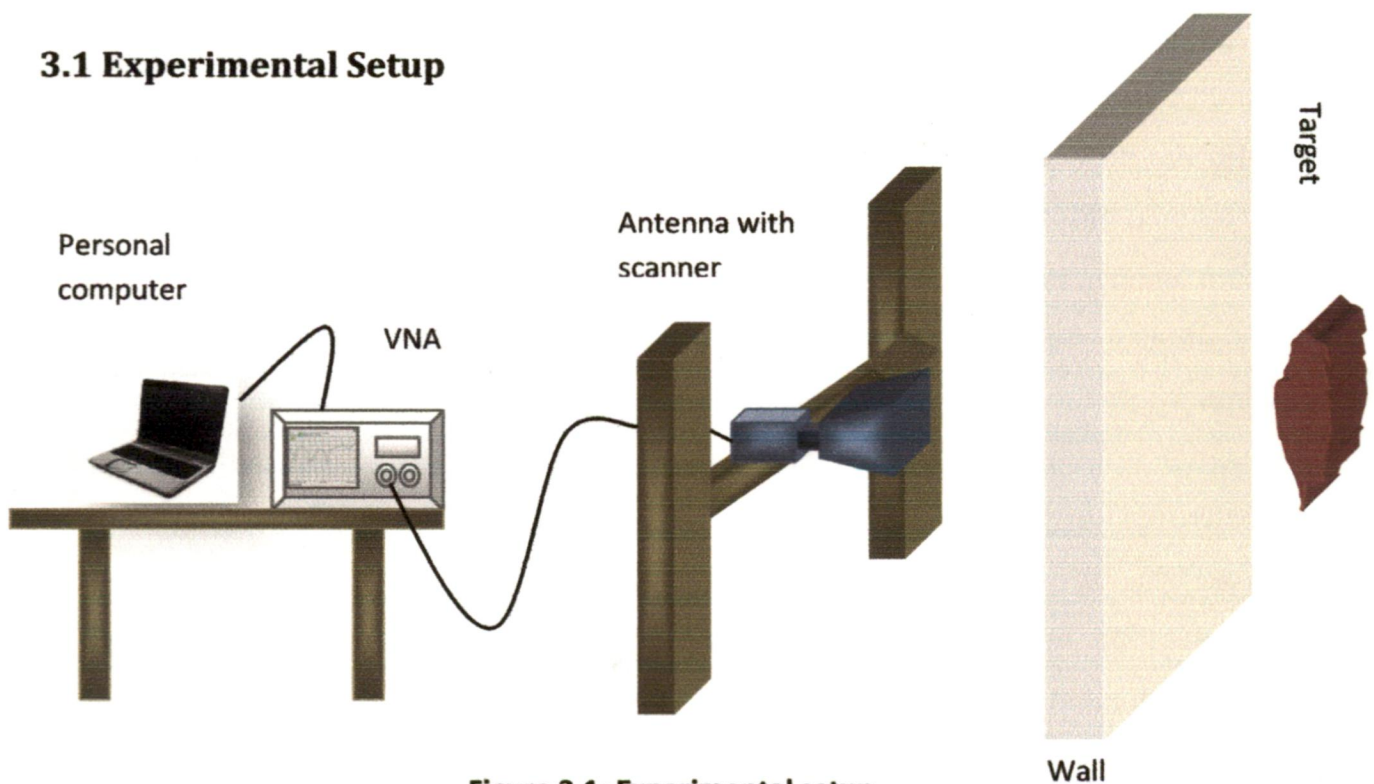


Figure 3.1: Experimental setup

The experimental setup for TWI is shown in the figure (3.1). The setup consists of VNA which act as a power source, laptop connected to VNA using LAN connection that is use for real time application. Two coaxial cables, length of 1m and 5m are used. Double rigid horn antenna R&S HF 906, operating in a frequency range of 1-18 GHz used as a transmitter and receiver. Walls of different type such as plywood, asbestos and brick and target used are of Teflon and metal. For scanning purpose 2D scanner of wooden frame was used on which the antenna was moved and target is placed on a wooden platform. The detailed description of the components is given in coming subsections.

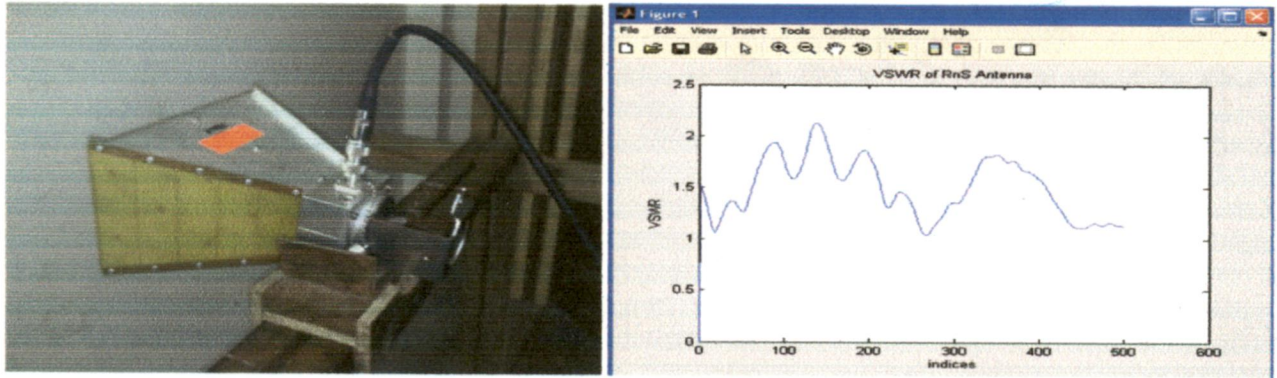
3.2 TWI Components and Properties

The detailed of components such as VNA, Antenna, Cables and their properties are detailed below.

3.2.1 Antenna

Electromagnetic horn antennas are radiating elements which can be characterized by their ability to effect transition from a medium supporting limited number of modes to a medium supporting large number of modes i.e. from a waveguide to free space.

The horn antenna may be considered as an RF transformer or impedance match between the waveguide feeder and free space which has an impedance of 377 ohms. By having a tapered or having a flared end to the waveguide the horn antenna is formed and this enables the impedance to be matched. Although the waveguide will radiate without a horn antenna, this provides a far more efficient match. However the main advantage of the horn antenna is that it provides a significant level of directivity and gain. For greater levels of gain the horn antenna should have a large aperture. Also to achieve the maximum gain for a given aperture size, the taper should be long so that the phase of the wave-front is as nearly constant as possible across the aperture. Thus the radiation characteristics depend on the flare angle, aperture dimension, type of flare, length of the flare etc. The lowest frequency of operation of a horn is fixed by the cut-off frequency of the waveguide and the neck dimension. The highest frequency gets limited on deterioration in radiation characteristic.



(a)

(b)

Figure 3.2: (a) HF 906 antenna (b) VSWR of antenna

Frequency range	1 GHz to 18 GHz
polarization	Linear
RF connector	N female
Nominal impedance	50
Gain	7 dBi to 14 dBi
VSWR	< 2.5
Max. RF input power	300 W CW , 500 W PEAK
Max. height	160 mm
Max. width	250 mm
Max. length	290 mm
Weight	1.5 kg
MTBF	>250.000 h
Environmental conditions:	
Rated temperature range	0°C to + 50°C
	40°C to +70°C

Table 3.1: Antenna Specification

3.2.1.1 Antenna pattern

At the mouth of the horn antenna (E-plane height b , H-plane width a) the fields are given by the rectangular waveguide mode with a phase curvature essentially equal to the flare

length of the horn. The radiation pattern of horn antenna used was calculated by taking E plane and H plane observations in the anechoic chamber.

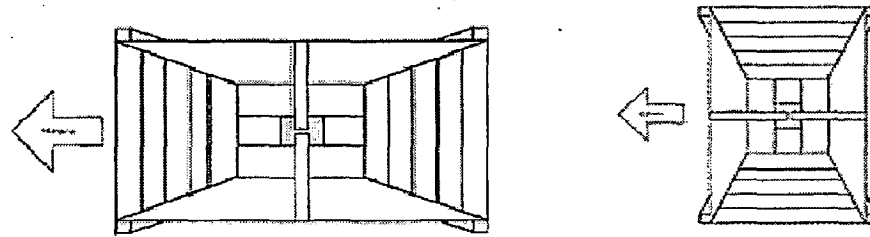


Figure 3.3: Diagram indicating H-plane (Vertical Polarization) and E-plane (Horizontal Polarization) cuts for Horn antenna [16].

The polar graph shown above is E-plane characteristics of the antenna at frequency 3 GHz. The half power beam width of antenna is called elevation angle. It is 35° in this case.

The polar graph of H-plane characteristics of the antenna at frequency 3 GHz is shown below. The half power beam width of antenna is called azimuth angle. It is 33° in this case.

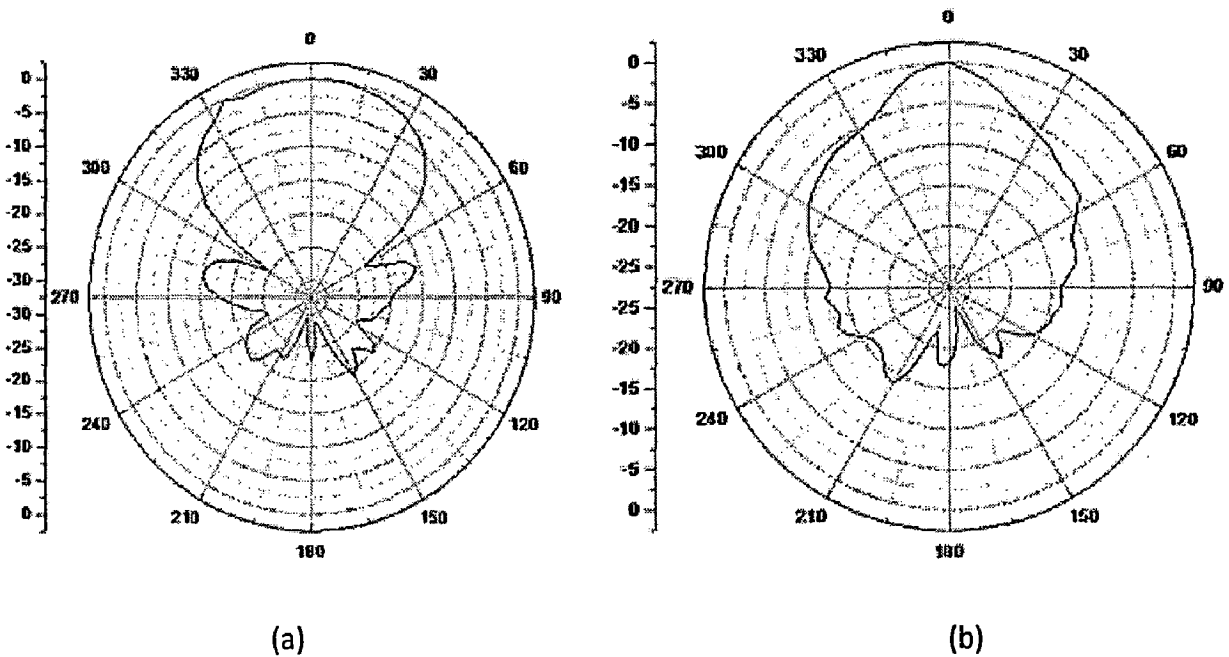


Figure 3.4: Antenna Pattern (a) E Plane (b) H-Plane

3.2.2 Vector Network Analyzer (VNA)

Commercial available network analyzer is used as both a generator and radar receiver. A synthetic pulse is reconstructed from a step frequency signal and then transmitted to the antenna. The major advantages of such system are controlling an ultra wideband around the central frequency and for obtaining higher dynamic range. A ZVL3 has been chosen for the experimental work. The synthetic pulse signal is generated by continuous step frequency signal with a maximum output power of 20 dBm, selected number of frequencies as 4001. It is able to measure a variety of different parameters including the amplitude response as well as the network scattering parameters, or S-parameters, which are the transmission and reflection coefficients for the device under test. These S-parameters contain both amplitude and phase information, and therefore a vector network analyzer, VNA is able to give a very comprehensive view of the device.

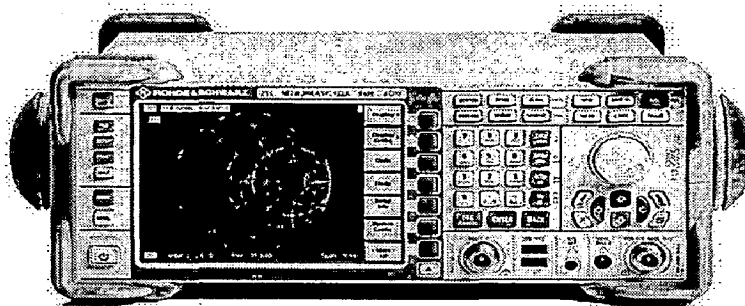


Figure 3.5: Front view of R&S ZVL3 vector network analyzer

3.2.2.1 Selection of frequency band:

For the application of TWI, the radar must provide low frequencies for deep penetration. For the absorption of electromagnetic fields in various types of wall the frequency is such that it can penetrate through the wall. The resolution should be as small as a few centimeters so that it can separate the closely related scattered. The reflection through the target is function of power higher the power higher should be the reflection, but higher power is dangerous for human being so an adjustment should be made for the purpose of our goal. High absolute bandwidth ensures high resolution of the system, it can be seen that lower center frequency ensures that attenuation of the signal through the wall is not very high. This makes UWB signals ideal for Through Wall Imaging applications as they allow us to deal effectively with the resolution-power trade-off. By specifying the start

and stop frequencies, f_{start} and f_{stop} , and the number of frequencies N_f , we can easily derive the frequency step by equation [47].

$$\Delta f = \frac{f_{stop} - f_{start}}{N_f - 1} \quad (3.1)$$

The maximum unambiguous range R_u and the frequency step size Δf of the stepped frequency signal are related by $R_u = c/2\Delta f$. since our aim is to achieve high resolution, first we chosen number of frequency points (4001). The used frequency range the calculated step size will be 475 KHz which will give unambiguous range of 315.78 m.

3.2.2.2 VNA calibration

Calibration is the process of eliminating systematic, reproducible errors from the measurement results. Calibration plays an important role in determining the accuracy of the measurement system. The process involves the following stages:

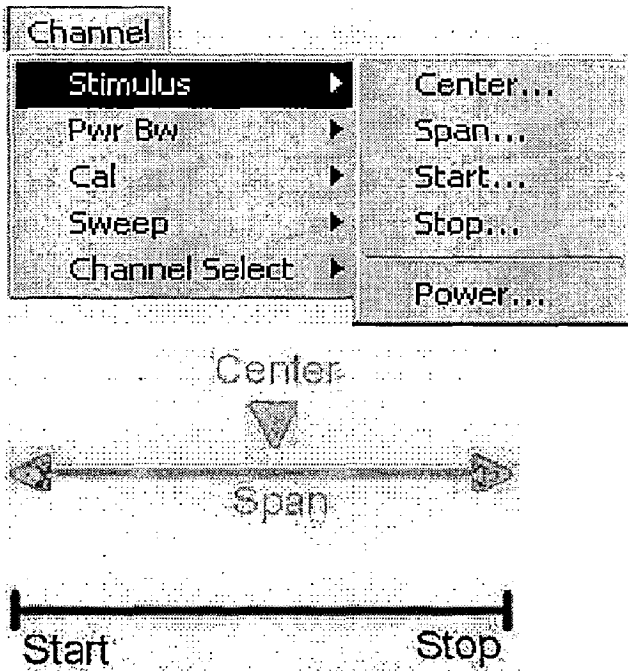
1. A set of calibration standards is selected and measured over the required sweep range.
2. The analyzer compares the measurement data of the standards with their known, ideal response. The difference is used to calculate the system errors using a particular error model (calibration type) and derive a set of system error correction data.
3. The system error correction data is used to correct the measurement results of a DUT that is measured instead of the standards.

Based upon the requirement one or two port calibration will take place. A full one port calibration requires a short, an open and a match standards to be connected to a single test port. The three standard measurements are used to derive all three reflection error terms:

- The short and open standards are used to derive the **source match** and the **reflection tracking** error terms.
- The match standard is used to derive the **directivity** error.

Calibration procedure is as follows:

- A channel contains hardware-related settings to specify how the network analyzer collects data. Therefore first the channel setting is done.



- After channel setting one port calibration is performed.

Standard cal kit	ZV-Z132
------------------	---------

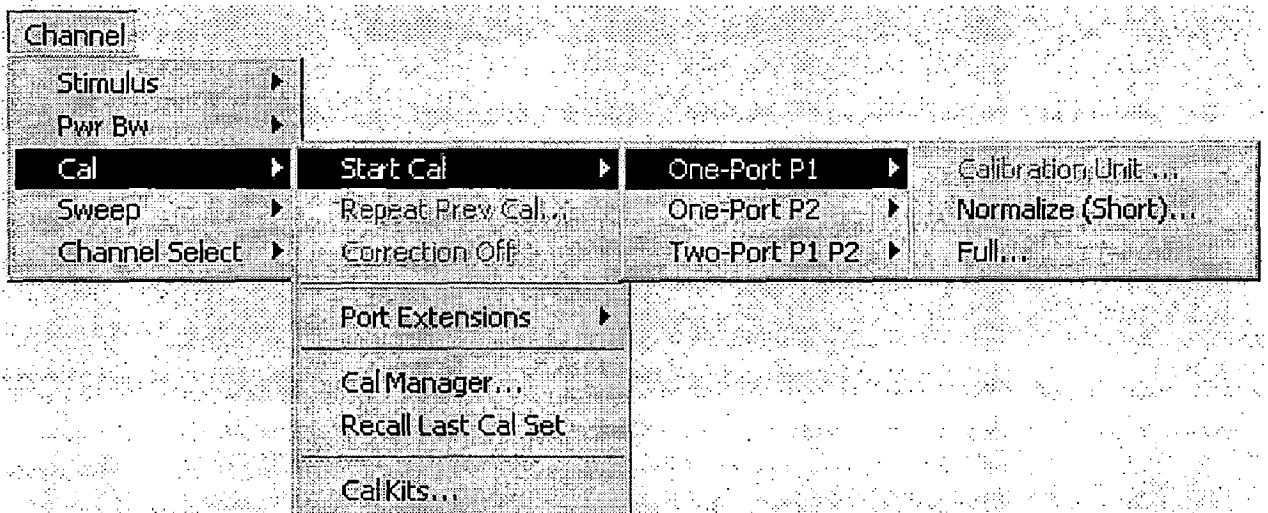


Figure 3.6: One port calibration menu in VNA

A two-port VNA with S-parameter test set can measure four scattering parameters, S_{11} , S_{21} , S_{12} and S_{22} of the device under test (DUT). In through wall imaging only one reflection (S_{11}) coefficient is recorded for image development. Only for wall parameters measurement need both S_{11} and S_{21} but it is not applicable for real time application.

3.2.3 Scanner

A wooden scanner is used for positioning the radar. The scanner has 30 positions along the horizontal direction and 20 positions along the vertical direction. Thus a total of 600 different positions for the radar are possible.

3.2.4 Cables

The two coaxial cables are used to connect the network analyzer to the antenna. When the cables move during the scanning operation a change in amplitude and phase response occurs. Length of cable is 5 m and 1m respectively.

3.2.5 Personal Computer

A laptop is used which is connected to the Vector Network Analyzer (VNA) using a LAN connection. The PC is important for real time implementation. The software used is Math works MATLAB. Virtual Instrument Software Architecture (VISA) provided by National Instruments (NI) was used to provide an interface between hardware (VNA) and the development environment (MATLAB).

3.3 Data Collection

Measurements were carried out with different type of walls, different type of targets, different shape and size of targets and with different distance between antenna scanner and wall.

All three scans, namely A-scan, B-scan and C-scan, were used to collect data.

- The signal received at any measurement point is called the **A-scan**. A-scan will be used to detect and locate the target.
- B-scan is a succession of stacked A-scans. Here we take a series of A-scans recorded along a scanning line.

- The C-scan (or three-dimensional data presentation) signal is obtained from the ensemble of B-scans, measured by repeated line scans along the plane. In addition to range, the C-scan provides valuable information about the target extent in length, height and width.

3.3.1 Wall characterization

For the wall characterization using insertion transfer function, two low loss cables were connected between the horn antennas and the two ports of VNA. Three different wall materials which are used in through wall imaging are selected for characterization. These include plywood, asbestos and brick wall of room. In case of brick wall, the two antennas were kept in two adjacent rooms so that wall dividing them can be used for experiment. VNA system was calibrated (two port calibration TOSM) and the reference positions were set to be at the output ports of coaxial cables that will be connected to antennas. The transmitted power, frequency range and number of frequency points are 20 dBm, 2 GHz to 3 GHz and 201 respectively. Transmitting antenna is kept at a distance of 1 m and receiving antenna is placed at distance 60 and 70 cm, so that variation of dielectric constant with distance can be calculated. Table 3.2 shows three different wall type used for experiment with their dimensions and distance between antennas and wall.

Sr. no.	Material	Dimension (cm)	Distance between transmitting antenna and wall	Distance between wall and receiving antenna
1	Plywood	12×365.76×121.92	1 m	60 and 70 cm
2	Asbestos	0.04×121.92×121.92	1 m	60 and 70 cm
3	Brick wall	0.012×184×123	1 m	60 and 70 cm

Table 3.2: Data collection for wall characterization

For the wall characterization by using reflection method, measurement has been done only from one side of the wall. VNA system was calibrated by using one port scattering parameter S_{11} and the reference positions were set to be at the output ports of coaxial

cable that will be connected to antennas. The transmitted power, frequency range and number of frequency points are 20 dBm, 1 GHz to 3 GHz and 201 respectively. Transmitting antenna is kept at a distance of 75, 82.5, 90, 97.5, 105 and 112.5cm from the wall.

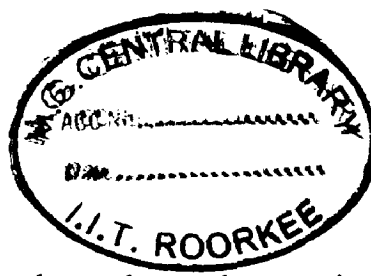
3.3.2 Single Target

In first experiment a single metal plate was chosen as a target. Table 4.1 shows the different type of walls used with different type of shapes of target at different distances. The readings were taken for 30 antenna position in cross range (azimuth) direction and 20 antenna position in vertical (upward) direction means a matrix of 30×20 is scanned by shifting the antenna by 5cm at each scanning point.

Sr. no	Type of Wall	Thickness of wall (cm)	Shape of Single Metal target	Size of target	Distance between antenna and wall (cm)	Distance between wall and target (cm)	Height of stand on which target is placed	Height at which scanning start above ground
1	Brick Wall	12.5	Square	58 cm × 58 cm	41	50	105	47
2	Brick Wall	12.5	Circular	58 cm diameter	41	50	105	47
3	Brick Wall	12.5	Eq. triangle	58 cm side	41	50	105	47
4	Plywood	1.2	Square	58 cm × 58 cm	41	50	105	47
5	Plywood	1.2	Circular	58 cm diameter	41	50	105	47
6	Plywood	1.2	Eq. triangle	58 cm side	41	50	105	47

Table 3.3: Data collection for single Target

VNA system was calibrated by using one port scattering parameter S_{11} . The transmitted power, frequency range and number of frequency points are 20 dBm, 1 GHz to 3 GHz and 201 respectively. Plywood walls are mounted on wooden stand whereas brick wall is used from the room which is dividing two rooms. So in case of brick room antenna scanner is placed in one room and target is placed in another room which resembles the actual situation.



3.4 Data Processing

In this dissertation two main tasks have been done, characterization of wall parameters and auto focusing approach to improve image quality. To get good quality image at an exact position behind the wall, wall parameters must be known exactly. But clutter, system noise and radar range resolution effect the measurement and error in wall parameters shift the target from its true location and image that we obtain is smear and blur so focusing approach has been applied to achieve good quality image.

3.4.1 Properties of Wave Penetrating Through Wall

In Through wall imaging wave propagate through different types of wall as concrete wall, wooden wall, asbestos wall, plaster, dry wall etc. the transmitted signal gets attenuation due to free space loss, scattering from air wall interface, multiple reflection due to in homogeneities in wall material, loss in the wall and scattering from the targets. The wave propagate through the antenna is generally spherical wave, but for simplification purpose the wave assumed to be planner wave, so all the experiment has to be done in far field condition. UWB signal are able to penetrate through the wall without massive attenuation so it can be use for TWI purpose. TOA mainly refer the time require to reach the signal between transmitting antenna, wall and receiver for simplification we can divide it into two parts transmitting to the target and target to the receive antenna. The waves transmitted strike wall the at different angles and propagate through the wall but change in direction the same has been apply in wall-air interface, the velocity in free space is equal to the velocity of the light but in dielectric media it depend upon the value of ϵ_r , velocity decrease by square root of relative dielectric constant, so total flight time is equal to the travel distances in different part divided by velocity in different parts. When electromagnetic wave propagate through the wall loss in signal strength takes place, to see the losses let us consider a TEM wave propagating in '+z' direction can be represented using phasor expression $E(z, \omega) = E_0 e^{-\gamma z}$, where $\omega = 2\pi f$ is the radiation frequency (f will be in Hz) and γ is the propagation constant, given by:

$$\gamma(\omega) = \alpha(\omega) + j\beta(\omega) = j\omega\sqrt{\mu\epsilon} \quad (3.2)$$

It is assume that wall is a non magnetic material then $\mu = \mu_r \mu_0 = \mu_0$ as $\mu_r = 1$ and assume

$\sigma \cong 0$, The dielectric polarization loss may be accounted for by a complex permittivity $\varepsilon(\omega) = \varepsilon'(\omega) - j\varepsilon''(\omega)$. So the value of

$$\gamma(\omega) = j\omega\sqrt{\mu\varepsilon_0(\varepsilon_r' - j\varepsilon_r'')} = j\omega\sqrt{\mu\varepsilon_0\varepsilon_r'(1 - j\frac{\varepsilon_r''}{\varepsilon_r'})} \quad (3.3)$$

The second radical factor become unity as ε'' vanish so the value of α become zero, then it can be say that losses occurs if ε'' is present. It represents dielectric losses. If material is of finite conductivity the Maxwell equation become

$$\nabla \times H = (\sigma + j\omega\varepsilon')E \quad (3.4)$$

And in dielectric material

$$\nabla \times H = j\omega(\varepsilon' - j\varepsilon'')E \quad (3.5)$$

By comparing (3.6) to (3.7) it has been observed that $\varepsilon'' = \sigma / \omega$ in any conducting media. In wall conductive loss cannot be easily separated from dielectric loss but the combination of two terms gives effective loss tangent [50].

$$p_e(\omega) = \frac{\varepsilon'' + \sigma / \omega}{\varepsilon'} = \frac{\varepsilon''}{\varepsilon'} + \frac{\sigma}{\omega\varepsilon'} \quad (3.6)$$

So complex effective relative permittivity can now be define as

$$\varepsilon_{re}(\omega) = \varepsilon_r(\omega)[1 - jp_e(\omega)] \quad (3.7)$$

So we can characterize the wall by its relative permittivity and effective loss tangent.

3.4.2 Measurement of wall Parameters

As discussed earlier through wall imaging use for the purpose of terrorist's localization or weapon detection behind walls, the detection of illegal immigrants, the detection, localization and tracking of the moving objects behind a wall becomes more and more important nowadays. Ultra-wideband radar imaging presents an interesting technology for that purpose. However, the imaging algorithms need the wall parameters such as thickness and permittivity in order to correct and to improve the obtained results. There are a few methods for estimation of the wall parameters [10, 16, 40, 43, 50]. In one

method the wall parameters can measure precisely when the wall is placed in between [40, 50] the antennas. However this is not practical especially in the case with terrorists or fire since it is meaningless for the intended applications to measure the wall from both sides.

In other wall parameters have been measured by using reflection coefficient [16, 28]. The main attention was paid to a practical estimation method that can be used in the real environment. The measurement is carried out from one side of the wall, thus there is no need to enter a dangerous space.

3.4.2.1 Measurement by Insertion Transfer Function

The transmission scattering signal related to the transmitted and incident signal by

$$S_{21}(j\omega) = \frac{FFT\{v_r(t)\}}{FFT\{v_i(t)\}} \quad (3.8)$$

Measurement is given in figure (3.7). Where v_r is the voltage at the output terminals of the receive antenna and is proportional to E_r , while v_i is the voltage at the input terminals of the transmit antenna and is proportional to E_i . Instead of measuring the transmitted and received voltage signals, it is more convenient to measure the following two signals on the receive side [25].

- A transmit 'through' signal, $v_i(t)$, which is received with the material layer in place, and
- A free-space reference signal, $v_i^{fs}(t)$, which is the received signal without the wall.

So the two measurements have been done exactly same distance with same antenna set up. Now the insertion transfer function can be written as [50]

$$H(j\omega) = \frac{E_r(j\omega) / E_i(j\omega)}{E_r^{fs}(j\omega) / E_i(j\omega)} = \frac{E_r(j\omega)}{E_r^{fs}(j\omega)} = \frac{FFT\{v_r(t)\}}{FFT\{v_r^{fs}(t)\}} = \frac{v_r(j\omega)}{v_r^{fs}(j\omega)} \quad (3.9)$$

In time domain the delay between two pulses has been measure to obtain the approximate dielectric constant of the wall. By measuring the total signal power in free space case and through the material, power loss through the material can be obtained.

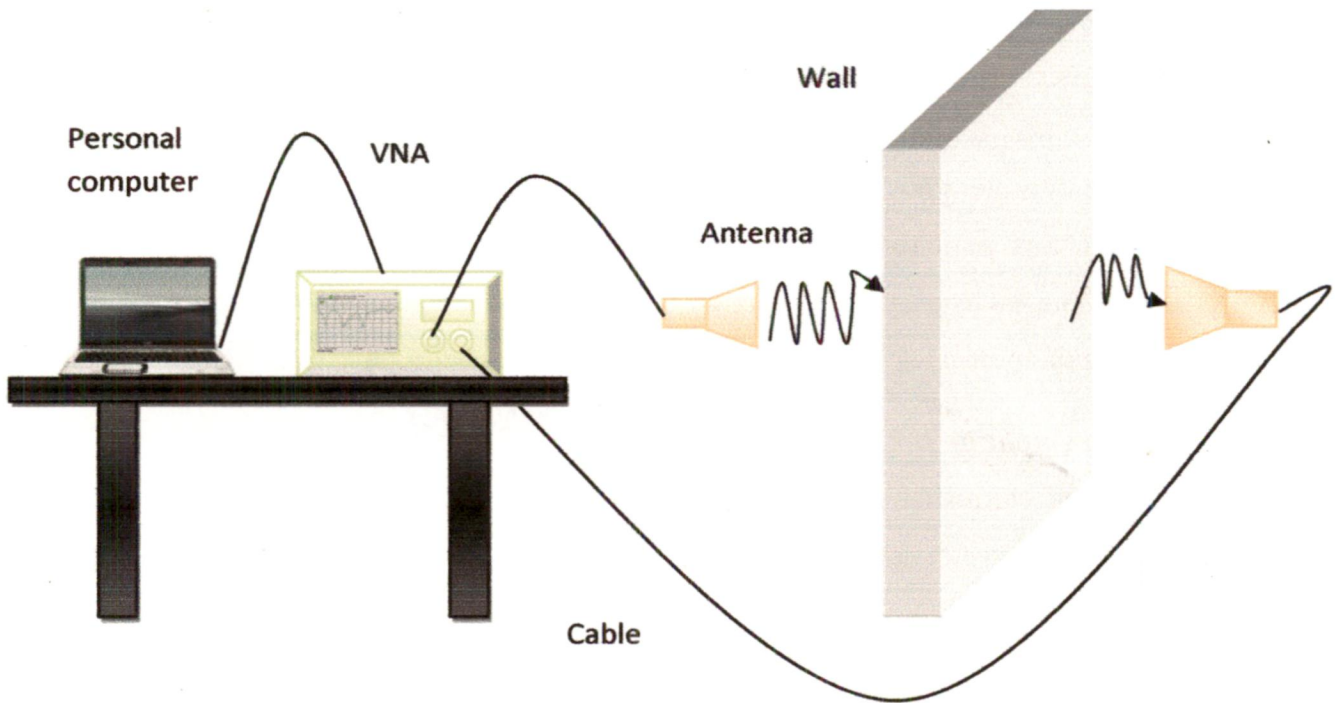


Figure 3.7: Model for characterizing wall parameters

3.4.2.1.1 Analysis Technique:

In real time environment reflection from the clutters and multiple reflections come into the picture so it is very difficult task to obtain the exact parameters. Measurement has to be done in far field to avoid spherical radiations. For measurement purpose two techniques can be applied [16, 40, 50] based on time domain and frequency domain, single-pass, multiple-pass, and approximate solutions for low loss materials by using multi-pass technique, are presented.

I. Single Pass Technique:

Electromagnetic wave of short duration has been applied to the homogenous, isotropic medium. It was assume that the wave incident on the wall normally and width of the wall is much larger so the pulse duration is much small then the time travel through the wall. The derivation of the measurement is given in [50].

$$\varepsilon_r(f) = \left[1 + \frac{\Delta\tau(f)}{\tau_0} \right]^2 \quad (3.10)$$

II. Multi – Pass Technique:

Single pass technique is not effective if the time taken by the signal through the wall is less than applied pulse width because of its multiple reflections through the wall cannot account. So the multiple pass technique can be applied, in this the data is obtained in frequency domain.

To obtain the expression for the insertion transfer function it is assumed that TEM wave propagating in '+z' direction. In which electric field directed towards '+x' and magnetic field is towards '+y', when it is incident on the wall some part of it is transmitted and some is reflected back. The wall has a complex dielectric constant of $\varepsilon(\omega) = \varepsilon'(\omega) - j\varepsilon''(\omega)$. It has been shown in figure (3.8).

Field in the region is given by

$$\vec{E} = a_x (E^+ e^{-\gamma z} + E^- e^{+\gamma z}) \quad (3.11)$$

$$\vec{H} = (H_0^+ e^{-\gamma z} - H_0^- e^{+\gamma z}) a_y \quad (3.12)$$

By applying boundary conditions at the interface the transmission that is obtained [40]

$$T = \frac{E_t e^{-j\beta z}}{E_i} = \frac{4}{e^{\gamma d} \left(2 + \frac{\eta_1}{\eta_2} + \frac{\eta_2}{\eta_1}\right) + e^{-\gamma d} \left(2 - \frac{\eta_1}{\eta_2} - \frac{\eta_2}{\eta_1}\right)} \quad (3.13)$$

The complex frequency response of the transmission channel can be obtained by measuring the scattering parameter S_{21} with this system. The transmission coefficient is obtained by comparing the measured S_{21} with and without wall and it is related to the insertion transfer function $S_{21} = H(\omega)$. Once the insertion transfer function is obtained, numerical methods are used to extract the attenuation coefficient and dielectric constant. From the complex insertion transfer function, the dielectric constant and loss tangent of the material under test are to be extracted.

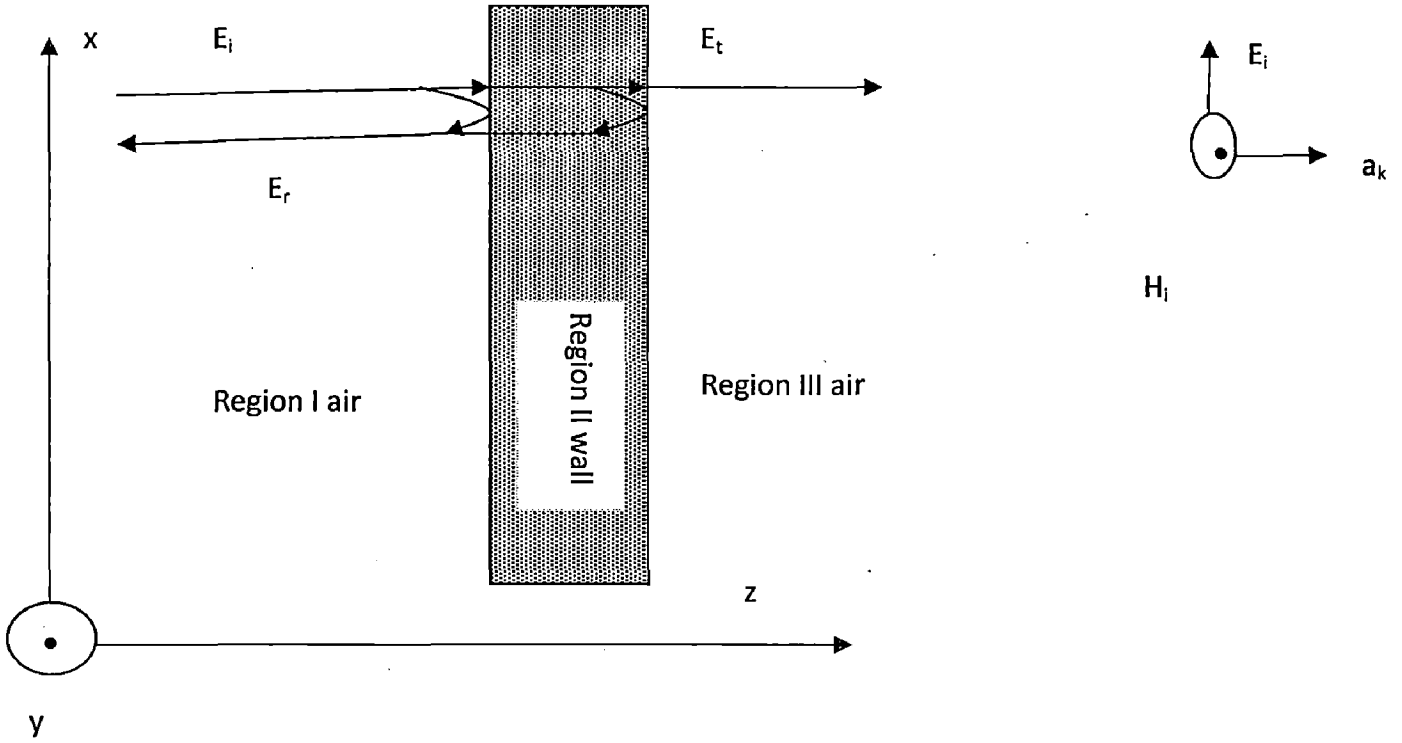


Figure 3.8: EM wave propagation through the wall

3.4.2.1.2 Calculation of Dielectric Constant of the Wall:

Due to Dielectric constant of the wall, velocity of the signals propagate through the wall is reduce by square root of dielectric constant of the wall.

$$V_{\text{wall}} = \frac{c}{\sqrt{\epsilon}} \quad (3.14)$$

While dielectric constant is the relative permittivity of the wall. After determination of insertion transfer function following equations have to be solved [40]

$$H(j\omega) = \frac{4e^{j\beta_0 d}}{e^{\gamma d} \left(2 + \frac{\eta_1}{\eta_2} + \frac{\eta_2}{\eta_1}\right) + e^{-\gamma d} \left(2 - \frac{\eta_1}{\eta_2} - \frac{\eta_2}{\eta_1}\right)} \quad (3.15)$$

While

$$\eta_1 = \sqrt{\frac{\mu_0}{\epsilon_0}} \quad \eta_2 = \sqrt{\frac{\mu_0}{\epsilon_0 (\epsilon_r' - j\epsilon_r'')}}$$

$$H(j\omega) = \frac{4e^{j\beta_0 d}}{e^{\gamma d} \left(2 + \frac{\epsilon_r' + 1}{\sqrt{\epsilon_r'}}\right) + e^{-\gamma d} \left(2 - \frac{\epsilon_r' + 1}{\sqrt{\epsilon_r'}}\right)} \quad (3.16)$$

thickness of the wall is d . Generally gives the complex solutions and can be solved by reducing it into one dimensional approximate solutions given by following equations and can be deduced where only ϵ is present.

$$\tan(\beta_0 d - \angle H(j\omega)) + \frac{1 - QX}{1 + QX} \tan \beta d = 0 \quad (3.17)$$

$$Q = -\left(\frac{\sqrt{\epsilon'} - 1}{\sqrt{\epsilon'} + 1}\right)^2 \quad (3.18)$$

$$\beta = \beta_0 \sqrt{\epsilon'}$$

$$X = e^{-2\alpha d} = \frac{[\cos 2\beta d (\epsilon' - 1)^2 + 8 \frac{\epsilon'}{|H(j\omega)|}] - \sqrt{[\cos 2\beta d (\epsilon' - 1)^2 + 8 \frac{\epsilon'}{|H(j\omega)|}]^2 - (\epsilon' - 1)^4}}{(\sqrt{\epsilon'} - 1)^4} \quad (3.19)$$

These equations are used to find ϵ' (real part of dielectric constant), which is required to calculate the speed of wave inside the wall so that a suitable velocity correction can be applied. Attenuation constant (α) can be calculated by using (3.17) assuming conductivity of walls to be zero the loss tangent can be calculated using

$$\epsilon'' = \frac{2c\alpha\sqrt{\epsilon'}}{\omega} \quad (3.20)$$

$$\tan(\delta) = \frac{\epsilon''}{\epsilon'} \quad (3.21)$$

By solving these equations we can find out the dielectric constant, attenuation constant and loss tangent. As describe in section 3.4.1, loss tangent of wall contain both dielectric

and conductive properties of the wall so it is difficult to extract the conductivity of the wall from loss tangent.

3.4.2.2 Measurement by Reflection Method:

Practically insertion method cannot be used in real time application, especially in the case when there is some harmful object behind the wall, terrorist or fire since it is become meaningless to measure the wall from both sides. So here an approach has been applied to measure the thickness and permittivity of the wall. Measurement has been done from one side of the wall so there is no need to enter in dangerous zone. It can be easily applied in real time environment. The processing takes only 3-4 second by using mat-lab.

In this method we use time domain reflection. The Fresnel equations at the wall interface and plane wave propagation within the wall is applied. The whole wave propagation is assumed to be planner; this is not the practical situation so measurement has been done in far field environment.

Figure (3.9) show the model of wave propagation within the wall, in this figure perpendicular polarization means electric field is perpendicular to the plane of incident.

Let the wave incident on the wall by making an angle θ with z axis then incident electric and magnetic field can be define as

$$\vec{E} = E_0 e^{-\gamma(x \sin \theta + z \cos \theta) a_y} \quad (3.22)$$

$$\vec{H} = \frac{E_0}{\eta} (-\cos \theta a_x + \sin \theta a_z) e^{-\gamma(x \sin \theta + z \cos \theta) a_y} \quad (3.23)$$

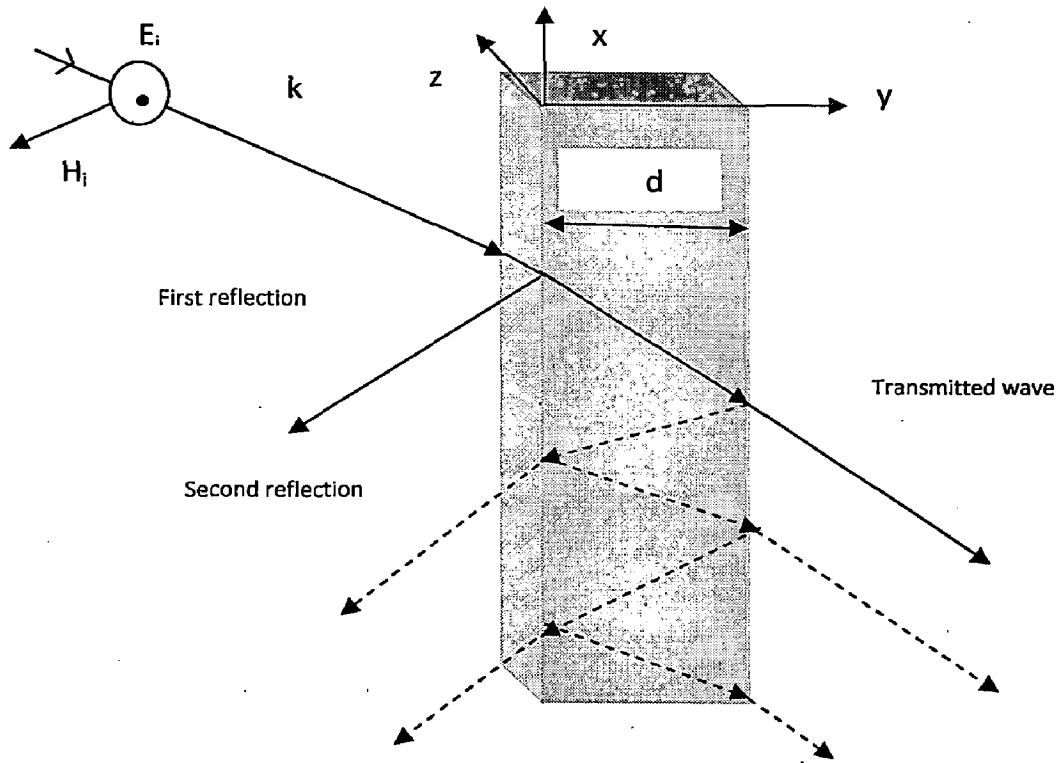


Figure 3.9: Model of wave propagation through the wall

By taking reflected and transmitted wave into the consideration and applying boundary condition the Fresnel equations for reflected and transmitted wave can be obtain. In this approach we can assume spherical wave and oblique incident but for simplicity we assume planner wave and normal incident of the wave, the error obtained by this approximation is negligible since only spreading loss has been neglected. For this case we assume wall structure is planner, homogenous and isotropic and frequency independent wall permittivity and permeability more over it has been assume that wall material is non magnetic then $\mu_r=1$. In this case reflections at the wall surfaces have been taken into the account.

Reflections of higher order have negligible amplitude so it can be neglected. The Fresnel equation for perpendicular incident is given by

$$\Gamma = \frac{E_r}{E_i} = \frac{\eta_2 - \eta_1}{\eta_2 + \eta_1} \quad (3.24)$$

$$\tau = \frac{E_t}{E_i} = \frac{2\eta_2}{\eta_2 + \eta_1} \quad (3.25)$$

While

$$\eta_1 = \sqrt{\frac{\mu_0}{\epsilon_0}}, \quad \eta_2 = \sqrt{\frac{\mu_0}{\epsilon_r \epsilon_0}}$$

$$\text{So, } \Gamma = \frac{\sqrt{\epsilon_a} - \sqrt{\epsilon_r}}{\sqrt{\epsilon_a} + \sqrt{\epsilon_r}} \quad (3.26)$$

Where Γ is a reflection coefficient; τ is a transmission coefficient, ϵ_a is the permittivity of the air and ϵ_r is the permittivity of the wall. When EM wave propagate through the wall attenuation in the wave occurs, which is usually determine for the frequency domain:

$$\alpha = \omega \sqrt{\frac{\mu\epsilon}{2} \left[\sqrt{1 + \left(\frac{\sigma}{\omega\epsilon}\right)^2} - 1 \right]} \quad (3.27)$$

It can be easily interpret that attenuation through the wall increase with frequency since the conductivity of the wall is very low then attenuation can assume to be zero. And the phase constant is linearly varied with frequency.

From this set of simple equations, it is possible to estimate the wanted wall parameters. The first reflection will provide the permittivity of the wall. From that the propagation speed can be calculated. Hence, the time delay of the inner wall reflection will give us the wall thickness. Thus, there is no iteration required and the data may be taken directly from radar measurements which are usually given in the time domain but in our case data has been taken into frequency domain and then by using inverse Fourier transform frequency domain data can be converted into time domain.

3.4.2.2.1 Clutter reduction

To obtain precisely reflections from wall-air interface or second reflection from the wall is a difficult task because of clutters, antenna ringing and system noise. It can overlap with the wall reflection and make calculation difficult.

In order to separate wall reflection from unwanted component some changes in scanning has to be done.

If we scan the wall in horizontal direction in front of wall then at each point we will get same reflection from the wall due to homogenous structure but the clutter signal will change their distances from the antenna, so by averaging the data the clutters can be

reduces. So by averaging the data in horizontal we clearly get the first two reflections from the wall that can be use for further calculations.

3.4.2.2.2 Wall Parameters calculation

The first step is to determine the reflection coefficient Γ of the outer surface in order to be able to determine the wall permittivity. Since the incident wave is not known in practice, a reference measurement $hm(n)$ was made before and stored in the device memory. For that purpose, we used a large sheet of metal whose reflectivity is approximately equal to 1, and measured the reflection at different distance. Since the wall parameters are not frequency dependent, we can determine Γ of the first surface from the peak values of the measured data, by using reflection we can find out dielectric constant of the wall by using equation as given in equation (3.28).

$$\Gamma = \frac{\sqrt{\varepsilon_a} - \sqrt{\varepsilon_r}}{\sqrt{\varepsilon_a} + \sqrt{\varepsilon_r}}$$

For this case ε_a is the permittivity of the air and ε_r is the permittivity of the wall.

Then the value of [28]

$$\Gamma = \frac{\|h_1(n)\|}{\|h_m(n)\|} \quad (3.28)$$

After that we can calculate the value of ε_r

$$\Gamma = \frac{(1 + \varepsilon_r)^2}{(1 - \varepsilon_r)^2} \quad (3.29)$$

The propagation time Δt within the wall will give the wall thickness

$$D_w = \frac{v_w \Delta t}{2} \quad (3.30)$$

Time Δt results from the time position of the maximum of $h2(n)$ referred to the second reflection.

We first subtract the first reflection $h1(n)$ from the data in order to gain the improved reflection from the inner surface. Since the wall parameters are frequency independent, we can suppose that $h1(n)$ and $hm(n)$ have the same time shape [16], then

$$h2(n) = h(n) - \frac{\|h1(n)\|_{\infty}}{\|hm(n)\|_{\infty}} hm(n) \quad (3.31)$$

3.4.3 Through-Wall TOA Estimation

For the accurate measurement wave propagation through the wall must be clearly estimated. Some conventional method uses constant velocity propagation produce error in object shape and position [12-13]. It is assumed that wall is homogenous in structure then problem has been converted to three layer model (air, wall and, air) for simplicity it can be also transform to the two layer (air-wall) model. By using iteration method we can calculate the TOA and it can easily use in real time application. If multilayer wall has been assumed then it converted to complex model and requires some numerical minimization method [28]. The number of variables is equal to the number of layers. This is a very time consuming process, but for small number of layers (especially for air-wall-air structure) a few improvements that significantly reduce the computation complexity will be presented.

3.4.3.1 Calculation of TOA between Antenna and target

To calculate true position of target behind the wall TOA between wall and antenna has to be known. For the computation the model has been given in the figure (3.10).

The wall assumes to be homogenous with constant permittivity and constant thickness, the relative permittivity of the air in front of the wall and behind the wall is same and equal to one. Horizontal scanning assume in '-x' direction vertical scanning in '+z' direction and target assume to be in '+y' direction. It is assume that target and are have same 'z' co-ordinate. Initial position of antenna is $(0, -d, z_0)$, target is at (x_0, y_0, z_0) , wave transmitted from transmitting antenna incident on the wall at a angle of θ_1 ; angle of refraction is θ_2 . The relative permittivity of the wall is ϵ_r and thickness is t . the radar has standoff distance d from the wall. The position of target from the radar is R_0 . The equivalent travel distance L calculated from equation (3.32)-(3.34) [35].

$$\sin \theta_1 = \sqrt{\epsilon_r} \sin \theta_2 \quad (3.32)$$

$$(R_0 \cos \theta_0 - t - d) \tan \theta_1 + \tan \theta_2 + d \tan \theta_1 = R_0 \sin \theta_0 \quad (3.33)$$

$$L = L_1 + \sqrt{\epsilon_r} L_2 + L_3$$

$$= \frac{R_0 \cos \theta_0 - t - d}{\cos \theta_1} + \sqrt{\epsilon_r} \frac{t}{\cos \theta_2} + \frac{d}{\cos \theta_1} \quad (3.34)$$

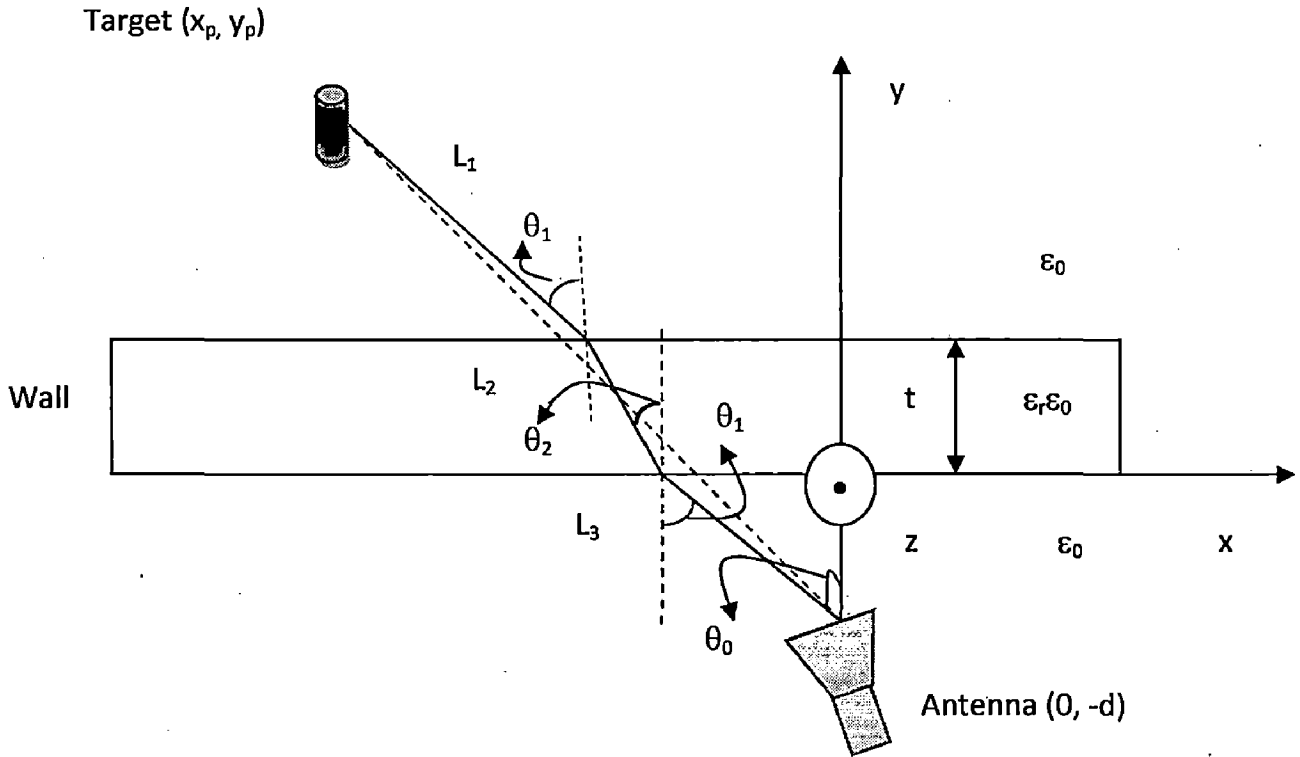


Figure 3.10: Model for calculation of True TOA [35].

The propagation delays are given by

$$\tau = \frac{L_1}{c} + \frac{L_2}{v} + \frac{L_3}{c} \quad (3.35)$$

3.4.4 Imaging: Beamforming

Beam forming is a technique used for directional signal transmission and reception. In this process the array has been design in such a way that the signals at a particular angle experience constructive interference and while others experience destructive interference. Beam forming has been found numerous applications in radar, sonar, seismology, wireless communications, radio astronomy, speech, acoustics, and biomedicine. Adaptive beam forming is used to detect and estimate the signal-of-interest at the output of a sensor array by means of data-adaptive spatial filtering and interference rejection.

3.4.4.1 Beam forming Concept

Consider the case of single transmitter and receiver, both located along the x-axis. Target is located along the positive z-axis. And scanning in longitudinal direction has been done along positive y-axis. In y-axis radar is at fixed location y_0 and it only move along positive x-direction. Let the transmitter is placed at m th position, $(x_{tm}, 0)$, transmitted a signal towards the target located at $x_p=(x_p, z_p)$ making an angle θ_0 with z-axis. Then the output at the receiver is given by $a(x_p)s(t-\tau_{mn})$ where n is the receiver location, where $a(x_p)$ is the complex reflectivity of the point target. As shown in the figure (3.11) propagation delay τ_{mn} is the time travel by the signal as it travels from m th transmitter to target and from target to n th receiver. That is given by [5]

$$\tau_{mn} = \frac{d(x_{tm}, x_p)}{c} + \frac{d(x_p, x_{rn})}{c} \quad (3.36)$$

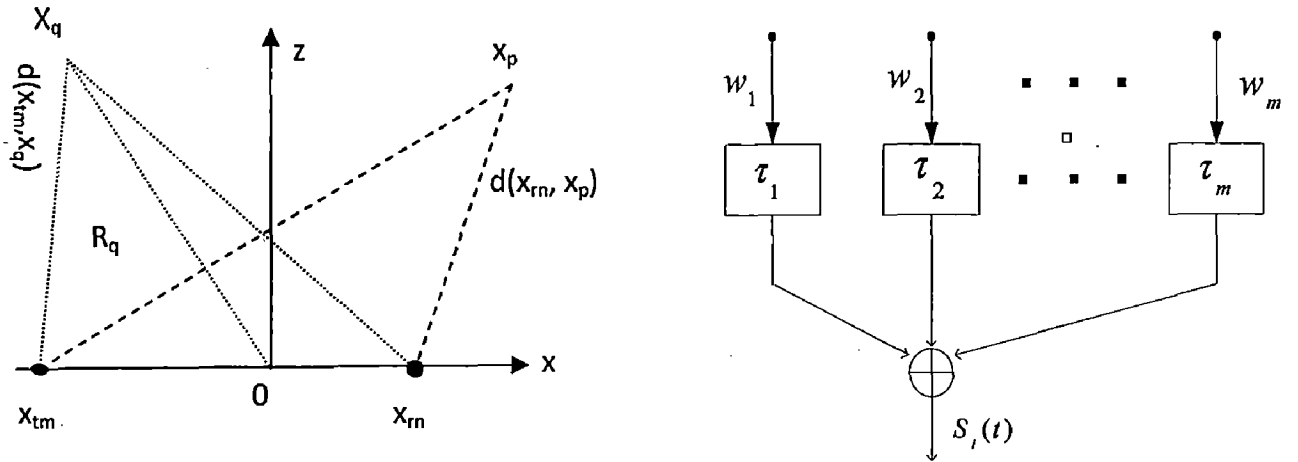


Figure 3.11: Layout representing the free space and block diagram of time domain beam former [5]

Where c is the speed of light and $d(x, y)$ denotes the Cartesian distance between locations x and y . this process is repeat till M^{th} location. If the target is divided into finite number of pixels in range and angle. Then the signal corresponds to image of the pixel located at x_q , is obtain applying time delay and weights to M receive corresponds to M transmitter locations, and summing the results. Then the output

$$z_{mq}(t) = \sum_{m=1}^M w_{rm} a(x_p) s(t - \tau_{mn} - \tilde{\tau}_{mn}) \quad (3.37)$$

Where w_{rm} is weight applied to the receiver and $\tilde{\tau}_{mn}$ is the focusing delay applied to the receiver. The focusing delay is given by figure (3.11).

$$\tilde{\tau}_{mn} = \frac{2R_q}{c} - \frac{d(x_{tm}, x_p)}{c} - \frac{d(x_p, x_{rm})}{c} \quad (3.38)$$

The weight applied to the transmitter and receiver are independent to the pixel location the complex value of image x_q is obtain by passing the signal $z_q(t)$ to through a filter matched to the transmitted pulse and sampling the output of a filter at a time $t=2R_q/c$

$$I(x_q) = (z_q(t) * h(t)) |_{t=2R_q/c} \quad (3.39)$$

The time-domain beam former can be implemented as follows:

- i. Divide the whole region into small pixels in range and angle.
- ii. For each pixel, synchronizes the outputs of the M receivers to gain the corresponding signal by using Eq. 3.37.
- iii. Pass the corresponding signal through a match filter to obtain the pixel's image value by using Eq. 3.39.
- iv. Repeat step ii and iii for all pixels to generate the composite image of the region.

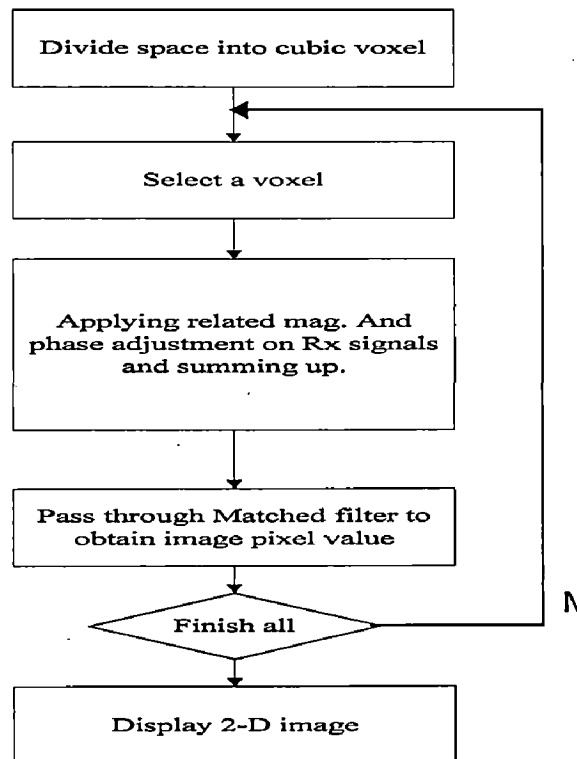


Figure 3.12: 2-D beamformer flow chart

3.4.4.2 Effect of Dielectric Wall on Beam forming

The characteristic of signal propagating through the wall has been affected by dielectric constant, thickness of the wall and angle of incident of the wave. The propagating wave slows down, encounters refraction, and attenuated as it passes through the wall.

As referring the figure (3.10) length L_1 , L_2 , and L_3 can be calculated from equation (3.34) in which radar act as a transmitter, length L_1 and L_3 is the free space length that can be combine and make a composite length L . when radar act as a receiver length can be represented as a L' , and L_2' .

The incident angle θ_1 can also be calculated by equation (3.33). We assume that the thickness of the wall and its dielectric constant are known exactly. The effects of the estimation errors in the wall thickness and its dielectric constant on beam forming are analyzed further. The sequential transmission and reception as describe in section 3.4.4.1 and after coherent combination of the delayed and weighted versions of the received signals, the complex signal corresponding to the pixel located at x_q , due to a single target located at x_p , is given by [5]

$$z_q(t) = \sum_{m=1}^M w_{tm} w_{rm} a(x_p) \exp(-\alpha(L_2 + L_2')) s(t - \tau_{mn} - \tau_{mn}^{\sim}) \quad (3.40)$$

Where α is the attenuation constant of the wall. And

$$\begin{aligned} \tau_{mn} &= \frac{L_p}{c} + \frac{L_{2p}}{v} + \frac{L'_p}{c} + \frac{L_{2p}'}{v} \text{ and} \\ \tau_{mn}^{\sim} &= T - \frac{L_q}{c} + \frac{L_{2q}}{v} + \frac{L'_q}{c} + \frac{L_{2q}'}{v} \end{aligned} \quad (3.41)$$

Where $T = (2L/c) + (2L'/v)$

Finally, the complex amplitude image value for the pixel located at x_q is obtained by filtering the signal using a filter matched to the transmitted pulse and sampling the output at $t = T$,

$$I(x_q) = \sum_{m=1}^M w_{tm} w_{rm} a(x_p) \exp(-\alpha(L_2 + L_2')) s(t - \tau_{mn} - \tau_{mn}^{\sim}) * h(t) |_{t=T} \quad (3.42)$$

By using this equation B-scan image can be obtained.

3.4.4.3 Effect of Wall Parameters Ambiguities on Beam forming image

If the wall parameters are known exactly, the focusing delay cancels the propagation delay and then $x_q = x_p$ and all receive pulse align and add together to produce a coherently combine output, it means that all the receive signal focus on a single point then output image intensity of the beam former is maximize. But in real time situation wall parameters are not known and it has to be calculated and these parameters have to be used for computing the focusing delay. By result of it, distorted image has been obtained. This degradation of image quality will be more pronounced in wall materials with high dielectric constants. Let δ_ϵ , δ_w denote the error in the dielectric constant and dielectric constant respectively. In this case the value of v , d_w , and ϵ are replaced by $c/(\epsilon+\delta_\epsilon)^{1/2}$, $d_w+\delta_w$ and $\epsilon+\delta_\epsilon$, respectively for τ_{mn} and T value. The value of focusing delay because of these errors become

$$\tau' = \tau + \Delta\tau \quad (3.43)$$

The change in focusing delay due to wall and dielectric errors [12]

i. Due to wall thickness error

$$\Delta\tau = \frac{\Delta d}{c} \left(\frac{\sin(\Phi_i - \theta_i)}{\sin(\theta_i)} + \frac{\sin(\Phi_r - \theta_r)}{\sin(\theta_r)} \right) \quad (3.44)$$

ii. Due to dielectric error

$$\Delta\tau = \frac{\Delta\epsilon d}{2\sqrt{\epsilon c}} \left(\frac{1}{\cos(\theta_i)} + \frac{1}{\cos(\theta_r)} \right) \quad (3.45)$$

Where Φ is the angle at refraction angle at wall-air interface and θ is the incident angle at air-wall interface, these angles are measure from the axis perpendicular to the incident plane.

Putting the value of focusing delay to the equation (3.40) then

$$z_q(t) = \sum_{m=1}^M w_{tm} w_{rm} a(x_p) \exp(-\alpha(L_2 + L_2)) s(t - T + \Delta\tau) \quad (3.46)$$

From equation (3.43) it is clear due to $\Delta\tau$ all the signal will not focus at same point and distortion in image will occurs, and because of thickness error target will shift from its true position. This degradation in image quality will be more when wall material having high dielectric constant and in presence of multiple wall separating the target from the

radar. So to neglect the effect of wall ambiguities auto focusing approach can be applied and obtained good quality of image.

3.4.5 Auto focusing Approach

As discussed earlier to locate and image the target behind the wall, wall parameters should be exactly known, ambiguities in wall parameters smear and blur the image and shift the target from its true position. Some algorithms has been developed in previous sections to obtain the wall parameters but because of low resolutions of radar systems and effect of clutters parameters cannot be exactly estimated, and some errors remains in estimation of parameters that errors are sufficient for distortion of the image so focusing approach can be applied to neglect these errors and obtained good quality of image. In this process image intensity profile has been generated for different values of dielectric and thickness. The approximate values of wall parameters can be assume as calculated values in previous sections. Then the values of thickness and dielectric have been put in the range of approximated value.

In this method both conventional contrast values and higher order standardized moments measures for measuring the degree of searing and blurriness of TWI of stationary target distributions. The block diagram for image quality estimation or to calculate the degree of smearing and blurriness of the image has been shown in figure (3.13)

In the process the measuring module that measure the image quality by using quality indices and feedback system that develop the image at change the wall parameters, the process continued till high quality image is not obtain.

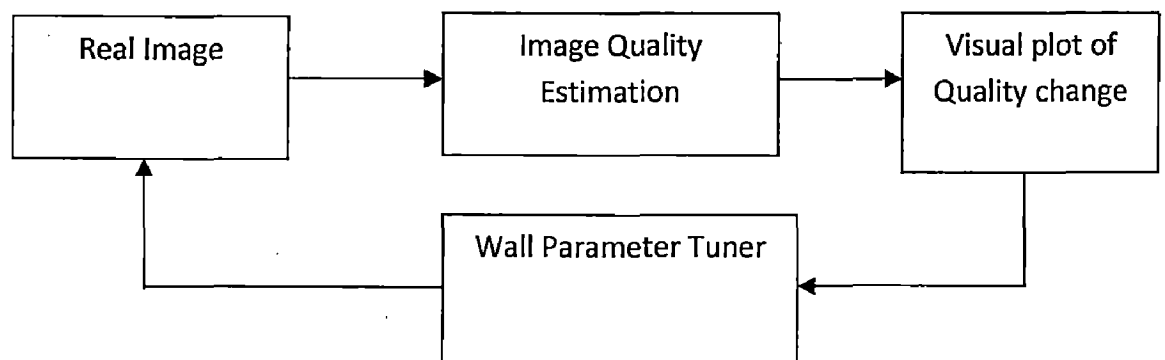


Figure 3.13: Image quality measurement feedback systems [51]

For measurement of image quality beam forming image has been generated, and use iteration for measurement. At each iteration, the assumed wall parameters are changed and image has been generated on the updated wall parameters. At exact wall parameter all signal will converge at a single point and focused image has been obtained so at this point the quality indices will show its maximum value. This analysis shows that exact, as well as incorrect, assumed wall characteristics, defined by wall thickness and dielectric constant, can lead to focused images with imaged target positions in close proximity to true target locations [51]

3.4.5.1 Image quality measurement:

Several metrics has been used for image quality measurement [52, 53, 54]. The following quality indices can be used for contrast measurement in TWI [51]

a) Normalized sum of image intensity:

$$C_1 = \frac{\sum_{q=1}^Q |I(x_q, y_q)|^2}{\left(\sum_{q=1}^Q |I(x_q, y_q)|^2 \right)} \quad (3.47)$$

b) Normalize sum of Squared intensity:

$$C_2 = \frac{\sum_{q=1}^Q |I(x_q, y_q)|^4}{\left(\sum_{q=1}^Q |I(x_q, y_q)| \right)^4} \quad (3.48)$$

c) Negative of image entropy

$$C_3 = \sum_{q=1}^Q ss(x_q, y_q) \ln [ss(x_q, y_q)] \quad (3.49)$$

Where $ss(x_q, y_q) = \left(|I(x_q, y_q)|^2 \right) / \left(\sum_{q=1}^Q |I(x_q, y_q)| \right)$

d) Ratio of standard deviation to mean amplitude:

$$C_4 = \frac{\sqrt{\sum_{q=1}^Q \left[|I(x_q, y_q)| - \frac{1}{Q} \sum_{q=1}^Q |I(x_q, y_q)| \right]^2}}{\sum_{q=1}^Q |I(x_q, y_q)|} \quad (3.50)$$

Where $I(x_q, y_q)$ is image pixel value and Q is total no of pixel in the image.

For good contrast measurement, the quality indices will show maximum or minimum value for undistorted image corresponds to the correct wall parameters. And the value of indices will decrease or increase monotonically as we increase the error in parameters.

It has been seen that value of standardize moments can also be use as indices for measurement of smearing and blurriness of the image. Let $P(x_q, y_q) = |I(x_q, y_q)|$ is the magnitude of the q th image pixel. Then, the n th standardized moment of $P(\cdot)$ is defined as the ratio of the n th moment-about-the-mean and the n th power of the standard deviation [27]. For an image consisting of Q pixels, this moment is given by [51]

$$\gamma_n = \frac{\sum_{q=1}^Q \left(P(x_q, y_q) - \hat{\mu} \right)^n}{(Q-1)\sigma^n} \quad (3.51)$$

Where μ and σ denote the sample mean and the sample standard deviation of $P(\cdot)$ and are, respectively, given by

$$\mu = \frac{1}{Q} \sum_{q=1}^Q P(x_q, y_q) \quad (3.52)$$

$$\sigma = \left[\frac{1}{Q-1} \sum_{q=1}^Q (P(x_q, y_q) - \hat{\mu})^2 \right]^{1/2} \quad (3.53)$$

For the higher value of n as we changes the wall parameters from its true value, there is sharpen change in moment will be observed, and it can be easily use for the multiple wall case where optimum parameters can be obtained by using standard moment.

It is not surprising that increasing the order of the standardized moment leads to an increased sensitivity to wall parameter errors. This is because the peaks in the image intensity profile become sharper as the image intensity is raised to a higher power, increasing the overall image contrast [51].

To develop statical model for focused image following steps have to be follow:

- i. Develop 2-D beam forming image.
- ii. Estimate image quality using quality indices value, and make a visual plot for it.
- iii. Change wall parameters.
- iv. Repeat steps from 1 to 3 till focused image has not developed.
- v. Develop a statical model for quality indices having wall parameters as an input.

The equation developed at step 5 shows its maximum value at correct parameters, so by solving this equations, accurate wall parameters can be obtain.

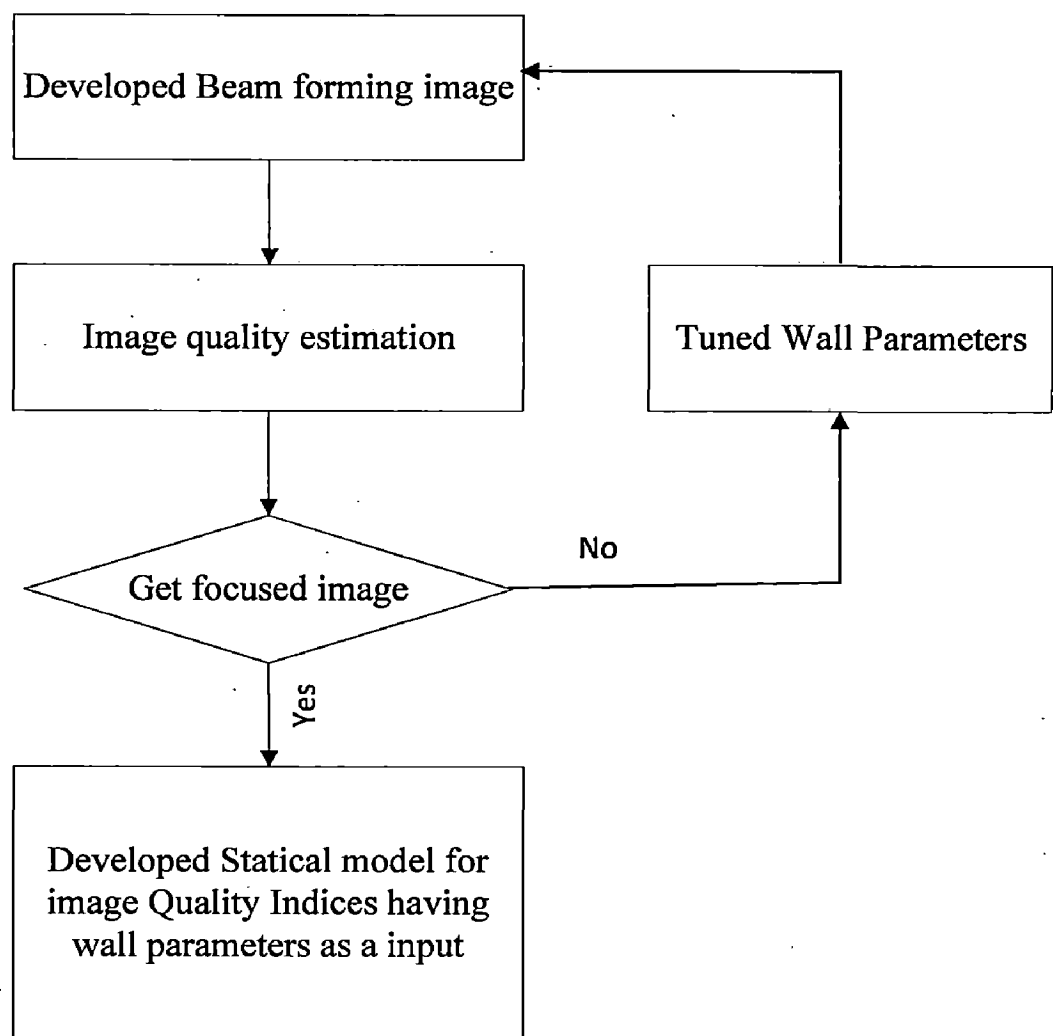


Figure 3.14: Flow chart for adaptive autofocusing algorithm

4. RESULTS AND DISCUSSION

4.1 Wall parameters Calculation by using insertion transfer function

For wall characterization data has been collected for brick wall, plywood wall and asbestos wall. Multi-pass technique has been applied for calculation purposes, S_{21} , with wall and without has been measure by using Vector Network Analyzer (VNA) ZVL3 over the frequency range of 2-3 GHz at 201 frequency points by using R&S HF 906 double ridge horn antenna working as a transmitter and S-band antenna used as a receiver. VNA output power has been set to 20dBm. A laptop is used which is connected to the Vector Network Analyzer (VNA) using a LAN connection. The PC is important for real time implementation. The software used for calculation is Math-works MATLAB.

Vector Network Analyzer	R&S ZVL	2 GHz – 3GHz
Antenna	Double-ridged waveguide type (HF 906)	1-18 GHz
VNA Power		20 dBm
Range resolution		15 cm
Azimuth resolution		29.8
Cable Loss		7 dB
Unambiguous range		600 m(for 4000 point)
Unambiguous range		30 m(for 201 points)

Table 4.1: System parameter

- i. After collecting the data (data collection for different walls have been shown in table 3.2) magnitude of transmission coefficient have been calculated by equation (3.9) and magnitude of transmission coefficient vs frequency has been plotted for all three walls and compare which are shown in figure (4.1).

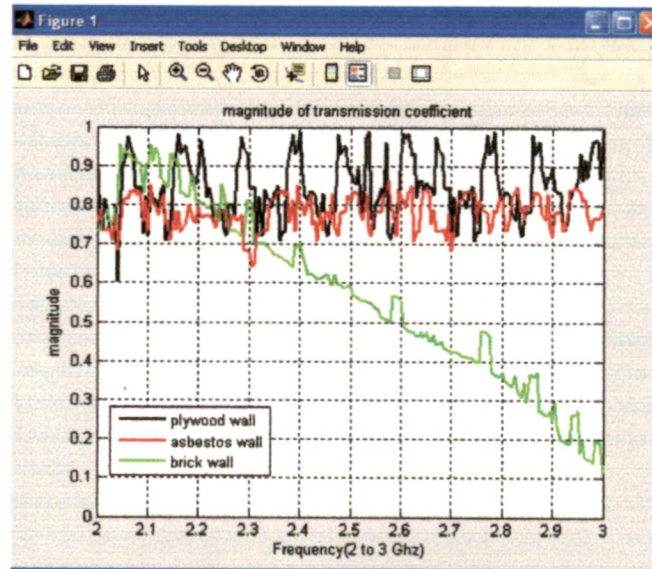


Figure 4.1: Transmission Coefficient; magnitude vs frequency

It has been observed that plywood wall has higher transmission coefficient and brick wall has lowest. Therefore brick wall provide the maximum attenuation and plywood wall provide the least attenuation.

a) Brick Wall (12×365.76×121.92 cm)

To calculate wall parameters for brick wall following steps have to be followed:

- i. As shown in step (i) of section 4.1 magnitude of transmission coefficient have to be calculated.
- ii. By using equations (3.16 to 3.18) real part of the dielectric constant has been calculated. Figure(4.2) showing variation of dielectric constant with frequency at distances 60 to 70 cm in the case of brick wall the dielectric constant is varying 4.2 to 6.5 and the mean value at 60cm, and 70cm is 5.34 and 5.50

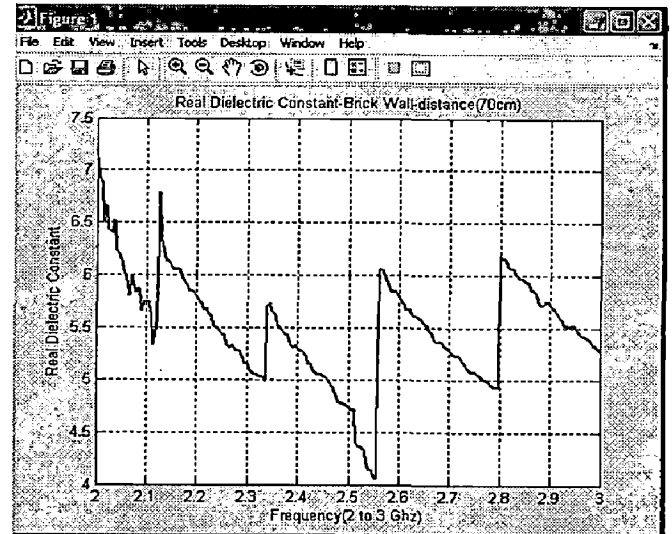
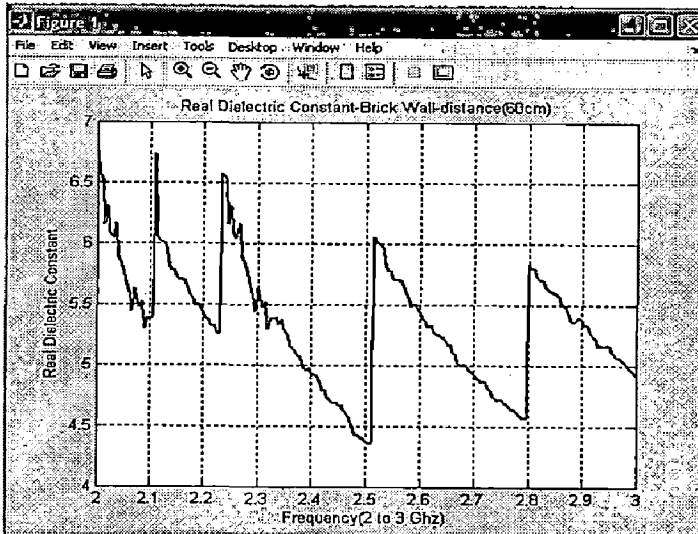


Figure 4.2: Variation of Dielectric Constant with frequency

Frequency(GHz)	Dielectric Constant	Frequency(GHz)	Dielectric Constant
2.0	6.756	2.0	7.116
2.1	5.38	2.1	5.74
2.2	5.432	2.2	5.792
2.3	5.631	2.3	5.156
2.4	4.933	2.4	5.293
2.5	4.376	2.5	4.732
2.6	5.432	2.6	5.792
2.7	4.926	2.7	5.286
2.8	5.826	2.8	6.186
2.9	5.372	2.9	5.732
3.0	34.918	3.0	5.278

Table 4.2: Variation of Dielectric Constant with frequency

- iii. Real part of dielectric constant, is required to calculate the speed of wave inside the wall so that a suitable velocity correction can be applied. Attenuation constant (α) can be calculated by using (3.19)

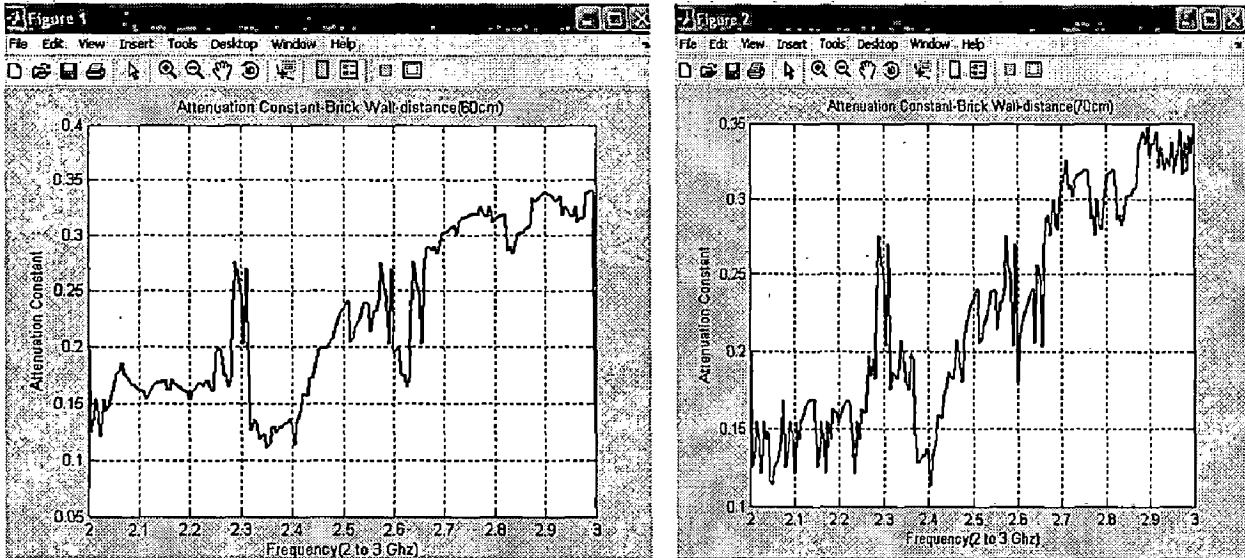


Figure 4.3: Variation of Attenuation Constant with frequency

- iv. Assuming conductivity of walls to be zero the loss tangent can be calculated using equations (3.20) to (3.21)

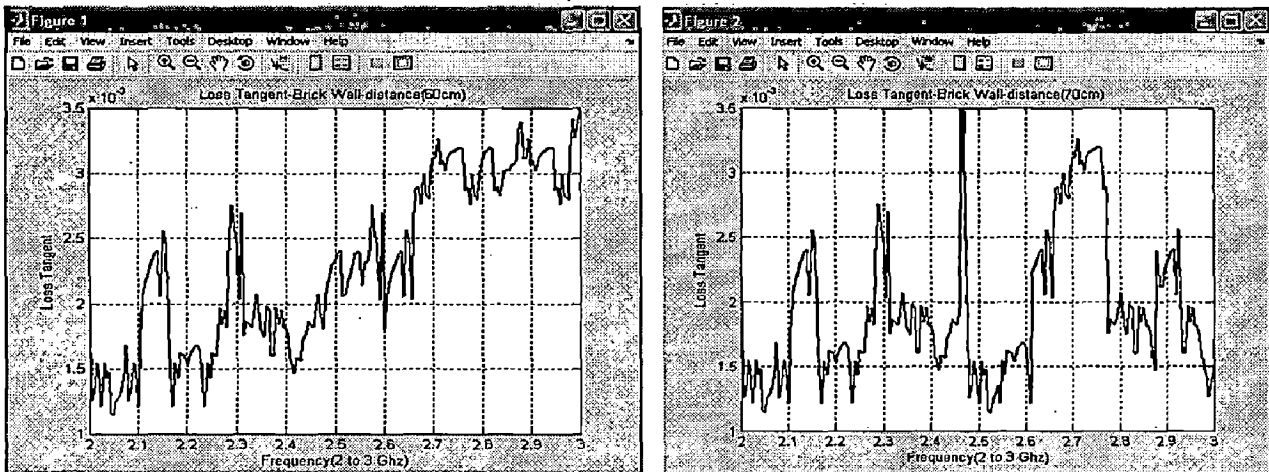


Figure 4.4: Variation of Loss Tangent with frequency

b) Ply wood Wall (0.012×184×123 cm)

The parameters for plywood wall have been calculated by using same equations as applied in section (a), results have been shown below:

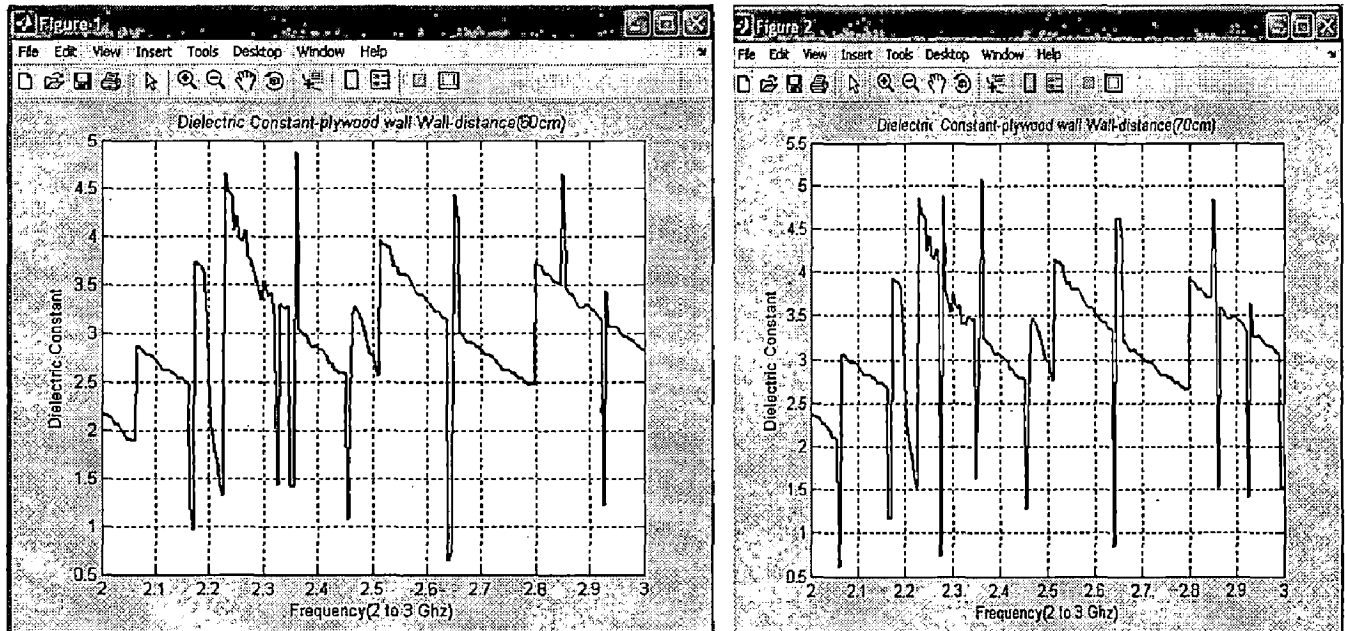


Figure 4.5: Variation of Dielectric Constant with frequency

Distance (60 cm)		Distance(70 cm)	
Frequency(GHz)	Dielectric Constant	Frequency(GHz)	Dielectric Constant
2.0	2.174	2.0	2.374
2.1	2.724	2.1	2.924
2.2	2.454	2.2	2.654
2.3	3.532	2.3	3.732
2.4	2.833	2.4	3.033
2.5	2.776	2.5	2.976
2.6	3.332	2.6	3.532
2.7	2.826	2.7	3.026
2.8	3.726	2.8	3.926
2.9	3.272	2.9	3.472
3.0	2.818	3.0	1.524

Table 4.3: Variation of Dielectric Constant with frequency

In the case of plywood wall we show the variation of dielectric constant with frequency. It is observed that dielectric constant of plywood wall is almost varying between 1 to 4.5. The mean value of dielectric constant at 60 and 70 cm is 2.95 and 3.146 respectively.

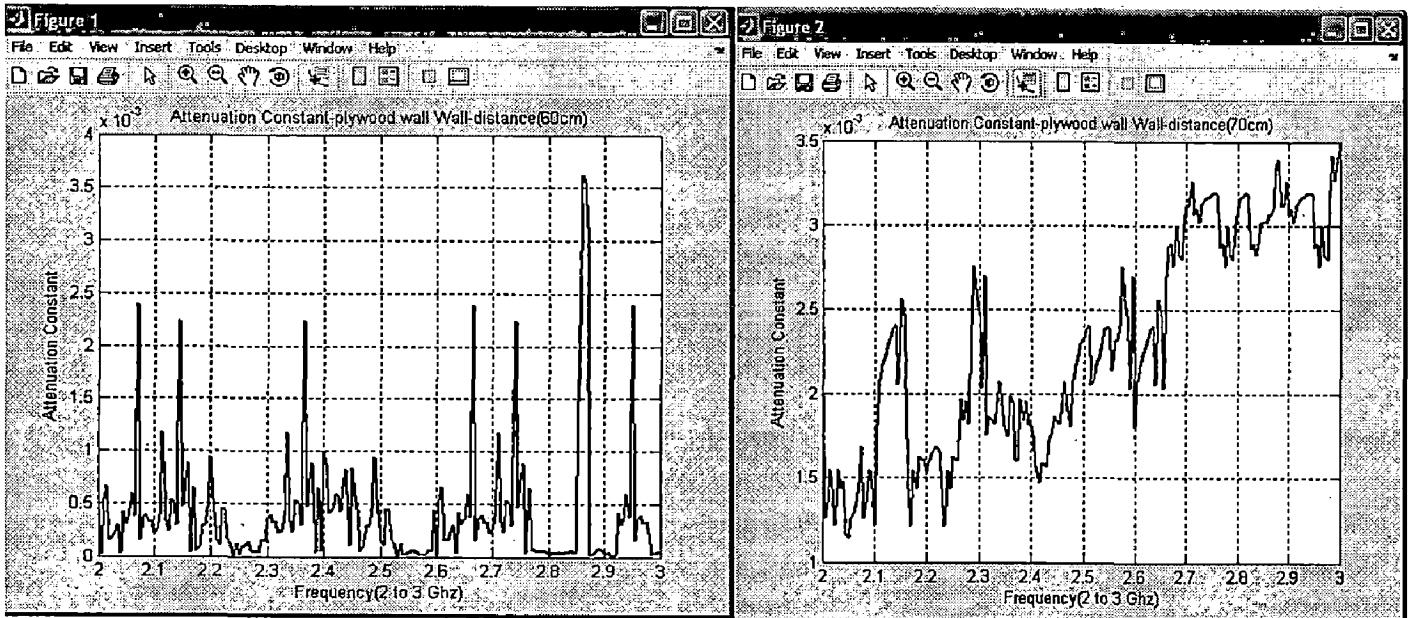


Figure 4.6: Variation of Attenuation Constant with frequency

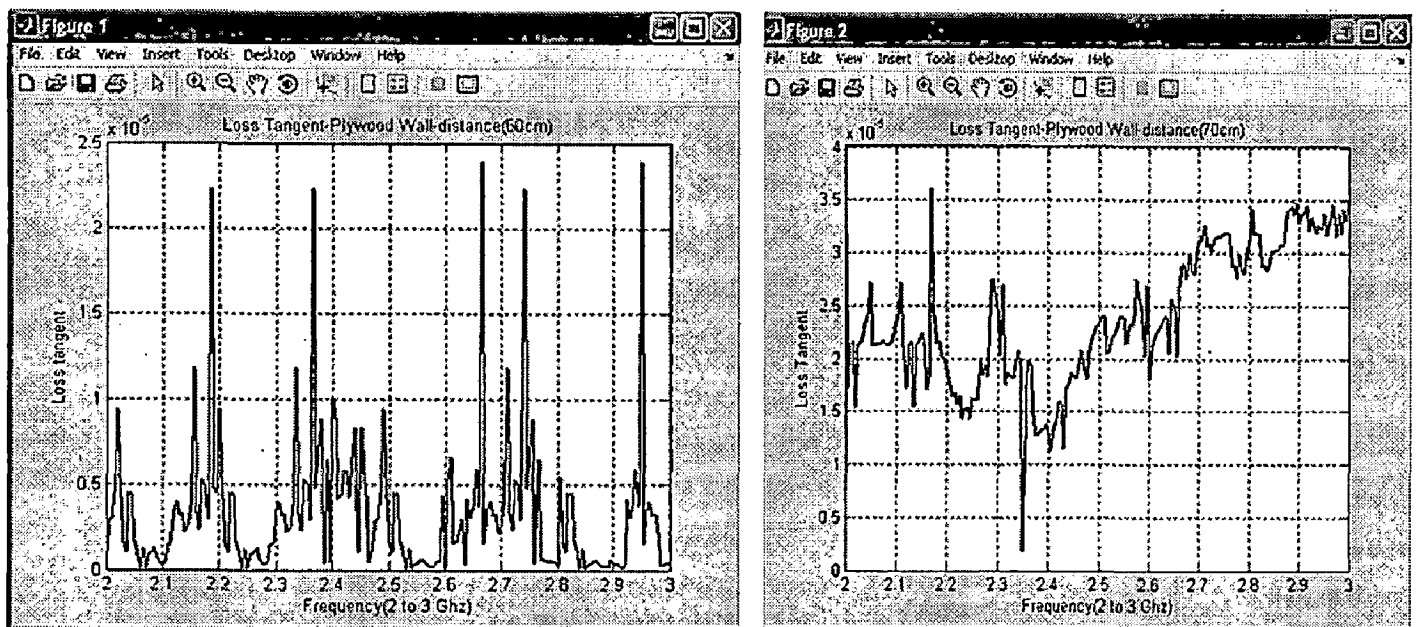


Figure 4.7: Variation of Loss Tangent with frequency

c) Asbestos Wall:

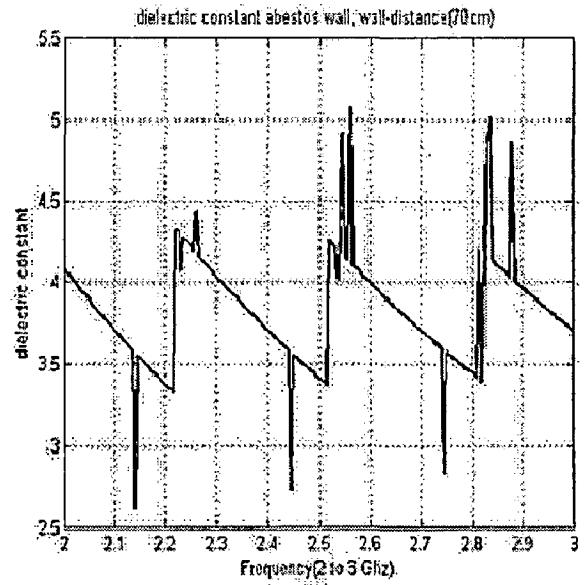
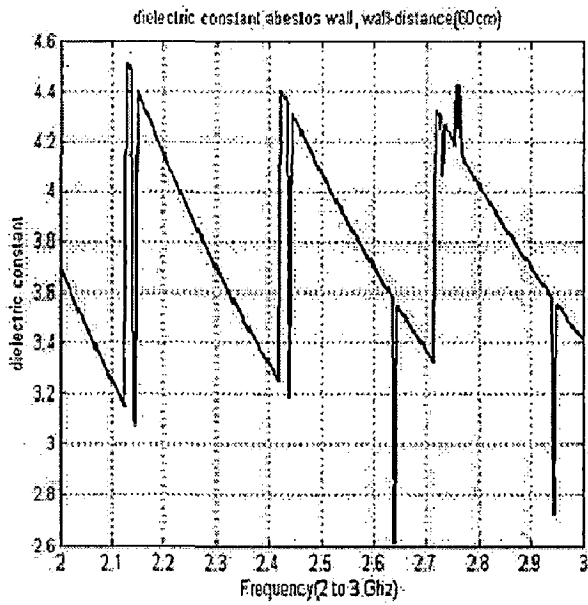


Figure 4.8: Variation of Dielectric Constant with frequency

Distance (60 cm)		Distance(70 cm)	
Frequency(GHz)	Dielectric Constant	Frequency(GHz)	Dielectric Constant
2.0	3.698	2.0	4.077
2.1	3.25	2.1	3.698
2.2	4.146	2.2	3.37
2.3	3.698	2.3	4.027
2.4	3.319	2.4	3.698
2.5	4.077	2.5	3.408
2.6	3.698	2.6	3.988
2.7	3.37	2.7	3.698
2.8	4.027	2.8	3.439
2.9	3.698	2.9	3.958
3.0	3.408	3.0	3.698

Table 4.4: Variation of Dielectric Constant with frequency

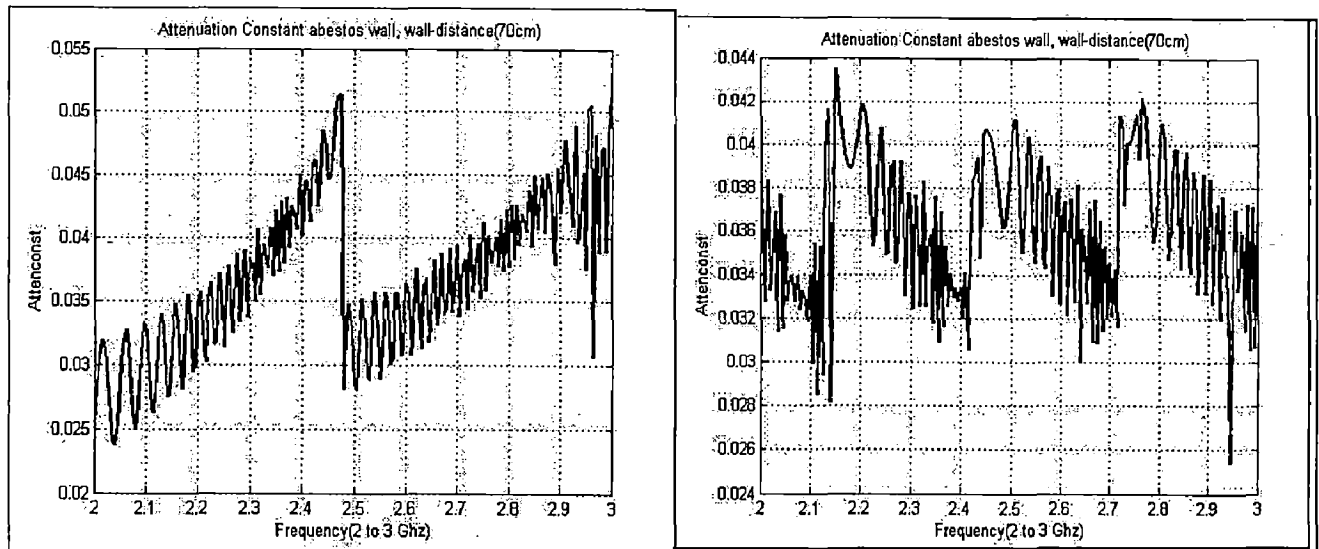


Figure 4.9: variation of Attenuation Constant with frequency

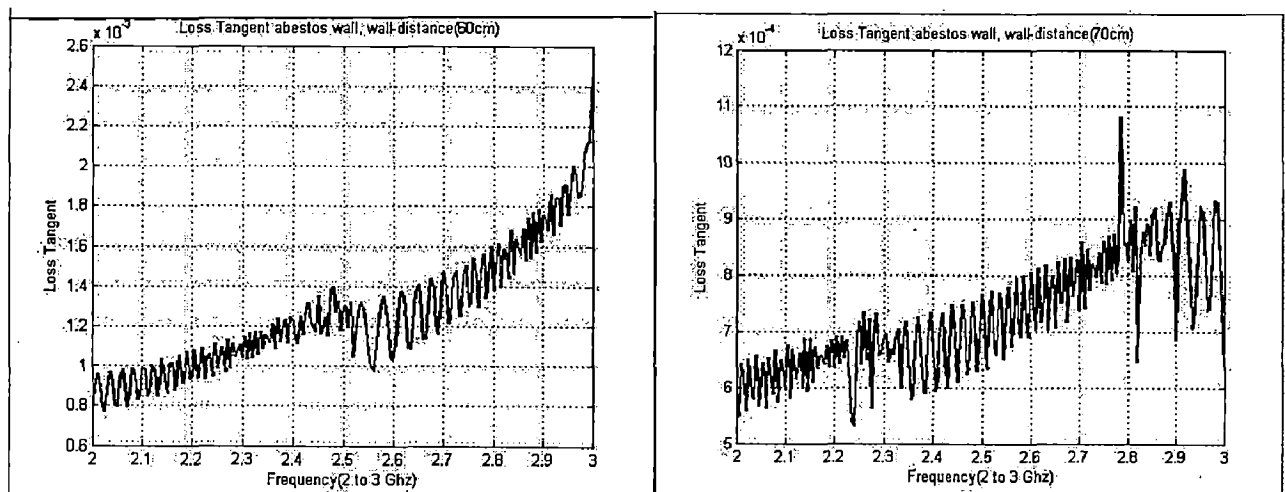


Figure 4.10: Variation of Loss tangent with frequency

4. 2 Reflection Method

a) Brick Wall

In the case of brick wall we keep our antenna at a distance of 75, 82.5, 90, 97.5, 105 and 112.5cm. The result has been shown at a distance of 90 cm from the wall. The system parameters is shown in table (4.4)

Vector Network Analyzer	R&S ZVL	1 GHz – 3GHz
Antenna	Double-ridged waveguide type (HF 906)	1-18 GHz
VNA Power		20 dBm
Range resolution		7.5 cm
Azimuth resolution		14.9 cm
Cable Loss		1-1.5 dB
Unambiguous range (4001 point)		300 m
Unambiguous range(201point)		15 m
Antenna-air reflection		0.225 m

Table 4.5: System parameter

For the calculation of wall parameters following steps have to be followed:

- i. Generate A-scan range profile for wall and metal. The data collected by the VNA is in the frequency domain at frequency points f_n which is converted to the time domain by inverse fast Fourier transform (IFFT). Mathematically,(see appendix I for detail description of algorithm), results have been shown in figure (4.11) and (4.12).

In fig two peaks have been displayed that is correspond to air wall reflection and wall air reflection. Multiple reflections inside the wall have been neglected.

The delay produce by antenna is 22.5 cm (see appendix I) so first wall air reflection will be shown at a distance of 105 cm.

- ii. Separate wall first and second reflections wall first reflection will be the same as metal, wall- air reflection can be separated by using equation (3.31). By these reflections width of the wall can be calculated.

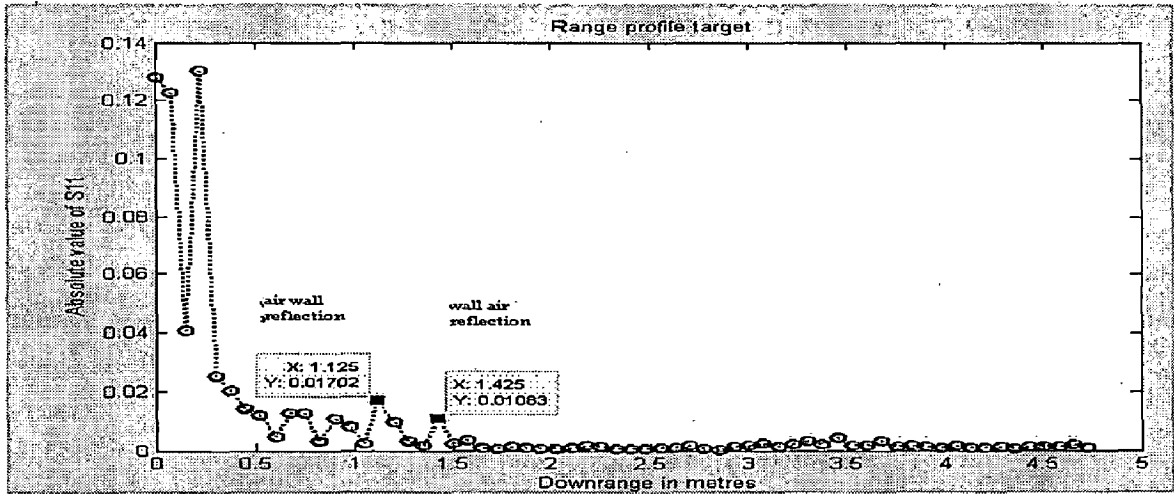


Figure 4.11: Range profile of wall (clearly showing the reflections)

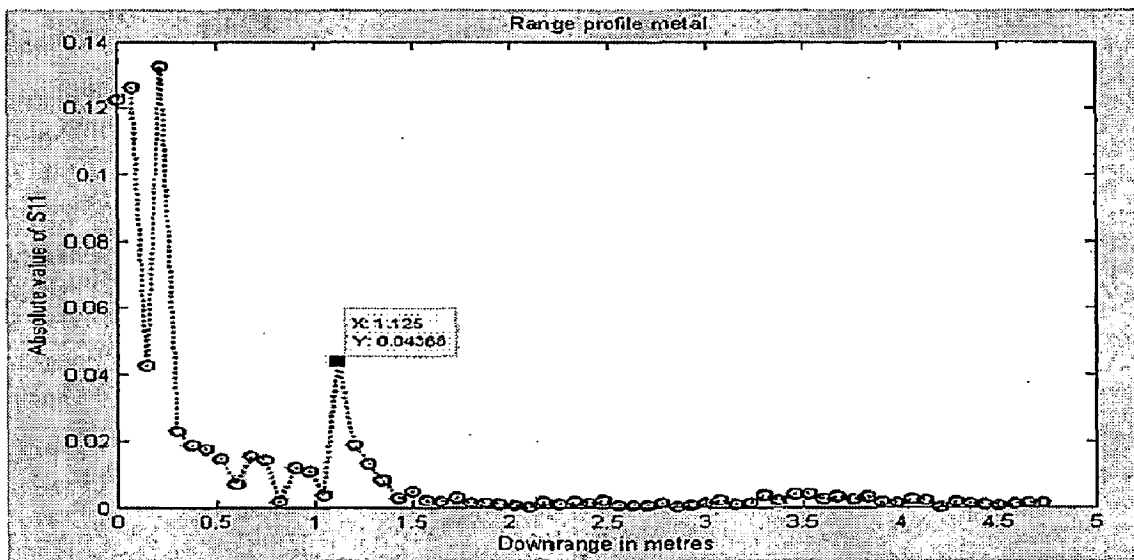


Figure 4.12: Range profile of metal (peak due to metal)

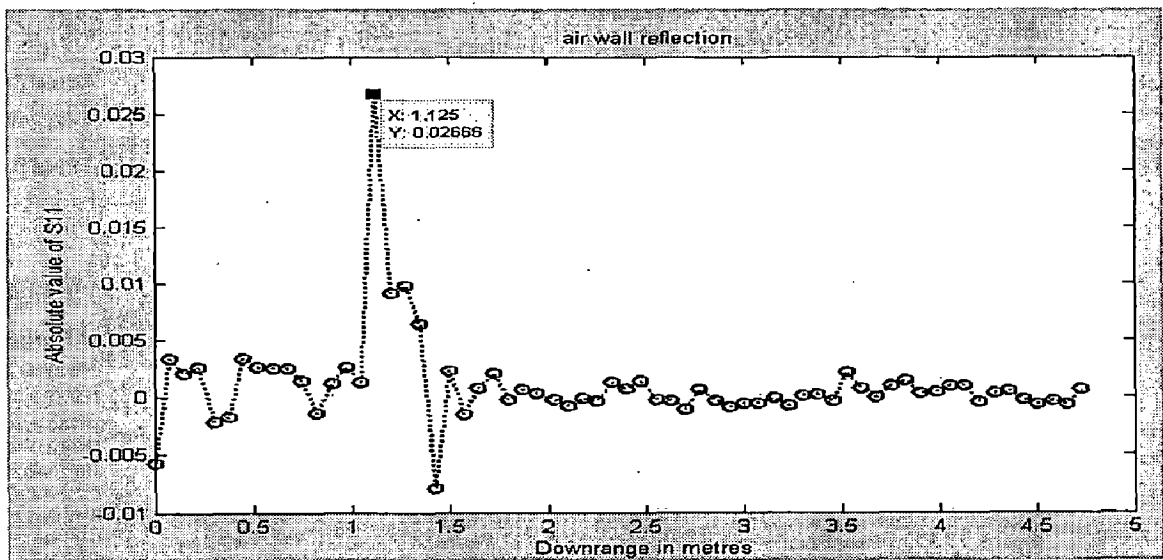


Figure 4.13: Reflection at air wall interface clear view

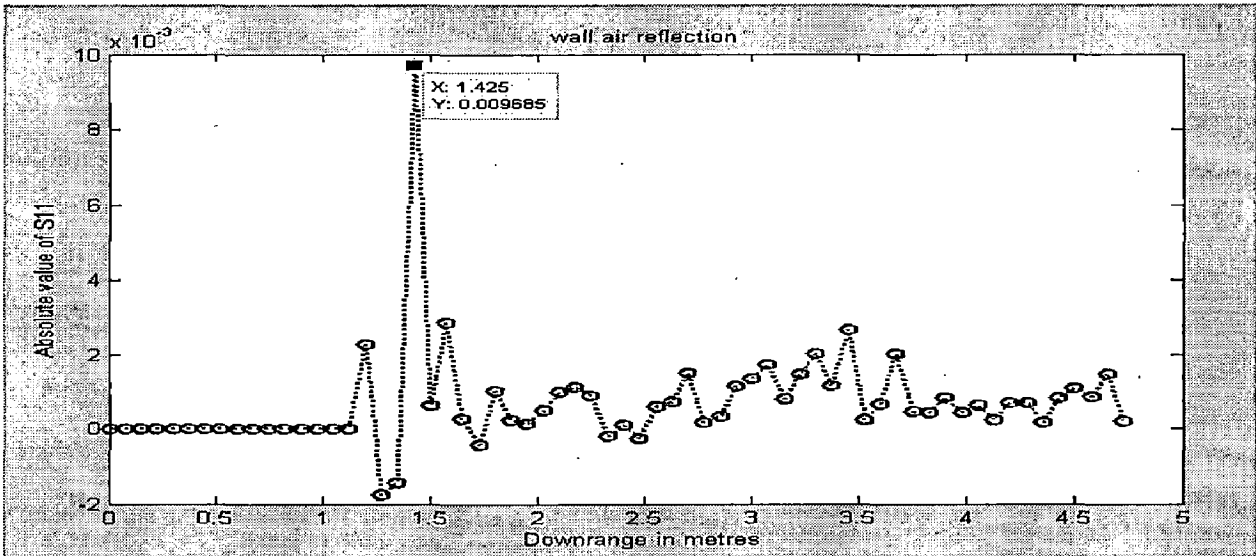


Figure 4.14: Reflection at wall air interface clear view

The peaks are due to reflection air-wall interface and at the wall-air interface. The distance between these two peaks to the square root of dielectric constant of the wall calculate width of the wall.

- iii. By using equation (3.28) reflection coefficient for wall calculated, then applying it to the equation (3.29) dielectric constant has been obtained.

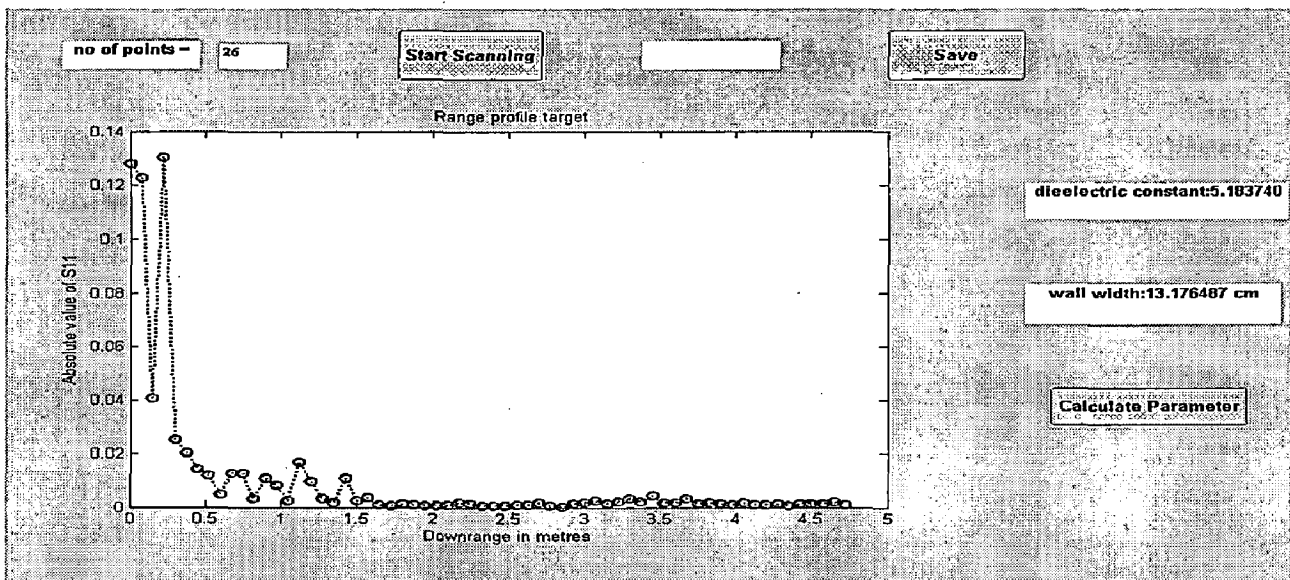


Figure 4.15: Calculation of parameter

Distance(cm)	Dielectric Constant
75	5.47
82.5	5.14
90	5.18
97.5	4.31
105	5.36
112.5	4.353

Table 4.6: Dielectric constant with distance

b) Plywood Wall

In the arrangement of plywood wall (184×123 cm) of 12mm of width. The range resolution of antenna is 7.5cm so we cannot calculate the width of the wall for calculation of width we put a large metal (150×120 cm) sheet at a distance of 40cm from the wall and calculate the distance between the wall. Calculation has been done at a distance of 75cm, 82.5cm, 90cm, 97.5cm, 105cm, and 112.5cm. The result has been shown at a distance of 105cm. For calculation of parameters steps are same as use in the case of brick wall.

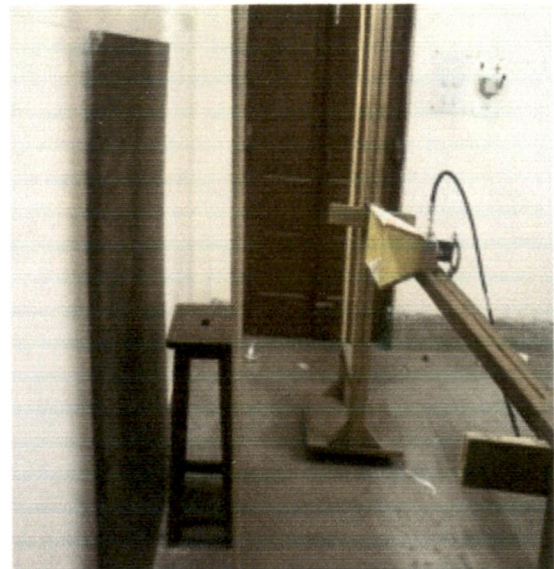
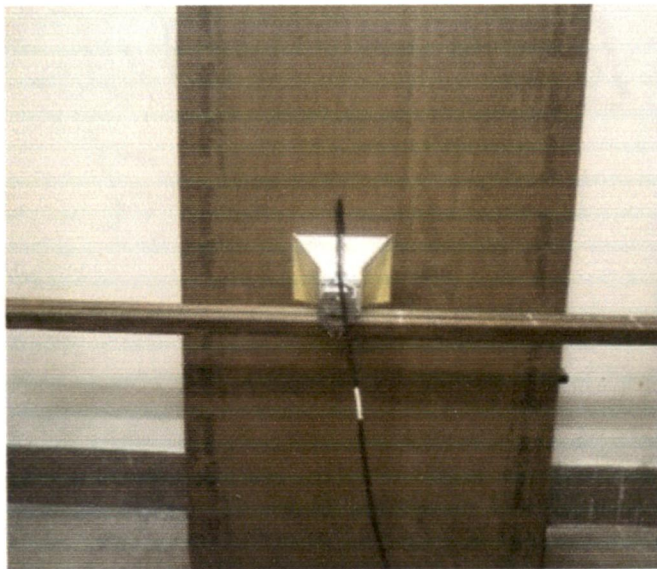


Figure 4.16: Experimental set up (front and side view)

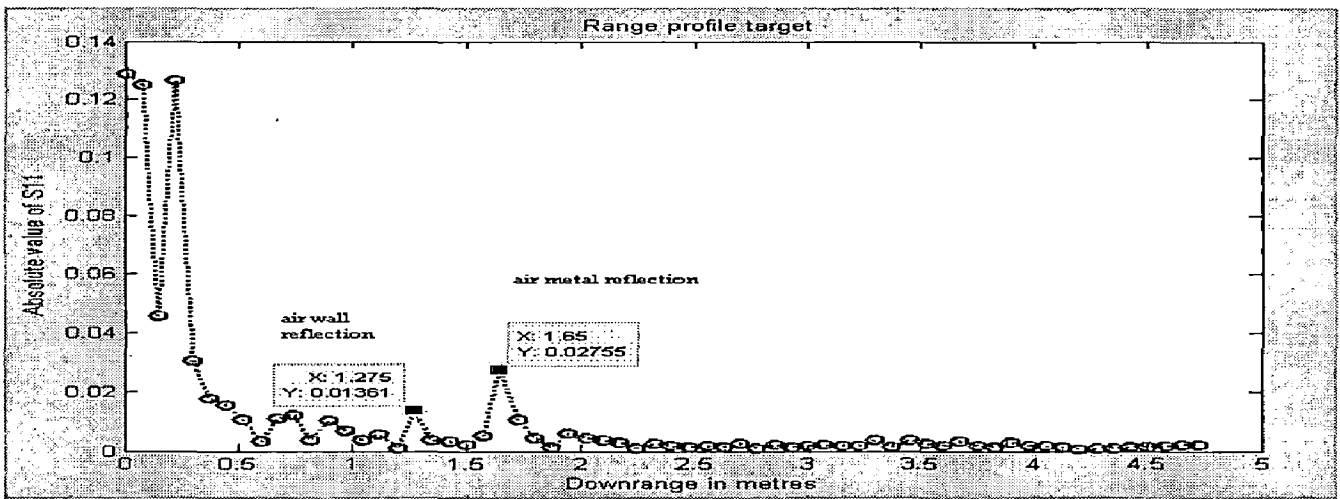


Figure 4.17: Range profile of plywood wall(clearly showing the reflections)

It is visible that first wall air reflection is at 127.5cm and air metal reflection is at 165cm.

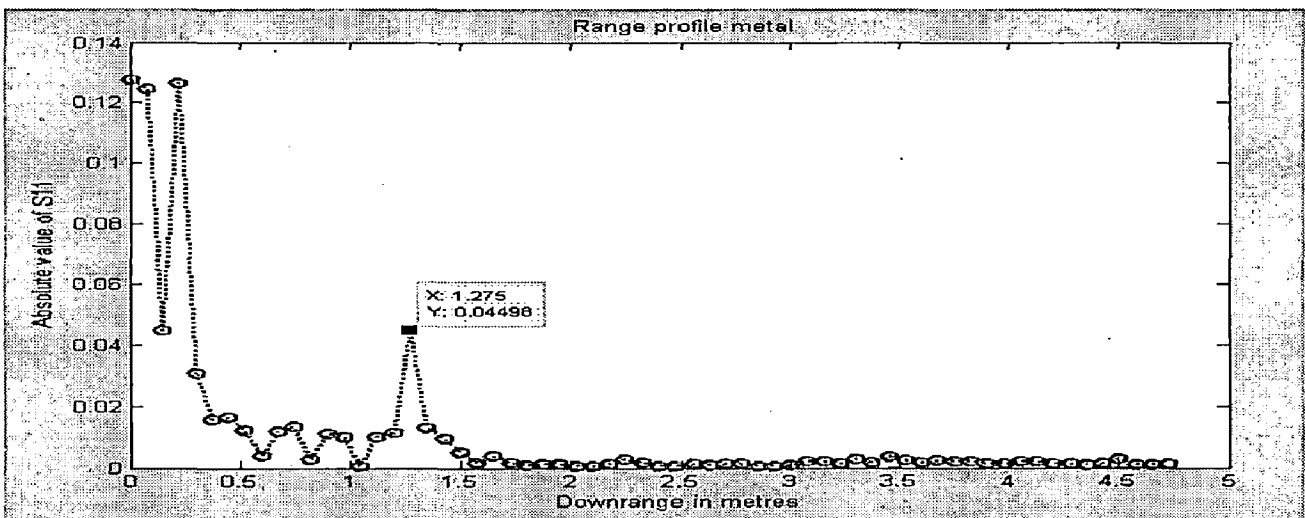


Figure 4.18: Range profile of metal (peak due to metal)

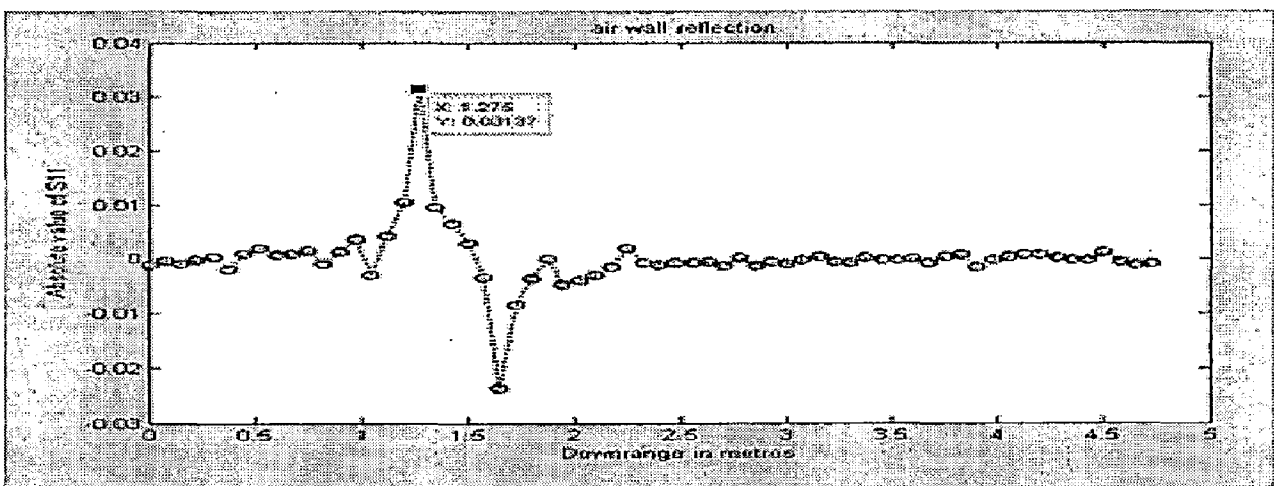


Figure 4.19: Reflection at air wall interface clear view

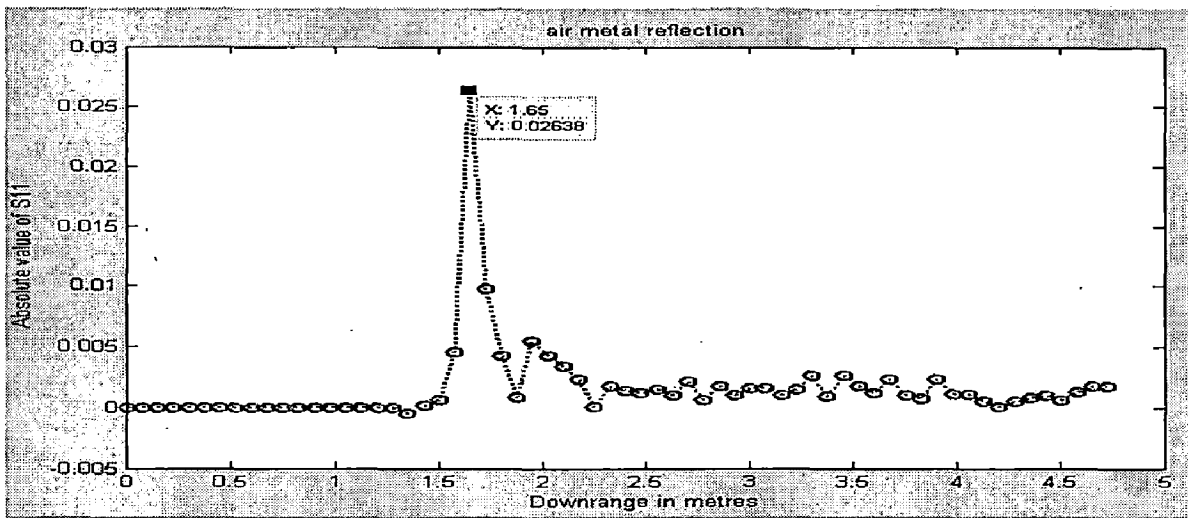


Figure 4.20: Reflection at air metal interface clear view

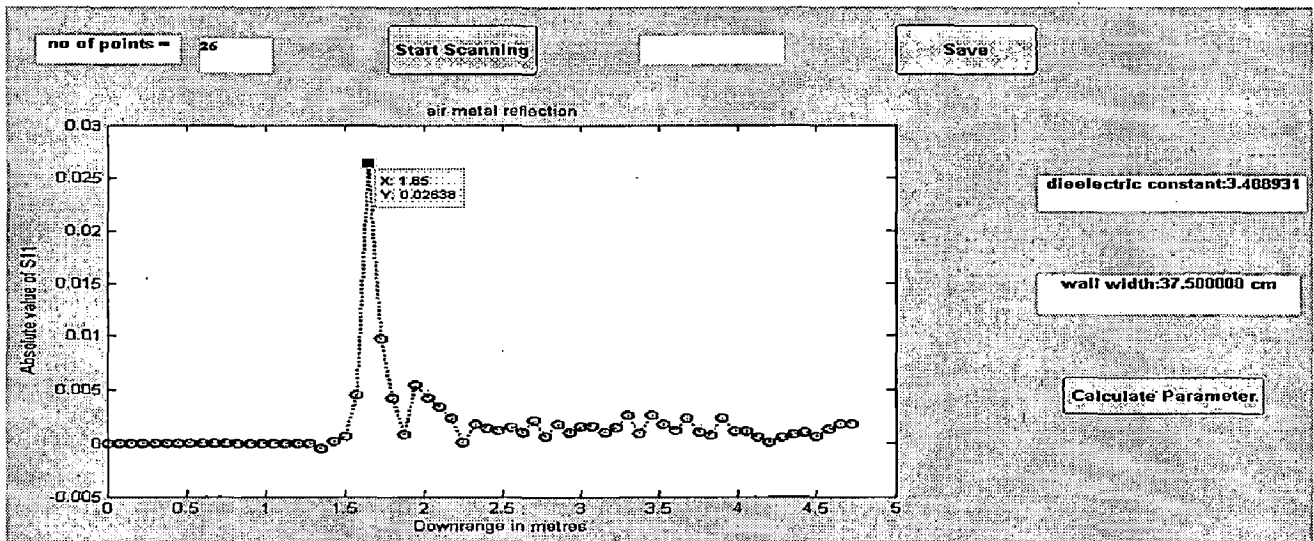


Figure 4.21: Calculation of parameter

In fig 5.17 it is shown that the dielectric constant is 3.488 and distance between wall and metal is around 37.5cm where the actual distance is 40 cm.

Distance (cm)	Dielectric Constant
75	2.7
82.5	2.5
90	3.5
105	3.448
112.5	3.29

Table 4.7: Dielectric constant with distance

c) Asbestos Wall

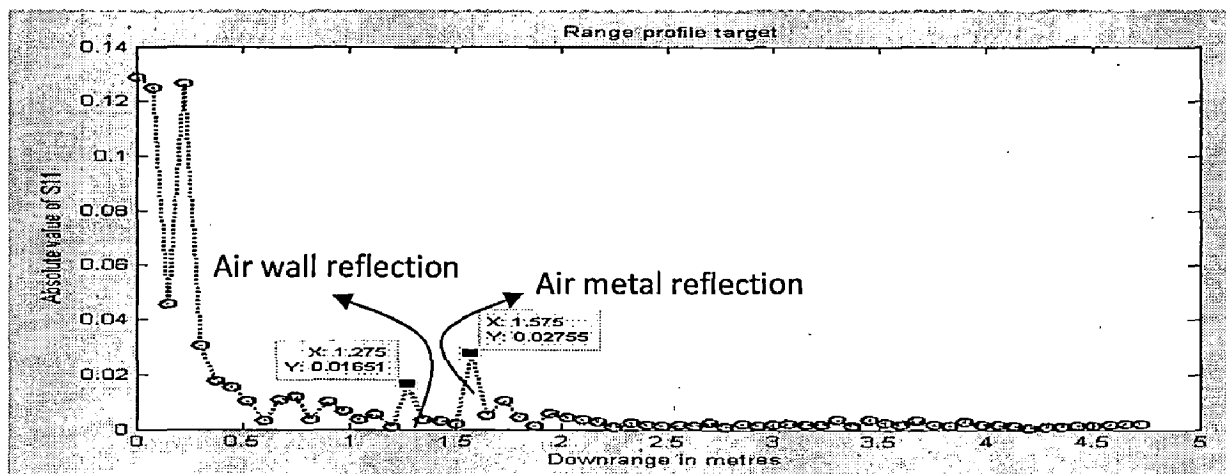


Figure 4.22: Range profile of Asbestos wall (clearly showing the reflections)

It is visible that first wall air reflection is at 127.5cm and air metal reflection is at 157.5cm

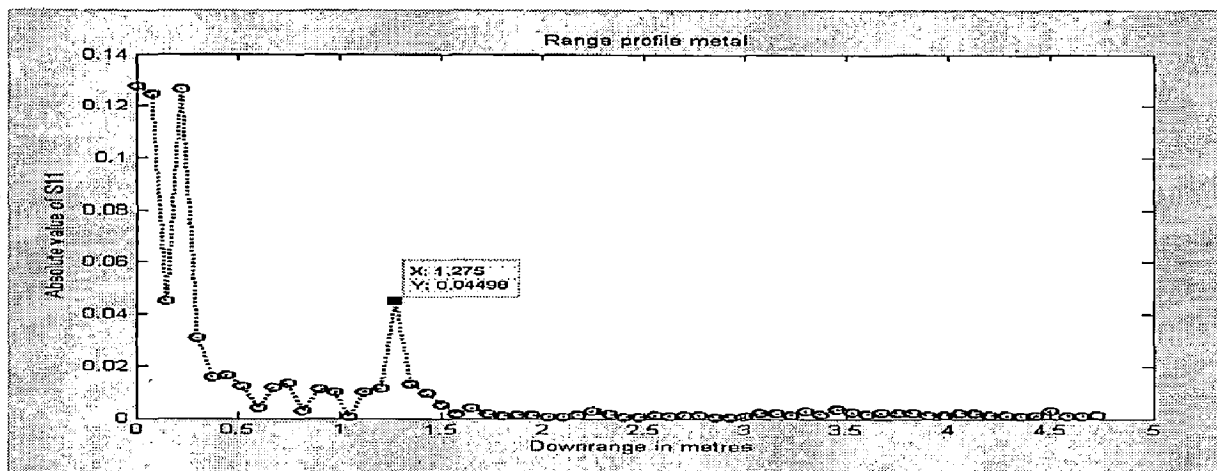


Figure 4.23: Range profile of metal (peak due to metal)

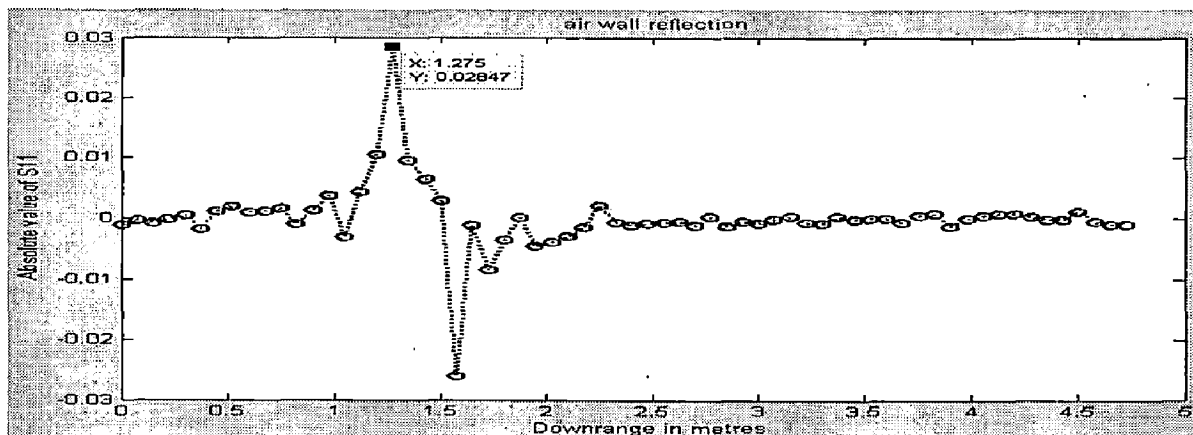


Figure 4.24: Reflection at air wall interface clear view

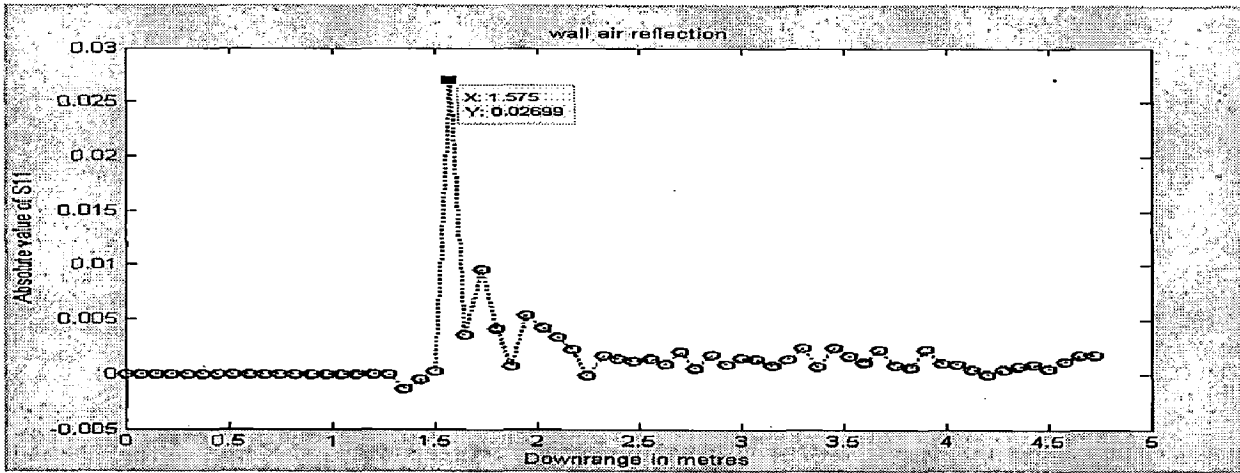


Figure 4.25: Reflection at air metal interface clear view

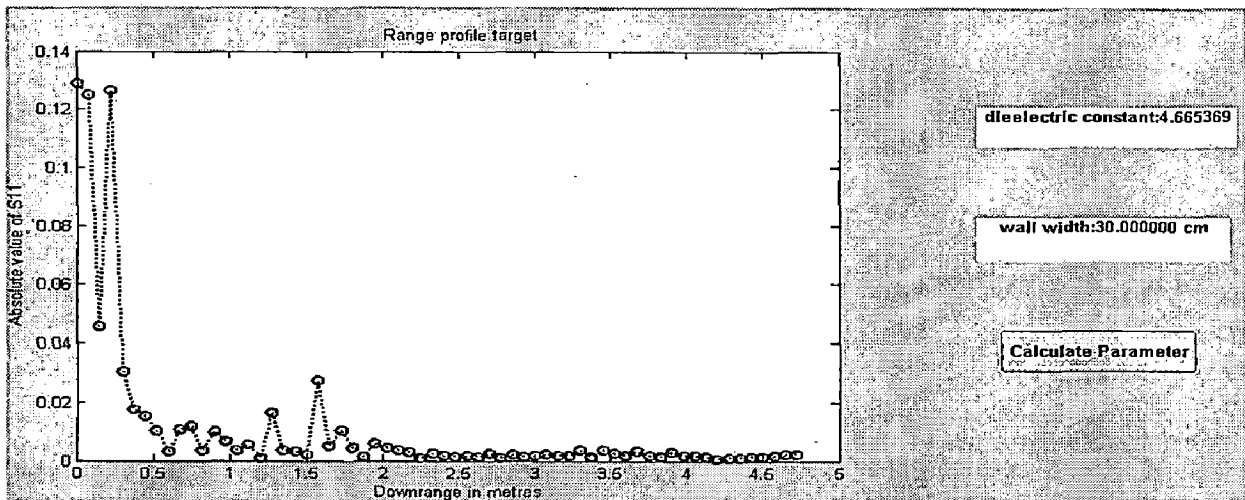


Figure 4.26: Calculation of parameter

In fig 5.17 it is shown that the dielectric constant is 3.488 and distance between wall and metal is around 37.5cm where the actual distance is 40 cm.

Distance (cm)	Dielectric Constant
75	2.7
82.5	2.5
90	3.5
105	3.448
112.5	3.29

Table 4.8: Dielectric constant with distance

4.3 Imaging: Beam forming

Beam forming image has been developed by keeping the different types by target behind the wall. By this imaging the effect of wall parameters can be show and parameters error can be reduce by focusing technique.

A metal target has been kept at a distance of 50 cm behind the brick wall of width about to 12.5cm. Data has been taken in frequency range by using Vector Network Analyzer (VNA) ZVL3 over the frequency range of 1-3 GHz at 201 frequency points by using R&S HF 906 double ridge horn antenna working in mono-static mode. The distance between antenna and wall is 41 cm. VNA output power has been set to 20dBm. A laptop is used which is connected to the Vector Network Analyzer (VNA) using a LAN connection. The PC is important for real time implementation. The software used for calculation is Math-works MATLAB. For proper C-scan imaging data has been taken at 20 points in down range and 30 points in cross range direction. The B-Scan image has been shown in figure (4.27) at different wall parameters.

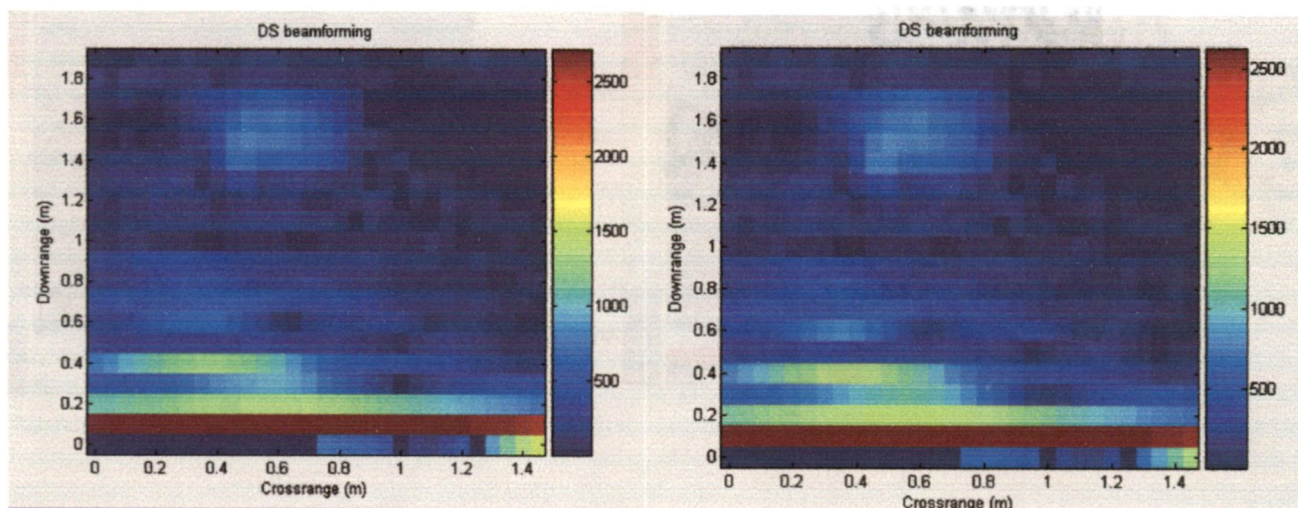
Vector Network Analyzer	R&S ZVL	1 GHz – 3GHz
Antenna	Double-ridged waveguide type (HF 906)	1-18 GHz
VNA Power		20 dBm
Range resolution		7.5 cm
Azimuth resolution		14.9 cm
Cable Loss		1-1.5 dB
Unambiguous range (4001 point)		300 m
Unambiguous range(201point)		15 m
Antenna-air reflection		0.225 m

Table 4.9: System Parameters

For the purpose of image formation following steps have to be followed:

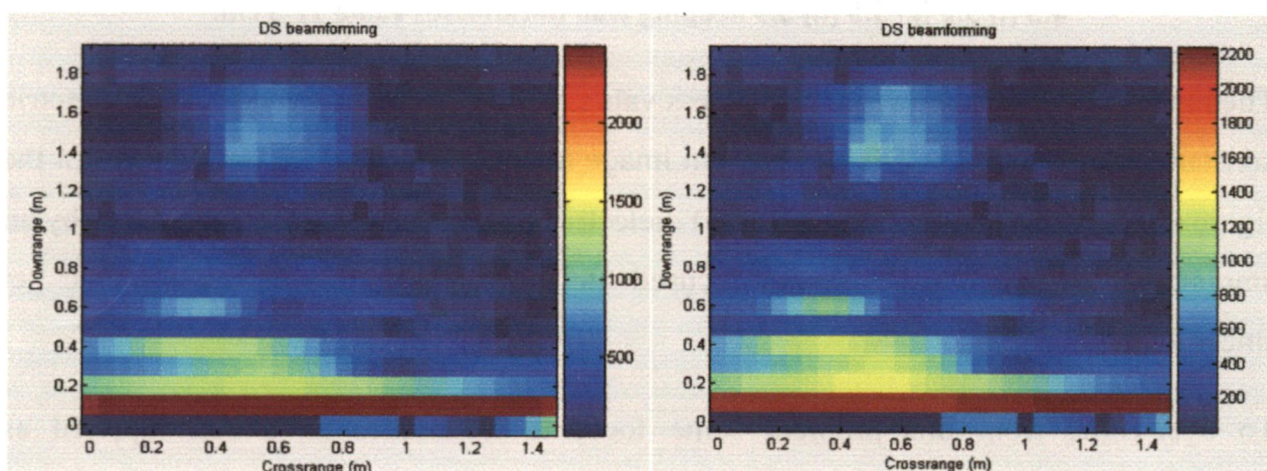
- i. Divide whole region into small pixel and for each pixel calculate reflection and refraction angle for the incident wave by solving equations (3.32) and (3.33).
- ii. For each pixel, synchronize the outputs of the M receiver to gain the corresponding signal by using equation (3.37).
- iii. Generate the composite image of the region.
- iv. Tune the wall parameters and then follow step i to iii for N number of times.

The results have been shown by keeping thickness constant and varying dielectric and by keeping dielectric constant and varying frequency.



(a)

(b)



(c)

(d)

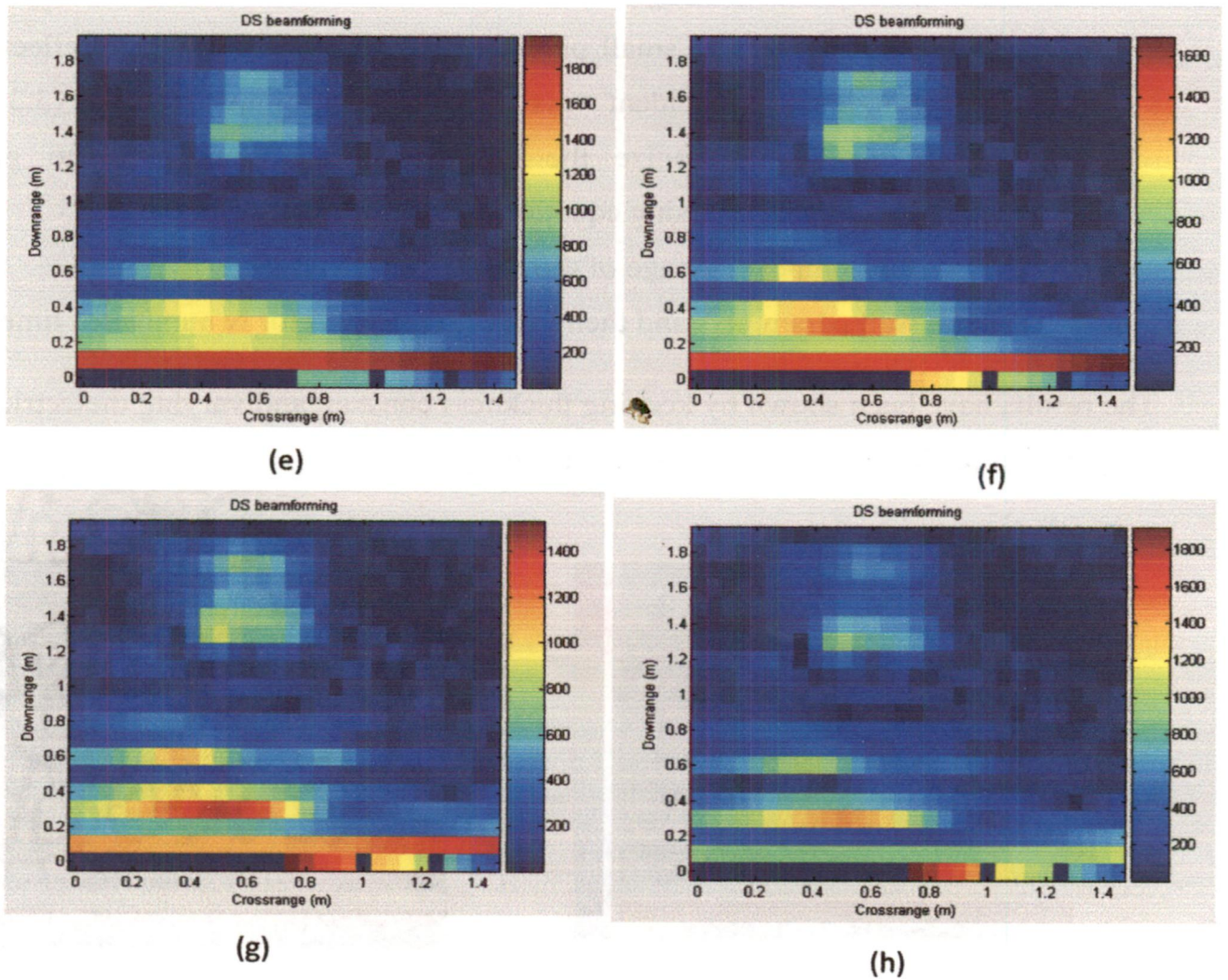


Figure 4.27: Beam forming image at different dielectric value (a) 3.9 (b) 4.1 (c) 4.3 (d) 4.6 (e) 4.9 (f) 5.2 (g) 5.5 (h) 5.9 keeping wall thicknesses value 12.5 cm.

The results have been shown at a thickness value of 12.5 cm and by varying the dielectric constant from 3.9 to 5.5. The variation in image intensity values have been shown in the figure (4.27) as shown in equation (3.45) dielectric error change the focusing delay by an amount and all the signals cannot be focused on the same point. Because of it, the image gets smeared and blurred.

To overcome this problem, some focusing techniques have been applied as discussed in chapter 3.4.5, and the results have been shown in section 4.4.

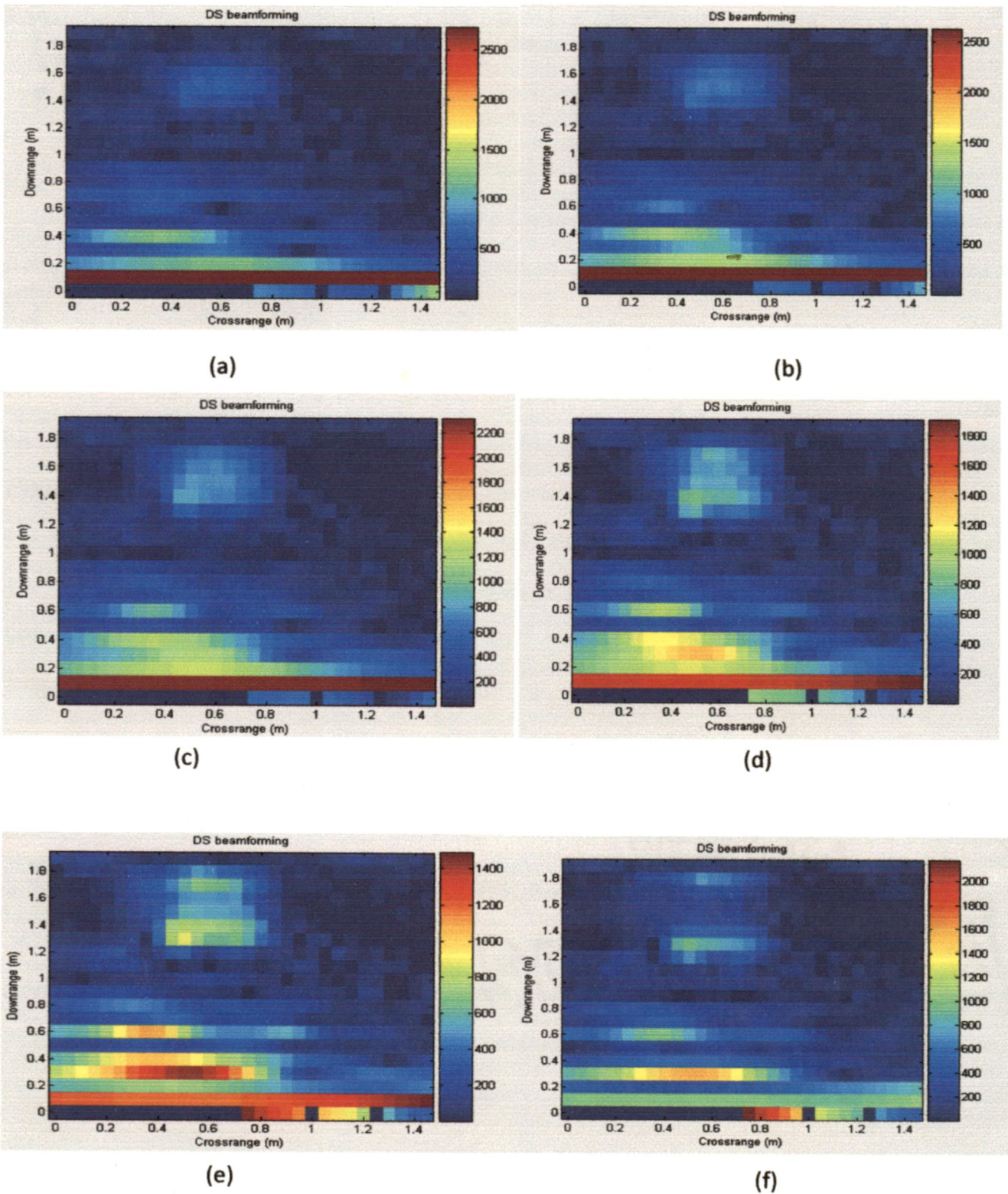


Figure 4.28: Beam forming image at different wall thickness value (a) 8.5 (b) 9.5 (c) 10.5 (d) 11.5 (e) 12.5 (f) 13.5 (g) 14.5 cm, keeping dielectric constant value constant 5.2 .

The results have been shown at a dielectric value of 5.2 cm and by varying the thickness from 8.5 to 14.5 cm. The variation in image intensity values have been shown in the

figure (4.28) as shown in equation (3.44) thickness error change the focusing delay by an amount and all the signals cannot focused on same point. Because of it image get smeared and blurred, and target shift from its true location.

4.4 Auto focusing Approach

In processing of developing beamforming image, If the wall parameters are known exactly, the focusing delay cancels the propagation delay (refer equation 3.38) and then $x_q = x_p$ (see figure 3.11) and all receive pulse align and add together to produce a coherently combine output, it means that all the receive signal focus on a single point then output image intensity of the beam former is maximize. But in real time situation wall parameters are not known and it has to be calculated and these parameters have to be used for computing the focusing delay. By result of it, distorted image has been obtained because of ambiguous wall parameters. To get high quality of image and nullify the effect of wall ambiguities autofocusing approach has to be used. By using image quality indices parameters, image quality estimation has been done. The steps to obtain high quality image has been followed:

- i. Develop 2-D beam forming image.
- ii. Estimate image quality using quality indices value, and make a visual plot for it.
- iii. Change wall parameters.
- iv. Repeat steps from i to iii, till focused image has not developed.
- v. Develop a statical model for quality indices having wall parameters as an input.

The equation developed at step (v) shows its maximum value at correct parameters, so by solving this equations, accurate wall parameters can be obtain.

For the process of it first look up technique has been applied and wall parameters have been obtain at maximum indices value, then develop a statical model for image quality indices and by solving it, parameters have been obtained. Results for both techniques have been shown in later sections.

- Calculation of Wall Thickness Value When Dielectric value is known

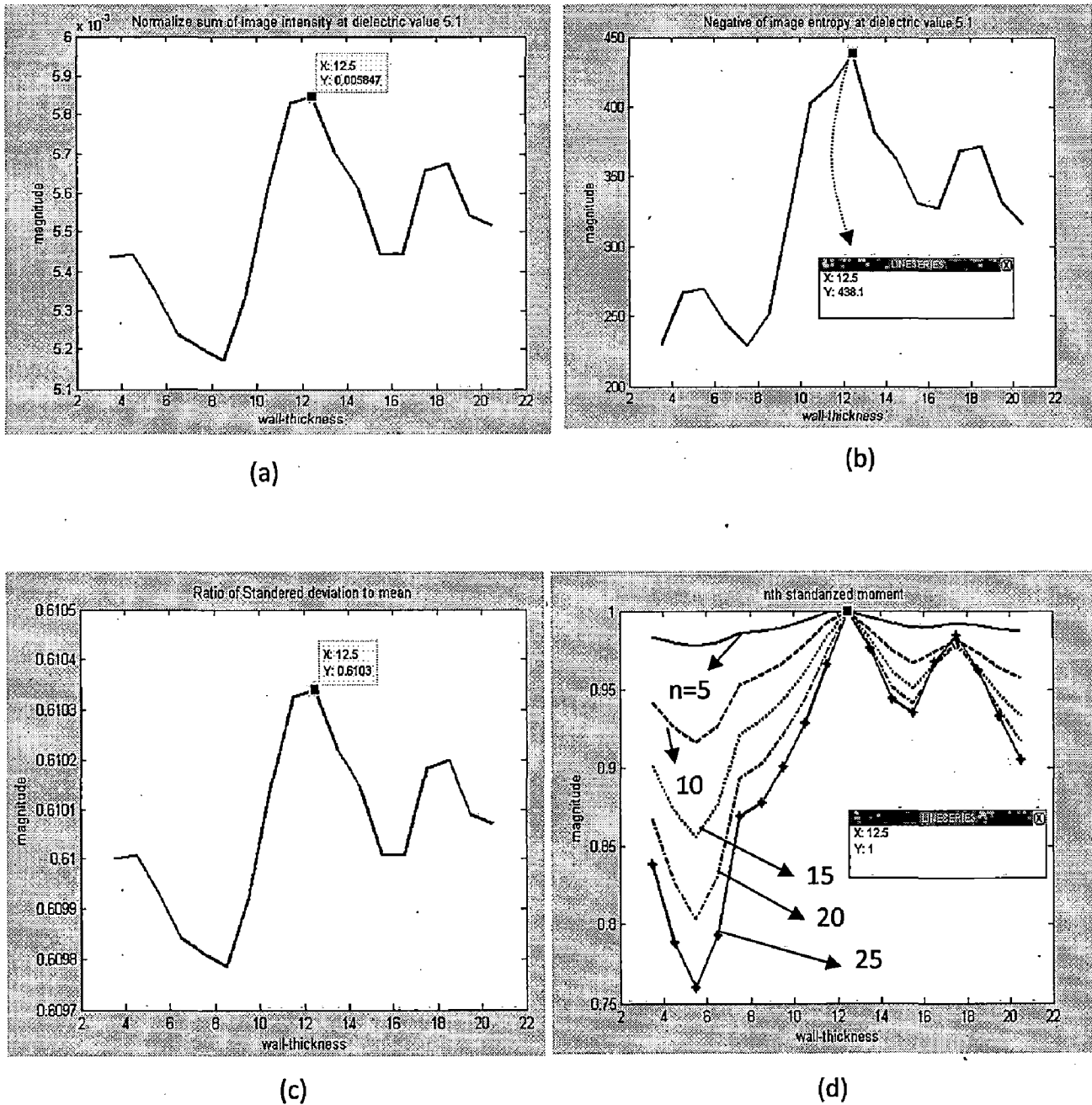


Figure 4.29: Plot of quality indices values (a) normalize sum of image intensity (b) Negative of image entropy (c) Ratio of Standard deviation to mean (d) Standardized moment at different values of n.

Quality indices parameters have been calculated at constant dielectric value of 5.1 and thickness have been changed from 3.5 cm to 20.5 cm. From the figure (4.29) it is clear that the value of quality indices is maximum at wall thickness 12.5 cm. So we can take it as an accurate wall thickness. So pair (5.1, 12.5 cm) can be assuming as a wall parameters by using lookup method.

- Calculation of dielectric at constant thickness

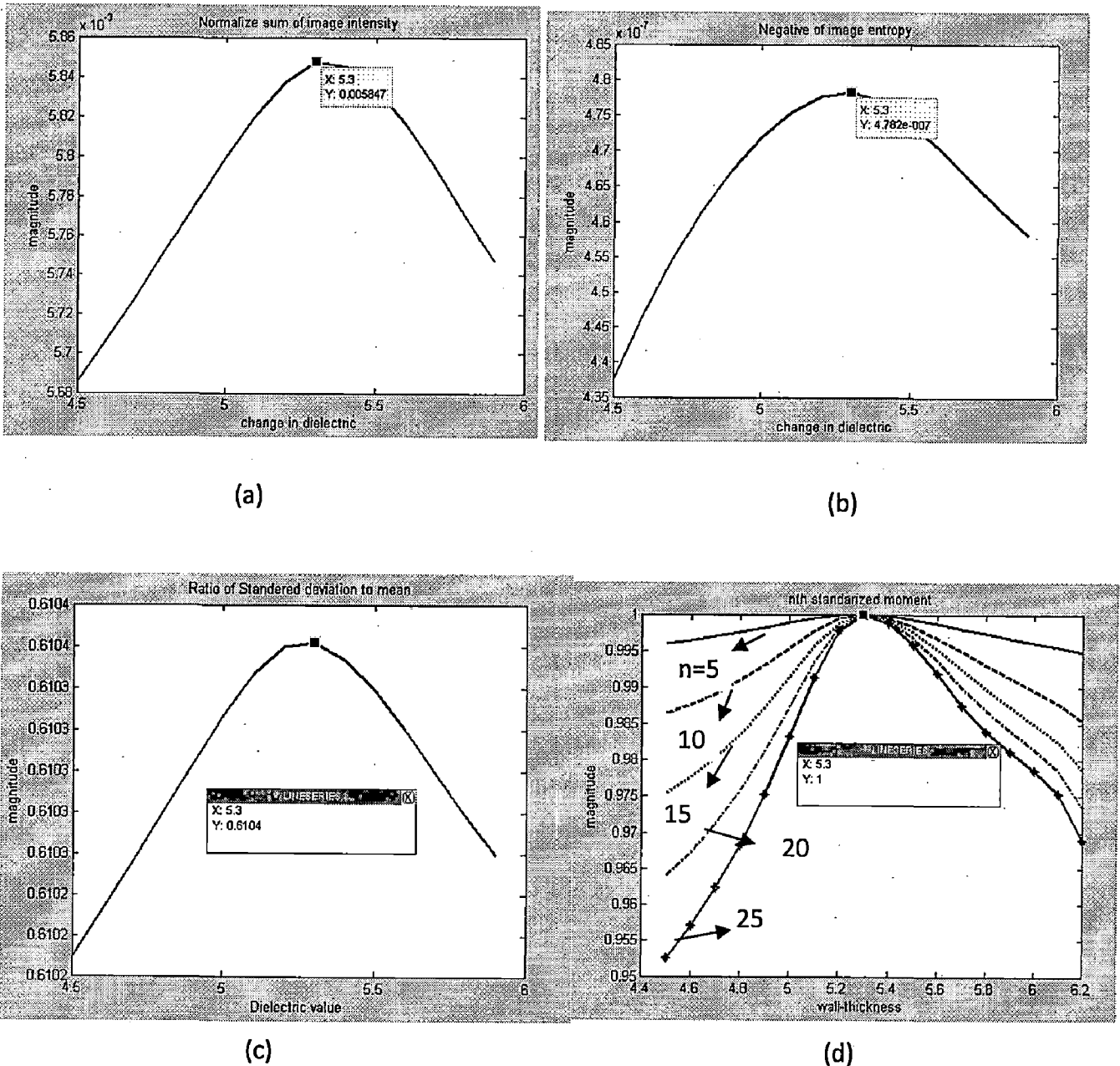


Figure 4.30: Plot of quality indices values (a) normalize sum of image intensity (b) Negative of image entropy (c) Ratio of Standard deviation to mean (d) Standardized moment at different values of n.

Quality indices parameters have been calculated at constant thickness value of 12.0 cm and thickness have been changed from 4.5 to 5.9 cm. From the figure (4.30) it is clear that the value of quality indices is maximum at wall dielectric 5.3. So we can take it as an accurate wall thickness. So pair (5.3, 12.0 cm) can be assuming as a wall parameters by using lookup method.

So we have seen from figure (4.29) to (4.30) as we change parameters, maximum values of the indices have been changed, and so for successfully applying this techniques one parameter should be exactly known.

- When Thickness and Dielectric Both are Unknown

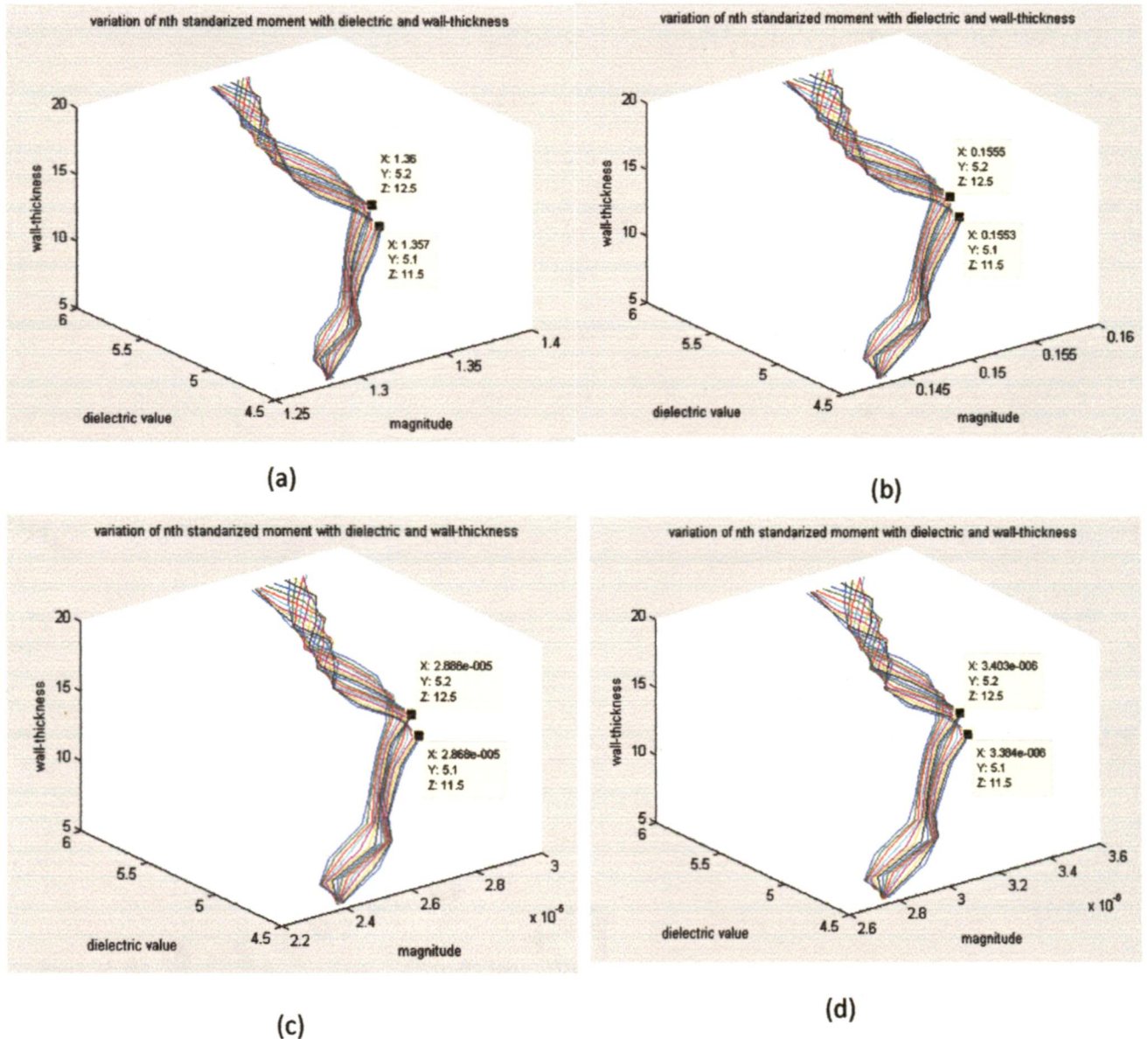


Figure 4.31: nth standardized moment for unknown dielectric and thickness value where n is equal to (a) 5 (b) 10 (c) 15 (d) 20.

As discussed earlier, for the higher value of n as we changes the wall parameters from its true value, there is sharpen change in moment will be observed, and it can be easily use for the multiple wall/ inhomogeneous wall case where optimum parameters can be obtained by using standard moment. So the value of standardized moment has been

calculate for different values of n by changing the thickness values from 5 to 20 cm and dielectric values form 4.5 to 6. As shown in the figure (4.31) the standardized moment shows its maximum value for dielectric, 5.1 and 5.2, and at a thickness value 11.5 cm and 12.5 cm. So by calculating quality indices at these values we may obtain more accurate solutions.

- At dielectric Value 5.1

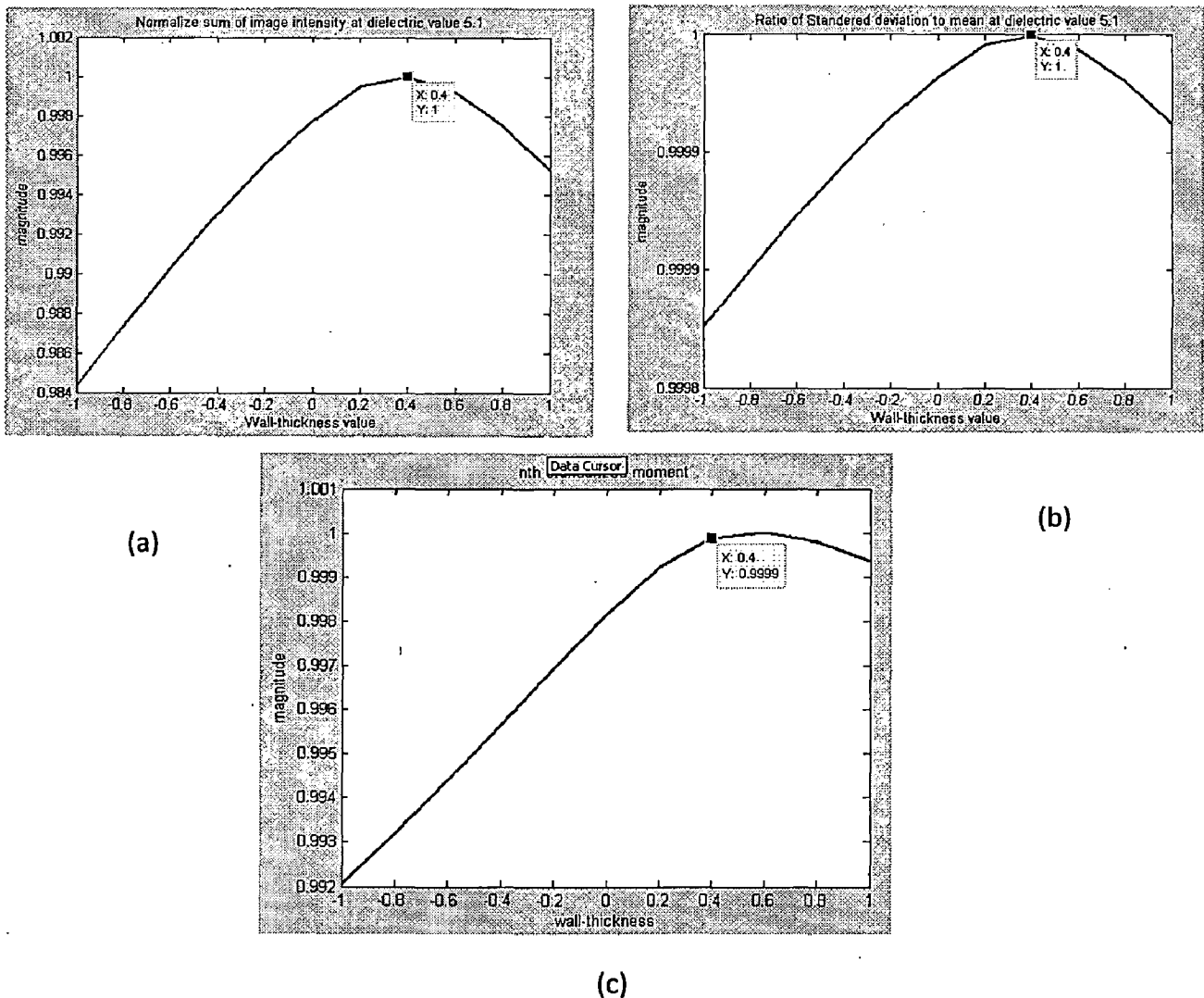


Figure 4.32: Quality indices plot at constant dielectric value and, varying thickness around 12.0cm by an amount of 0.2, (a) Normalize Sum of image intensity (b) Ration of standardizes deviation to mean (c) 20th moment.

It can be said that it is in the form of exponential function. So the function is assumed to be

$$F(t') = a1*exp(-((t'-b1)/c1)^2) + a2*exp(-((t'-b2)/c2)^2); \quad (4.1)$$

We change thickness value by an amount of 0.2, around 12.0 cm so, $t = 12.0+t'$ cm; by applying curve fitting method, equation has been obtain for quality indices value (see equation 4.1)

Normalize sum of image intensity							Ratio of Std deviation to mean							<i>n</i> th standard moment						
a1	b1	c1	a2	b2	c2	R ²	a1	b	c	a	b	c	R ²	a	b1	c	a	b2	c2	R ²
0.998	0.37	8.7	0.014	-1.4	0.69	0.9987	1	0.4	9.2	0.0	-1.8	0.996	1	0.61	1.4	.0	-1.4	0.43	0.995	

Table 4.10: Constant terms value for equation (4.1).

By solving equation (4.1), value of t' can be obtained.

- At Dielectric Value 5.2

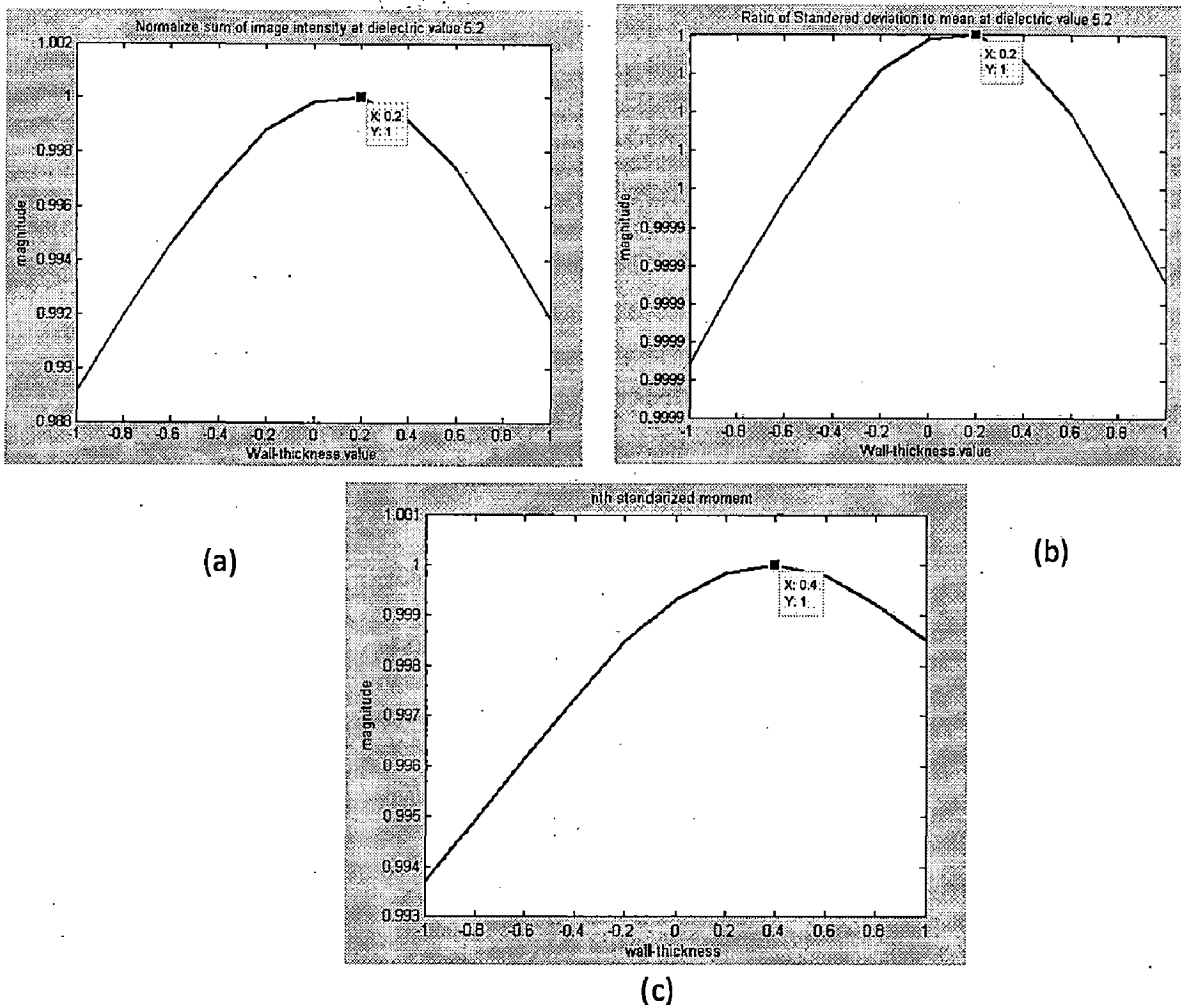


Figure 4.33: Quality indices plot at constant dielectric value and ,varying thickness around 12.0cm by an amount of 0.2.

We change thickness value by an amount of 0.2, around 12.0 cm so, $t = 12.0+t'$ cm; by applying curve fitting method, equation has been obtain for quality indices value (see equation 4.2)

$$F(t') = a1 * \exp(-((t'-b1)/c1)^2) + a2 * \exp(-((t'-b2)/c2)^2) \quad (4.2)$$

Where $t = 12.0+t'$ cm; by applying curve fitting method

Normalize sum of image intensity							Ratio of Std deviation to mean						
a1	b1	c1	a2	b2	c2	R ²	a1	b1	c1	a2	b2	c2	R ²
0.99	0.12	9.604	0.003	- 1.11	0.334	0.998	1	0.14	10.12	0.006	- 1.34	0.56	0.991

<i>n</i> th standard moment						
a1	b1	c1	a2	b2	c2	R ²
1	0.39	15.21	0.002	-1.10	0.35	0.9994

Table 4.11: Constant values for equation 4.2

It shows maximum value at accurate parameters so by differentiating the function wrt t' and equating it equal to zero give the accurate value.

- At Thickness 12.5 cm

$$F(n') = a1 * \exp(-((n'-b1)/c1)^2) + a2 * \exp(-((n'-b2)/c2)^2); \quad (4.3)$$

Where $n = 5.0+n'$; by applying curve fitting method

Normalize sum of image intensity							Ratio of Std deviation to mean						
a1	b1	c1	a2	b2	c2	R ²	a1	b1	c1	a2	b2	c2	R ²
0.99	0.18	7.604	0.0065	- 1.61	0.784	0.988	1	0.19	10.19	0.087	- 2.34	0.96	0.971

<i>n</i> th standard moment						
a1	b1	c1	a2	b2	c2	R ²
1	0.43	11.26	0.010	-1.34	0.597	0.9991

Table 4.12: Values of constant for equation 4.3

It shows maximum value at accurate parameters so by differentiating the function wrt n' and equating it equal to zero give the accurate value.

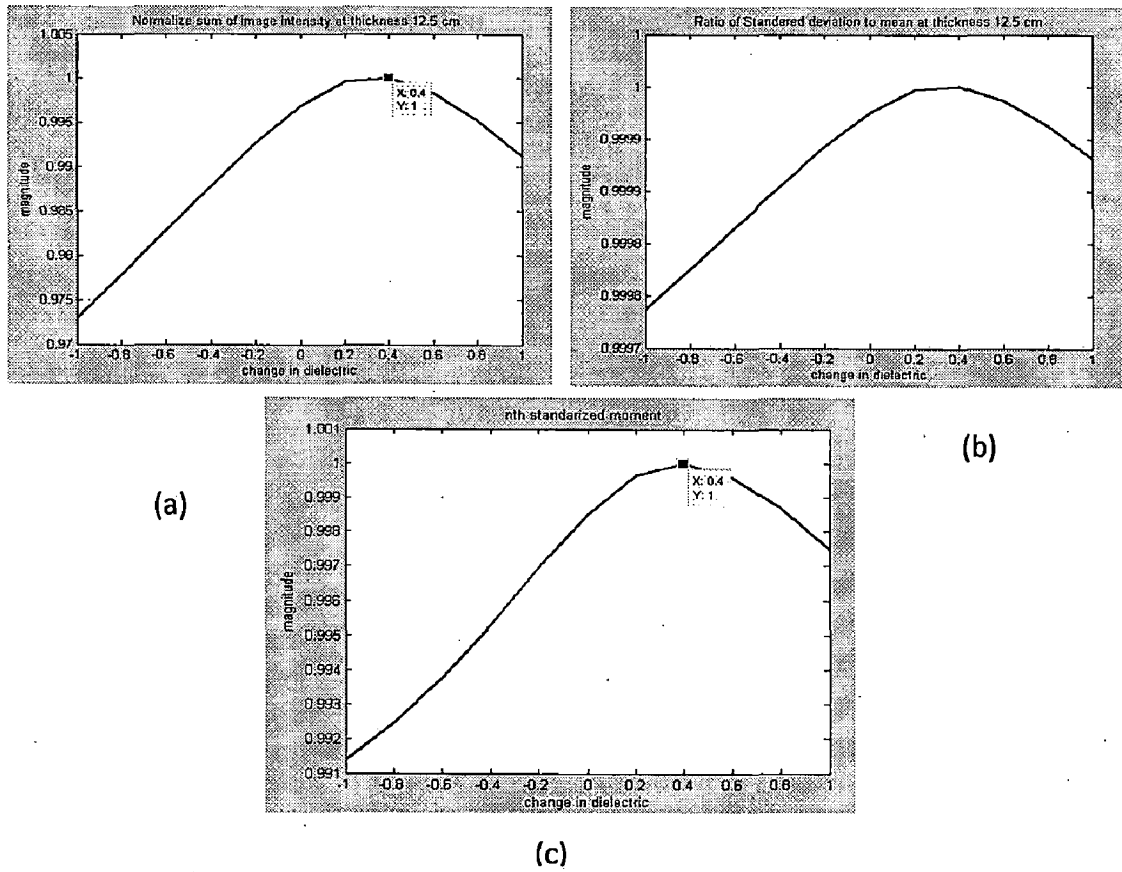


Figure 4.34: Quality indices plot at constant thickness value and, varying dielectric around 5.0 by an amount of 0.2.

- At Thickness 11.5 cm

$$F(n') = a1 * \exp(-((n'-b1)/c1)^2) + a2 * \exp(-((n'-b2)/c2)^2); \quad (4.4)$$

Where $n = 5.0 + n'$; by applying curve fitting method

Normalize sum of image intensity							Ratio of Std deviation to mean						
a1	b1	c1	a2	b2	c2	R ²	a1	b1	c1	a2	b2	c2	R ²
0.99	0.62	3.7	0.18	-	1.08	0.997	1	0.14	14.19	0.587	-	1.96	0.991
				1.81							4.74		

nth standard moment						
a1	b1	c1	a2	b2	c2	R ²
0.997	0.75	7.07	0.059	-1.55	0.961	0.9988

Table 4.13: Values of constant for equation 4.4

It shows maximum value at accurate parameters so by differentiating the function wrt n' and equating it equal to zero give the accurate value.

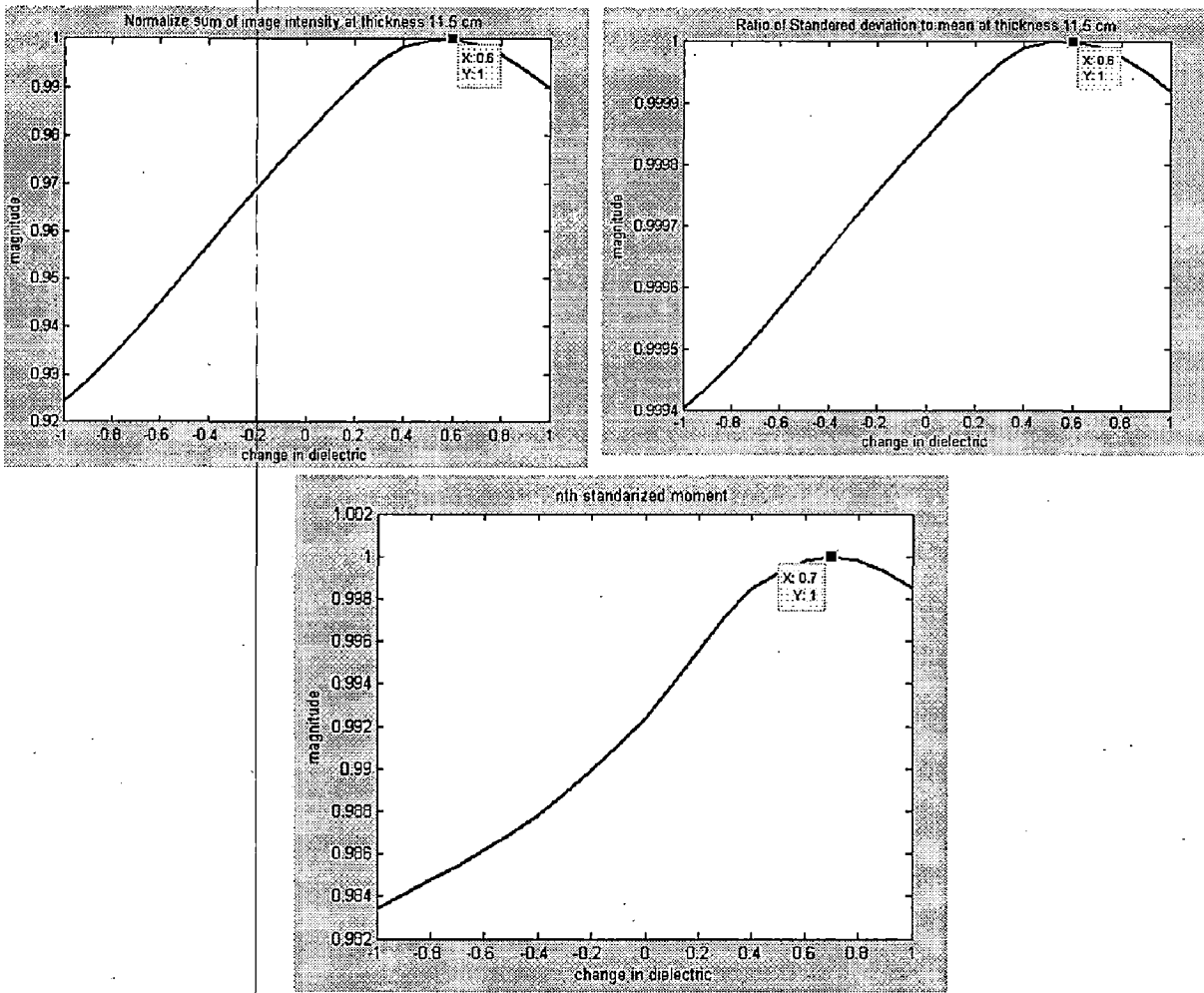


Figure 4.35: Quality indices plot at constant thickness value and, varying dielectric around 5.0 by an amount of 0.1.

- General Solution

From the figure (4.34 & 4.35) it is clear that changing the dielectric value by 0.1, there is negligible change in quality indices value, and the experiment had been done in real environment so clutter also affect the data. So by taking a data in wide ranges and then summing them, we can go for optimum solution.

Quality indices values had been calculated at different values of thickness, by varying the dielectric values from 3 to 7. By averaging a_1 , b_1 , c_1 , a_2 , b_2 , c_2 we got optimum values of these parameters. At true parameters quality indices shows its maximum value, so by differentiating the equation 4.5 with respect to Δn and then putting it equal to zero we will get optimum value of parameters.

Thickness (cm)	Normalize sum of image intensity							Ratio of Std deviation to mean						
	a1	b1	a2	b2	c1	c2	R ²	a1	b1	a2	b2	c1	c2	R ²
11.9	0.99	0.50	3.7	1.6	0.12	0.92	0.9862	1	0.33	42.38	0.0004	-1.05	0.31	0.9578
12.0	0.99	0.30	4.1	0.04	-1.2	0.48	0.9943	1	0.30	45.98	0.0078	-1.46	0.45	0.9786
12.1	0.99	0.30	4.1	0.04	-1.3	0.58	0.9862	0.99	0.26	31.25	0.008	-1.21	0.48	0.9862
12.2	0.99	0.20	4.4	0.02	-1.09	0.31	0.9811	0.99	.33	30.71	0.012	-1.131	0.06	0.9793
12.3	0.99	0.19	4.4	0.04	-1.09	0.31	0.9748	1	0.17	41.8	0.04	-1.03	0.58	0.9745
12.4	0.99	0.17	4.8	0.04	-1.03	0.58	0.9845	1	0.48	28.87	0.07	-1.76	0.59	0.9628

nth standard moment						
a1	b1	a2	b2	c1	c2	R ²
0.99	0.4	10.38	0.016	-1.44	0.731	0.9925
0.99	.33	10.71	0.012	-1.131	0.062	0.9893
0.99	0.26	11.25	0.008	-1.21	0.487	0.9862
0.99	0.20	11.58	0.005	-1.137	0.383	0.9708
0.99	0.13	11.97	0.004	-1.09	0.331	0.9598
1.03	1.543	15.79	-0.04931	2.59	3.077	0.9265

Table 4.14: Obtain values of constant by using curve fitting method for equation (4.5)

$$F(x) = a1 \cdot \exp(-((\Delta n - b1)/c1)^2) + a2 \cdot \exp(-((\Delta n - b2)/c2)^2) \quad (4.5)$$

$$\varepsilon = 5.0 + \Delta n;$$

Normalize sum of image intensity							Ratio of Std deviation to mean						
a1	b1	c1	a2	b2	c2	R ²	a1	b1	c1	a2	b2	c2	R ²
0.99	0.326	-1.61	4.93	0.734	0.29	0.988	1	0.19	-2.34	32.38	0.087	0.96	0.971

<i>n</i> th standard moment						
a1	b1	c1	a2	b2	c2	R ²
1	0.43	-1.34	0.012	-1.34	0.597	0.9991

Table 4.15: Average value

Same as, quality indices values had been calculated at different values of dielectric, by varying the thickness values from 5 to 15 cm. by averaging a1, b1, c1, a2, b2, c2 we got optimum values of these parameters. At true parameters quality indices shows its maximum value, so by differentiating the equation (4.6) with respect to Δt and then putting it equal to zero we will get optimum value of parameters.

$$F(x) = a1 * \exp(-((\Delta t - b1)/c1)^2) + a2 * \exp(-((\Delta t - b2)/c2)^2) \quad (4.6)$$

$$t = 5.0 + \Delta t;$$

dielectric	Normalize sum of image intensity							Ratio of Std deviation to mean						
	a1	b1	a2	b2	c1	c2	R ²	a1	b1	a2	b2	c1	c2	R ²
4.9	0.99	0.60	5.7	1.9	0.42	0.62	0.9762	1	0.38	32.38	0.0087	-1.35	0.56	0.9678
5.1	0.99	0.37	6.1	0.94	-3.2	0.98	0.9843	0.9	0.32	25.98	0.0876	-1.786	0.75	0.9456
5.3	0.99	0.48	5.7	0.75	-4.3	1.68	0.9762	0.99	0.36	31.67	1.006	-1.31	0.68	0.9732
5.5	0.99	0.89	6.4	0.48	-3.09	0.71	0.9611	0.99	.43	29.61	1.09	-1.141	0.36	0.9433
5.7	0.99	0.98	7.4	0.72	-4.09	0.91	0.9748	1	0.47	37.6	0.87	-1.53	0.48	0.9845
5.9	0.99	0.63	4.9	1.76	-5.03	1.28	0.9887	1	0.28	30.77	0.089	-1.76	0.49	0.9528

<i>n</i> th standard moment						
a1	b1	a2	b2	c1	c2	R ²
0.99	0.78	18.38	0.018	-1.94	0.987	0.9885
0.99	1.33	7.71	1.012	-1.231	0.089	0.9763
0.99	1.27	13.25	1.008	-1.561	0.76	0.9892
0.99	1.20	12.58	0.045	-1.347	0.543	0.9878
0.98	1.23	17.97	0.304	-1.675	0.574	0.9788
1.03	2.443	17.89	-0.4931	2.129	3.987	0.9325

Table 4.16: Obtain values of constant for eq (4.6)

Normalize sum of image intensity							Ratio of Std deviation to mean						
a1	b1	c1	a2	b2	c2	R ²	a1	b1	c1	a2	b2	c2	R ²
0.99	0.65	- 3.215	6.035	1.09	1.03	0.978	1	0.37	- 1.47	31.33	.52	0.55	0.961

<i>n</i> th standard moment						
a1	b1	c1	a2	b2	c2	R ²
0.98	1.37	1.644	14.63	-0.315	1.15	0.9753

Table 4.17: Average value

By solving the equations (4.5) and (4.6) dielectric and thickness value 12.8 and 5.4 has been obtain, we have taken it as a optimum parameters and obtain beam forming image for it.

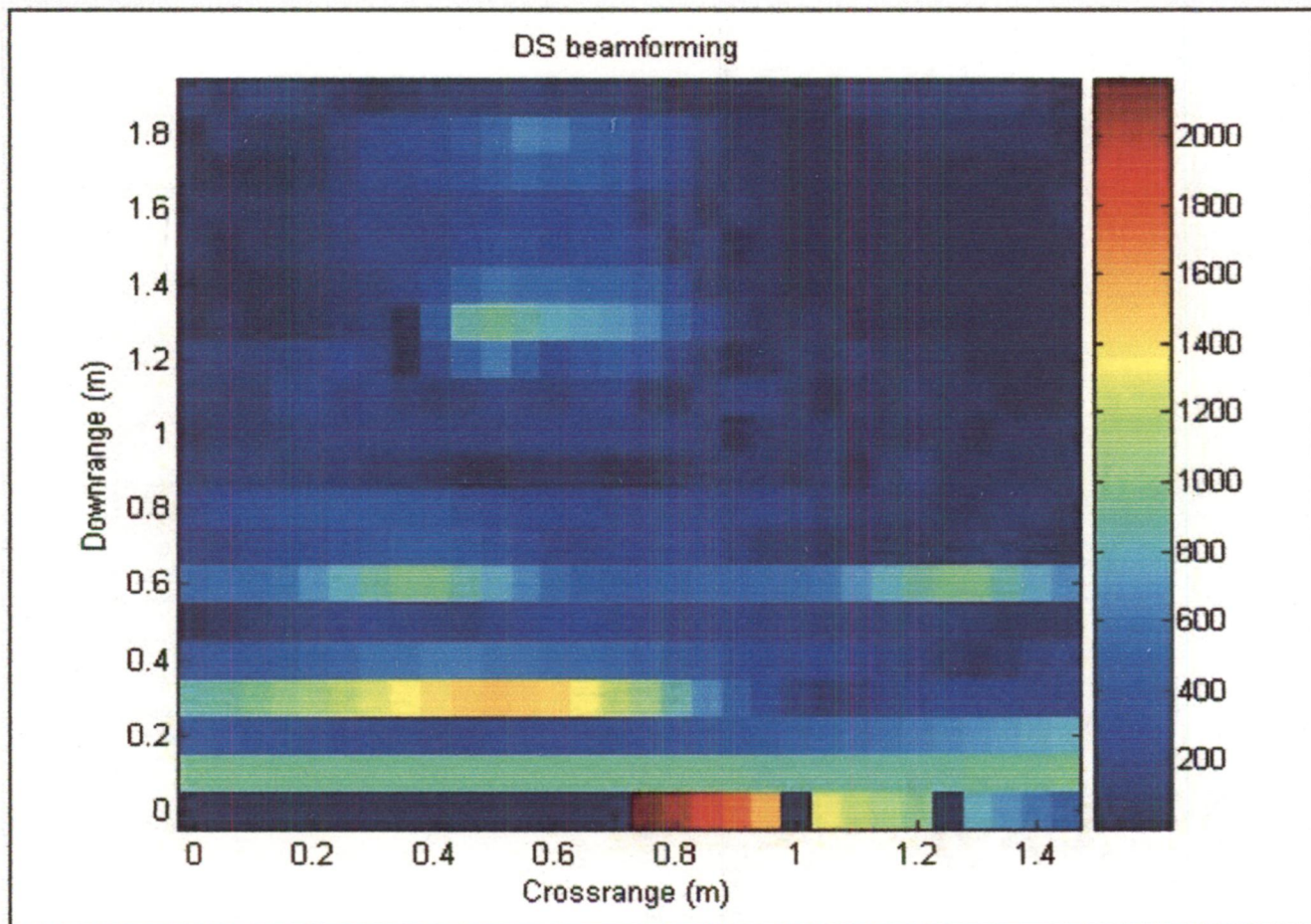


Figure 4.36: Beamforming image for dielectric value 5.4 and thickness 12.8cm.

5. CONCLUSION AND FUTURE SCOPE

5.1 Conclusion

Our main aim for this work is to characterize wall parameters and then apply focusing approach to improve results, so that we can get high quality of image. We have used here step frequency continuous wave radar (SFCW) which consists of mainly VNA and data is collected in frequency domain. The PC was interfaced with the VNA using MATLAB and NI VISA. For wall characterization insertion transfer function method and reflection method had been applied first. The insertion transfer function method provide variation of parameters with frequency, for this method complex equations have to be solved and it cannot be applied in real time applications. However, reflection method is simple, easy to use and can be used in real time environment but to the effect of multiple reflections from wall effect its accuracy. Further beam forming B-scan image had been developed and showed the effect of wall parameters in image intensity. The errors in these parameters smear and blur the image and shift the target from its true location. Then we presented an auto-focusing system for through-the-wall applications that focuses the image and corrects for shifts in imaged locations of stationary targets. We analyzed the intensity profile, for this system, under far-field and small error assumptions. We considered point targets and assumed single uniform walls. We examined potential image quality metrics that allow the system operator to perform imaging under wall parameter ambiguities. It was shown that higher order statistics are more sensitive to errors in wall parameters as compared to conventional contrast measures such as sum of squared intensity. This is because the peaks in the image intensity profile become sharper as the image intensity is raised to a higher power, increasing the overall image contrast.

5.2 Future Work

There are lots of applications where the imaging of the objects through the opaque obstacles could be used. It seems that the radar with the electromagnetic waves

penetration is a good way to achieve it. However, all the required techniques need to be improved in a large scale.

- To include the multilayer model approach for the measurements of the wall parameters. This would provide thickness, permittivity and conductivity for every layer of the wall such as brick wall, plaster, plywood etc.
- To include the multilayer model of the wall into the precise TOA estimation. By using this effects wall parameters on image can be precisely obtained.
- Since different clutter reduction techniques and their results show improvement in detection. But these results are influence by priory information about the presence of target. It will interesting to apply in unknown environment, particularly adaptive techniques should be applied.
- The process that takes into account multiple reflections between object and diffraction should be investigated.
- Investigate the ways to reduce data throughput, possibly by some type of preprocessing, and develop more efficient imaging algorithms.

Apart from it radar hardware has the great ability for improvement. By improving the radar range resolution detection of moving targets can make easy. It can be expected that more sophisticated methods with much larger computational requirements would be investigated in the future. They will require more powerful hardware that is available now.

REFERENCES

- [1] D. D. Ferris Jr. and N. C. Currie, "Microwave and millimeter wave systems for wall penetration," *Proc. SPIE*, vol. 3375, pp. 269-279, Apr. 1998.
- [2] D. J. Taylor, *Introduction to Ultra-wideband Radar Systems*, CRC press, 1995.
- [3] D. D. Ferris Jr. and N. C. Currie, "A survey of current technologies for through the wall Surveillance (TWS)," in *Proc. SPIE*, vol. 3577, pp. 62-72, Nov. 1998.
- [4] D. B. Lin and T. H. Chu, "Bistatic frequency swept microwave imaging: principle, methodology and experimental results," *IEEE Trans. Microwave Theory and Techniques*, vol. 41, no. 5, pp. 855-861, May 1993.
- [5] F. Ahmad, M. G. Amin and S. A. Kassam, "Synthetic aperture beamformer for imaging through a dielectric wall," *IEEE Trans. Aerosp. Electron. Syst.*, vol. 41, no. 1, pp. 271-283, Jan. 2005.
- [6] [Online]. Available: http://www.schafertmd.com/VisibuildingIndustryDay/documents/VisiBuilding_Proposers_Briefing.pdf
- [7] T. W. Barrett, "History of UltraWideBand (UWB) Radar & Communications," *Progress In Electromagnetic Symposium*, July 2000.
- [8] T. Gibson and D. Jenn, "Prediction and measurements of wall insertion loss," *IEEE Trans. Antennas Propagation*, vol. 47, pp. 55-57, Jan. 1999.
- [9] I. Cuinas and M. Sanchez, "Building material characterization from complex transmissivity measurements at 5.8 GHz," *IEEE Trans. Antennas Propagat.*, vol. 48, pp. 1269-1271, Aug. 2000
- [10] J. Zhang, M. Nakhsh, and Y. Huang, "In-situ characterization of building materials," *11th Int. Antennas and Propagation Conf.*, Apr. 17-20, Conf. Pub. 480, pp. 269-274, 2001.
- [11] J. Baker-Jarvis, R. G. Geyer, J. H. Grosvenor, Jr., M. D. Janecic, C. A. Jones, B. Riddle, C. M. Weil, and J. Krupka, "Dielectric characterization of low-loss materials: A comparison of techniques," *IEEE Trans. Dielect. Elect. Insulation*, vol. 5, pp. 571-577, Aug. 1998.

- [12] G. Wang and M. Amin, "Imaging Through Unknown Walls Using Different Standoff Distances," *IEEE Transactions on Signal Processing*, vol. 54, pp. 4015–4025, October 2006.
- [13] H. Wang, Z. Zhou and L. Kong, "Wall Parameters Estimation for Moving Target Localization with Through-the-Wall Radar," *Microwave and Millimeter Wave Technology*, 2007, pp. 1–4, April 2007.
- [14] H. Khatri and C. Le, "Identification of Electromagnetic Parameters of a Wall and Determination of Radar Signal Level Behind a Wall," *Proc 2006 SPIE, the International Society for Optical Engineering*, vol. 6210, pp. 1–7, April 2006.
- [15] M. Mahfouz, A. Fathy, Y. Yang, E. ElHak and A. Badawi, "See through wall imaging using ultra wideband pulse systems," *Proc. IEEE, 34th Applied Imagery and Pattern Recognition Workshop (AIPR05)*, pp. 8-16, Oct. 2005.
- [16] Michal Aftanas, Jargen Sachs, Milos Drutarovsky, Dus an Kocur," Efficient and Fast Method of Wall Parameter Estimation by Using UWB Radar System", *European Commission through the 6th framework*, pp. 231-235, 2009.
- [17] M. Dehmollaian and K. Sarabandi, "Refocusing through building walls using synthetic aperture radar," *IEEE Trans. Geosci. Remote Sens.*, vol. 46, no. 6, pp. 1589-1599, Jun. 2008.
- [18] [Online]. Available: <http://www.itl.nist.gov/div898/handbook/>
- [19] Attiya A. M., Bayram A., Safaai-Jazi A., Riad S. M., "UWB applications for through-wall detection," in *Antennas and Propagation Society International Symposium, IEEE*, vol. 3, pp. 3079 – 3082, 20-25 Jun. 2004.
- [20] J. B. Anderson, *Digital Transmission Engineering*, 2nd ed. Wiley-IEEE Press, 2005.
- [21] Eaves, J. J., and E. K. Reedy (eds.), *Principles of Modern Radar*, New York: Van Nostrand Reinhold, 1987.
- [22] Li, H. J., and S. H. Yang, "Using Range Profiles as Feature Vectors to Identify Aerospace Objects," *IEEE Trans. Aerospace and Electronic Systems*, Vol. 41, No. 3, pp. 261–268, 1993.

- [23] Zyweck, A., and R. E. Bogner, "Radar Target Classification of Commercial Aircraft," *IEEE Trans. Aerospace and Electronic Systems*, Vol. 32, No. 2, pp. 598–606, 1996.
- [24] Knott, E. F., "Radar Cross Section." In *Aspects of Modern Radar*, E. Brookner (ed.), Norwood, MA: Artech House, 1988
- [25] Wehner, D. R., *High-Resolution Radar, Second Edition*, Norwood, MA: Artech House, 1994.
- [26] R. Rau and J. H. McClellan, "Analytic models and post processing techniques for UWB SAR," *IEEE Trans. Aerospace and Electronic Systems*, vol. 36, no. 4, pp. 1058-1074, Oct. 2000.
- [27] R. Chandra, "Study of through wall imaging in UWB range for target detection," M.Tech. Thesis, Dept. of E and CE, IIT Roorkee, India, 2008.
- [28] Ing. Michal Aftanas, "Through Wall Imaging with UWB radar system", PhD Thesis, Department of Electronics and Multimedia Communications, Technical university of Kosice, Aug 2009.
- [29] E. M. Johansson and J. E. Mast, "Three-dimensional ground-penetrating radar imaging using synthetic aperture time-domain focusing," *AMMWD, Proceedings of SPIE*, vol. 2275, pp. 205-214, Sep. 1994.
- [30] S. Gauthier and W. Chamma, "Through-The-Wall Surveillance," *Technical Memorandum DRDC*, Ottawa, Oct. 2002.
- [31] Prof. Igor. I. Immoreev, PGS Dmitry V, Fedotov, "Ultra Wideband radar systems: advantages and disadvantages," *IEEE conference on Ultra Wideband system and technologies*, 2002.
- [32] G. Barrie, "Ultra-wideband synthetic aperture: data and image processing," *Defense R&D Canada DRDC Ottawa, Tech. Memorandum*, TM 2003-015, Jan. 2003.
- [33] N. C. Wild *et al.*, "Ultrasonic through-the wall surveillance system," *Proc. SPIE*, Boston, MA, vol. 4232, Enabling Techn. For Law Enforcement and Security, pp. 167–176 Nov. 2000.
- [34] A. R. Hunt, "Stepped-frequency CW radar for concealed weapon detection and through-the-wall surveillance," in *Proc. SPIE, Orlando, FLm*, vol. 4708, Sensors

- and C3I Techn. For Homeland Defense and Law Enforcement, pp. 99–105, Apr. 2002.
- [35] Yazhou Wang; Fathy, A.E, “Three-dimensional through wall imaging using an UWB SAR,” *IEEE Antennas and Propagation Society International Symposium* 2010.
- [36] P. Withington, H. Fluhler, and S. Nag, “Enhancing homeland security with advanced UWB sensors,” *IEEE Microw. Mag.*, vol. 4, no. 3, pp. 51–58, Sep. 2003.
- [37] C. Chen, K. Yao, and R. E. Hudson, “Source localization and beamforming,” *IEEE Signal Process. Mag.*, pp. 30–39, May 2002.
- [38] F. Ahmad and M. G. Amin, “A noncoherent radar system approach for through-the-wall imaging,” in *Proc. SPIE*, Bellingham, WA, vol. 5778, Sensor, and Command, Control, Communications, and Intelligence Technologies for Homeland Security and Homeland Defense IV, Mar.-April 2005.
- [39] G. Wang and M. G. Amin, “A new approach for target locations in the presence of wall ambiguities,” presented at the IEEE Symp. Signal Processing Information Technology (ISSPIT’04), Rome, Italy, Dec. 2004.
- [40] A. Muqaibel and A. Safaai-Jazi, “A new formulation for characterization of materials based on measured insertion transfer function,” *Microwave Theory and Techniques*, vol. 51, pp. 1946–1951, August 2003.
- [41] A. Muqaibel, A. Safaai-Jazi, A. Bayram, A. Attiya and S. Riad, “Ultrawideband through-the-wall propagation,” *Microwaves, Antennas and Propagation, IEE Proceedings*, vol. 153, pp. 581–588, Decembe 2005.
- [42] Nekoogar. Book, “Introduction to Ultra-Wideband Communications” August 5, 2005.
- [43] G. Cui, L. Kong, J. Yang and X. Wang, “A New Wall Compensation Algorithm for Through-the-wall Radar Imaging,” *Synthetic Aperture Radar, 2007. APSAR 2007*, pp. 393–396, November 2007.
- [44] A. T. S. Ho, W. H. Tham and K. S. Low, “Improving classification accuracy in through-wall radar imaging using hybrid prony’s and singular value decomposition method,” *Geoscience and Remote Sensing Symposium*, 2005, vol. 6, pp. 4267–4270, July 2005.

- [45] R. Linnehan, J. Schindler, D. Brady, R. Kozma, R. Deming and L. Perlovsky, "Dynamic Logic Applied to SAR Data for Parameter Estimation Behind Walls," *Radar Conference, 2007 IEEE*, pp. 850–855, April 2007.
- [46] F. Ahmad and M. G. Amin, "Through the wall radar imaging experiments," in *Proc. IEEE Workshop on Signal Processing Applications for Public Security and Forensics SAFE '07*, Washington D. C., pp. 1-5, Apr. 2007.
- [47] P. Van Genderen, "Multi- waveform SFCW radar," *33rd European Microwave Conference* , Vol 2, pp- 849-852, March 2003.
- [48] Mojiaba Dehmollaian, "Through-Wall Shape Reconstruction and Wall Parameters Estimation Using Differential Evolution," *IEEE Geoscience and Remote Sensing Letters*, Vol 8, No.2, Mar 2011.
- [49] Lianlin Li, Wenji Zhang, and Fang L, "A Novel Autofocusing Approach for Real-Time Through-Wall Imaging Under Unknown Wall Characteristics", *IEEE transactions on geoscience and remote sensing*, vol. 48, no. 1, january 2010.
- [50] Ahmad Safaai-Jazi, Sedki M. Riad, Ali Muqaibel, and Ahmet Bayram, "Through-the-Wall Propagation and Material Characterization," *DARPA NETEX Program*, November 18, 2002.
- [51] F. Ahmad, M. G. Amin, and G. Mandapati, "Autofocusing of through-the-wall radar imagery under unknown wall characteristics," *IEEE Trans. Image Process*, vol. 16, no. 7, pp. 1785–1795, Jul. 2007.
- [52] F. Berizzi and G. Corsini, "Autofocusing of inverse synthetic aperture radar images using contrast optimization," *IEEE Trans. Aerosp. Electron. Syst.*, vol. 32, no. 3, pp. 1185–1191, Jul. 1996.
- [53] J. R. Fienup, "Synthetic-aperture radar autofocus by maximizing sharpness," *Opt. Lett.*, vol. 25, no. 4, Feb. 2000.
- [54] S. Fortune, M. Hayes, and P. Gough, "Statistical autofocus of synthetic aperture sonar images using image contrast optimization," in *Proc. OCEANS*, vol. 1, pp. 163–169, 2001.
- [55] Online article, <http://www.fcc.gov/oet/info/rules>.

- [56] Gautam. R.S, Singh, D., Mittal, A., “An Efficient Contextual Algorithm to Detect Subsurface Fires With NOAA/AVHRR Data,” *IEEE Transactions on Geoscience and Remote Sensing*, VOL. 46, No. 7 July 2008.
- [57] F. Ahmed, Yimin Zhang, and M.G. Amin, “ Three-Dimensional beamforming for imaging through a single wall;” *IEEE Geoscience and Remote Sensing Letters* ,Vol 5 No. 2 April 2008.
- [58] S. A. Gauthier and W. Chamma, “Surveillance through concrete walls,” in *Proc. of SPIE*, pp. 597-608, 2004.

I. Experimental Setup, delay calculation of antenna and A-Scan algorithm

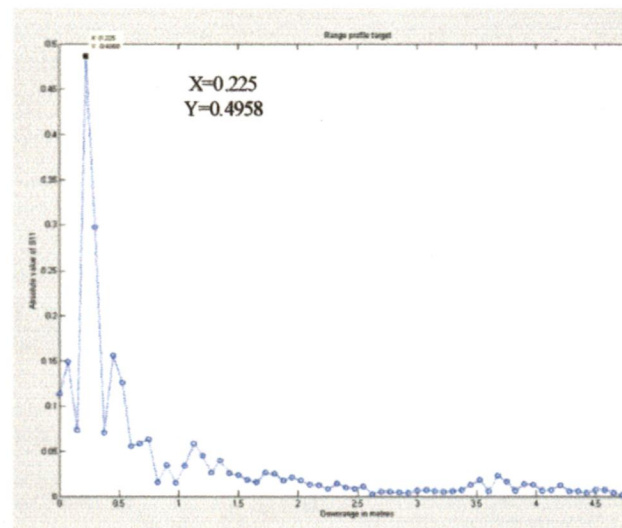
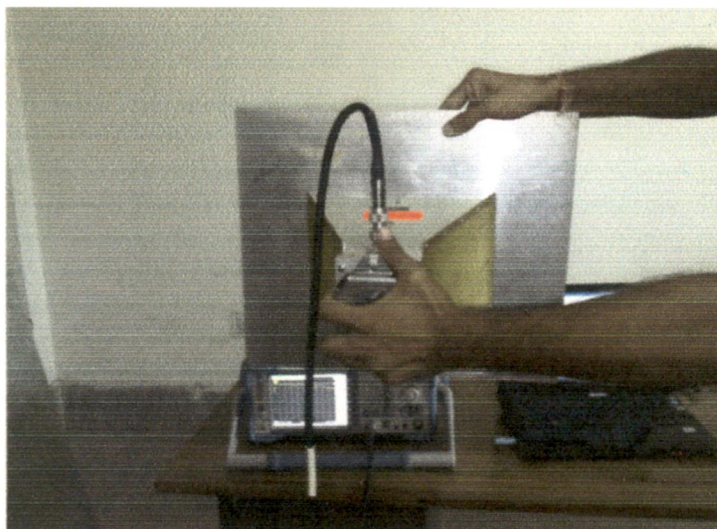
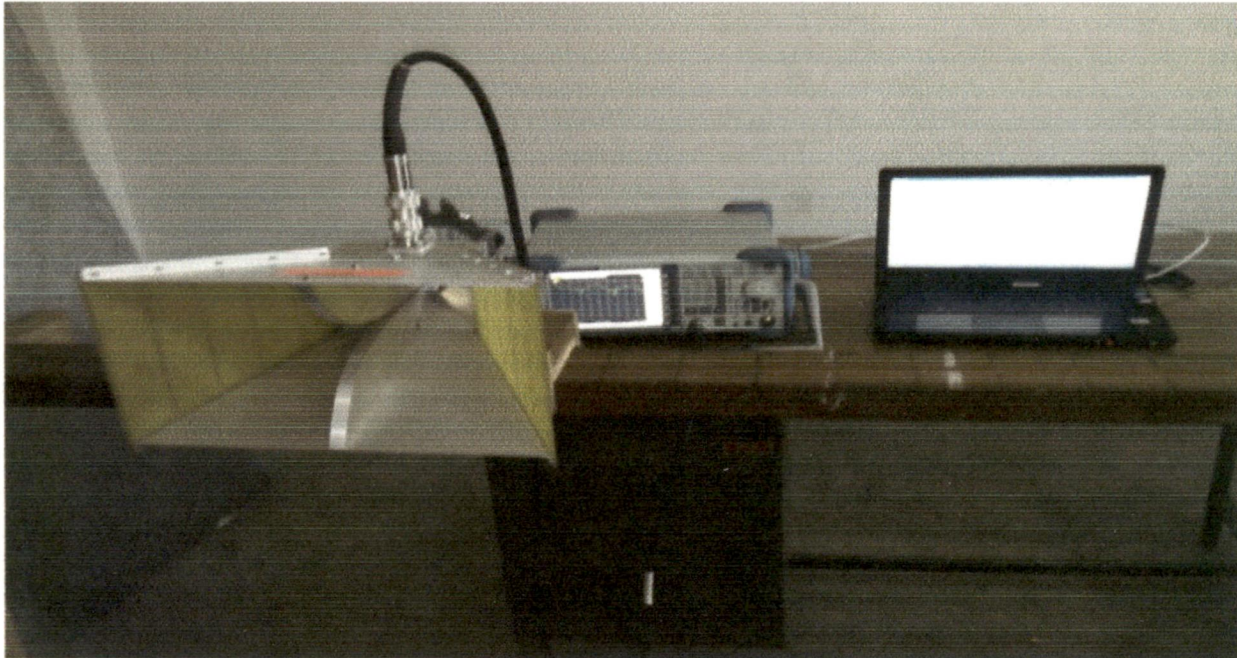


Fig: Experimental setup and Delay calculation of antenna

A Scan Algorithm: The data collected by the VNA is in the frequency domain at frequency points f_n which is converted to the time domain by inverse fast Fourier

transform (IFFT). Mathematically, a signal returned from a target at a distance in the frequency domain is given by equation :

$$S(f_n) = \frac{1}{\tau_{\max}} \int_0^{\tau_{\max}} S(t) \exp(-j2\pi f_n t) dt \quad (1)$$

$$\Delta\tau = \frac{1}{N_f \Delta f} \quad (2)$$

$$\tau_{\max} = \frac{N_f - 1}{BW} \quad (3)$$

Where $\Delta\tau$ is the time resolution possible with the stepped frequency waveform of N_f uniform steps of Δf , τ_{\max} is the maximum time possible and BW is the bandwidth of the system. For the present case, $N_f = 4001$ and $\Delta f = 0.5$ MHz Thus we see the need to choose $N = 4001$ for increased resolution.

The signal obtained in frequency domain is converted into time domain by performing inverse Fourier Transform. The time domain signal is represented as:

$$S(t) = \sum_{n=0}^{N_f-1} S(f_n) \exp(j2\pi f_n t) \quad (4)$$

Mapping from time domain to spatial domain is done according to following equation :

$$z = \frac{ct}{2} \quad (5)$$

The mapped spatial domain signal is represented as

$$S(z) = \sum_{n=0}^{N_f-1} S(f_n) \exp\left(j2\pi f_n \left(\frac{2z}{c}\right)\right) \quad (6)$$

II. MATLAB Code

```
// Code for characterization of wall parameters using insertion method
```

```
Dwall=.12;
c=3*10^8;
S21=importdata(' ');
S21W=importdata(' ');
freq=importdata('H:\freq.mat');
magS21=abs(S21);
angS21=angle(S21);
magS21W=abs(S21W);
angS21W=angle(S21W);
S21n=S21./S21W;
magS21n=abs(S21n);
angS21n=angle(S21n);
beta0=2*pi*freq/c;
initRealDielectricConst=5; // in the case of brickwall
options=optimset('Display','iter','NonlEqnAlgorithm','dogleg');
RealDielecConst=zeros(length(magS21n),1);
for var=1:length(magS21n)

RealDielecConst(var)=fsolve(@CalRealDielectricConstant,initRealDielectricConst,options,magS21n(var),
angS21n(var),freq(var),beta0(var),Dwall,c);
end
% save('H:\vishal','RealDielecConst');
% RealDielecConst=zeros(length(magS21n),1);
% for var=1:length(magS21n)
%
RealDielecConst(var)=CalRealDielectricConstant(initRealDielectricConst,magS21n(var),angS21n(var),fre
q(var),beta0(var),Dwall,c);
% end
% save('H:\vishalnm','RealDielecConst');
[AttenConst,ImagDielectric,LossTangent]=calImagDielectricConstant(RealDielecConst,magS21n,angS21n
,freq,beta0,Dwall,c);
kk=RealDielecConst;
figure(1), plot(freq/1e9,RealDielecConst,'-g','linewidth',2);
abs(mean( RealDielecConst))
figure(2), plot(freq/1e9,abs(AttenConst),'-r','linewidth',2);
mean(RealDielecConst)
figure(3), plot(freq/1e9,abs(LossTangent),'-k','linewidth',2);
```

```
// Function used in method //
```

```
// For calculation of Real Dielectric Constant //
```

```
function F=CalRealDielectricConstant(RealDielectricConstant,magS21n,angS21n,freq,beta0,Dwall,c)
```

```
beta=beta0.*sqrt(RealDielectricConstant);
```

```

b=cos(2.*beta.*Dwall).*(RealDielectricConstant-1)^2+(8*RealDielectricConstant)./(magS21n.^2);
X=(b-sqrt(b.^2-(RealDielectricConstant-1)^4))./(sqrt(RealDielectricConstant)-1)^4;
Q=-((sqrt(RealDielectricConstant)-1)/(sqrt(RealDielectricConstant)+1))^2;
F=tan(beta0.*Dwall-(angS21n+2*pi*freq.*(Dwall/c)))+((1-Q.*X)/(1+Q.*X)).*tan(beta.*Dwall);
end

```

// For Claculation of Loss tangent and Attenuation Constant //

```

function[AttenConst,ImagDielectric,LossTangent]=callImagDielectricConstant(RealDielectricConstant,mag
S21n,angS21n,freq,beta0,Dwall,c)

```

```

beta=beta0.*sqrt(RealDielectricConstant);
b=cos(2.*beta.*Dwall).*(RealDielectricConstant-1).^2+(8*RealDielectricConstant)./(magS21n.^2);
X=(b-sqrt(b.^2-(RealDielectricConstant-1).^4))./(sqrt(RealDielectricConstant)-1).^4;
AttenConst=-(1/2*Dwall)*log(X);
ImagDielectric=(2*c.*AttenConst.*sqrt(RealDielectricConstant))./(2*pi*freq);

```

```

LossTangent=ImagDielectric./RealDielectricConstant;

```

```

End

```

// Calculation of Dielectric Constant by using reflection method with Gui //

```

function varargout = final_prjct1(varargin)
% FINAL_PRJCT1 M-file for final_prjct1.fig
%   FINAL_PRJCT1, by itself, creates a new FINAL_PRJCT1 or raises the existing
%   singleton*.
%
%   H = FINAL_PRJCT1 returns the handle to a new FINAL_PRJCT1 or the handle to
%   the existing singleton*.
%
%   FINAL_PRJCT1('CALLBACK',hObject,eventData,handles,...) calls the local
%   function named CALLBACK in FINAL_PRJCT1.M with the given input arguments.
%
%   FINAL_PRJCT1('Property','Value',...) creates a new FINAL_PRJCT1 or raises the
%   existing singleton*. Starting from the left, property value pairs are
%   applied to the GUI before final_prjct1_OpeningFunction gets called. An
%   unrecognized property name or invalid value makes property application
%   stop. All inputs are passed to final_prjct1_OpeningFcn via varargin.
%
%   *See GUI Options on GUIDE's Tools menu. Choose "GUI allows only one
%   instance to run (singleton)".
%
% See also: GUIDE, GUIDATA, GUIHANDLES

% Edit the above text to modify the response to help final_prjct1

% Last Modified by GUIDE v2.5 24-Oct-2010 03:24:17

% Begin initialization code - DO NOT EDIT

```

```

gui_Singleton = 1;
gui_State = struct('gui_Name',    mfilename, ...
                  'gui_Singleton', gui_Singleton, ...
                  'gui_OpeningFcn', @final_prjct1_OpeningFcn, ...
                  'gui_OutputFcn', @final_prjct1_OutputFcn, ...
                  'gui_LayoutFcn', [] , ...
                  'gui_Callback', []);
if nargin && ischar(varargin{1})
    gui_State.gui_Callback = str2func(varargin{1});
end

if nargout
    [varargout{1:nargout}] = gui_mainfcn(gui_State, varargin{:});
else
    gui_mainfcn(gui_State, varargin{:});
end
% End initialization code - DO NOT EDIT

% --- Executes just before final_prjct1 is made visible.
function final_prjct1_OpeningFcn(hObject, eventdata, handles, varargin)
% This function has no output args, see OutputFcn.
% hObject    handle to figure
% eventdata  reserved - to be defined in a future version of MATLAB
% handles    structure with handles and user data (see GUIDATA)
% varargin   command line arguments to final_prjct1 (see VARARGIN)

% Choose default command line output for final_prjct1
handles.output = hObject;
%handles.wall={zeros(64,1),zeros(64,1),zeros(64,1)};
%handles.metal={zeros(64,1),zeros(64,1),zeros(64,1)};
handles.ref1=zeros(64,1);
handles.h2=zeros(64,1);
handles.valu=0;
handles.no=0;
handles.count=1;
set(handles.text1,'string','no of points =');
% Update handles structure
set(hObject,'toolbar','figure');
guidata(hObject, handles);

% UIWAIT makes final_prjct1 wait for user response (see UIRESUME)
% uiwait(handles.figure1);

% --- Outputs from this function are returned to the command line.
function varargout = final_prjct1_OutputFcn(hObject, eventdata, handles)
% varargout  cell array for returning output args (see VARARGOUT);
% hObject    handle to figure

```

```

% eventdata reserved - to be defined in a future version of MATLAB
% handles structure with handles and user data (see GUIDATA)

% Get default command line output from handles structure
varargout{1} = handles.output;

% --- Executes on button press in pushbutton1.
function pushbutton1_Callback(hObject, eventdata, handles)
% hObject handle to pushbutton1 (see GCBO)
% eventdata reserved - to be defined in a future version of MATLAB
% handles structure with handles and user data (see GUIDATA)
axes(handles.axes1);
dist=cal_dist();
%K11_1={zeros(201,1),zeros(201,1),zeros(201,1)};
input=get(handles.edit1,'string');
no=str2num(input);
vr = visa('ni','TCPIP::192.168.111.14::INSTR');
set(vr, 'InputBufferSize', 30000);
fopen(vr);
for ( i=1:1:no)

fprintf(vr , 'CALC:DATA:STIM? ');
fscanf(vr);
str2num(ans);
freq = ans;
fprintf(vr , 'CALC:DATA? SDAT ');
fscanf(vr);
data = str2num(ans);

%data2 = zeros(201,3);
data2{i}(:,1) = freq;
data2{i}(:,2) = data(1:2:401)';
data2{i}(:,3) = data(2:2:402)';
K11_1{i} = data2{i}(:,2)+sqrt(-1)*data2{i}(:,3);
str=sprintf('data:%d',i);
set(handles.text2,'string',str);
invF1 = ifft(K11_1{i},201);
ab1{i}(:,1) = abs(invF1);
    % ab1 = normalize(ab1);
target1{i}(:,1) = ab1{i}(1:64);
plot(dist,target1{i},':ob','linewidth',2);
title(' Range profile target');
ylabel('Absolute value of S11');
xlabel('Downrange in metres');
invF_g1=abs(invF1);
pwr=invF_g1(1:100,:);
wall_target(i,:)=pwr;
beep;
%handles.valu

```

```

if i==no
    break;
end
    pause;
end
pause(1);
set(handles.text2,'string','');
save('H:\S11_wallfake','K11_1');
fclose(vr);
    % v(i)=max(target1);

```

```

function edit1_Callback(hObject, eventdata, handles)
% hObject handle to edit1 (see GCBO)
% eventdata reserved - to be defined in a future version of MATLAB
% handles structure with handles and user data (see GUIDATA)

% Hints: get(hObject,'String') returns contents of edit1 as text
% str2double(get(hObject,'String')) returns contents of edit1 as a double

```

```

% --- Executes during object creation, after setting all properties.
function edit1_CreateFcn(hObject, eventdata, handles)
% hObject handle to edit1 (see GCBO)
% eventdata reserved - to be defined in a future version of MATLAB
% handles empty - handles not created until after all CreateFcns called

```

```

% Hint: edit controls usually have a white background on Windows.
% See ISPC and COMPUTER.
if ispc && isequal(get(hObject,'BackgroundColor'), get(0,'defaultUicontrolBackgroundColor'))
    set(hObject,'BackgroundColor','white');
end

```

```

% --- Executes on button press in pushbutton2.
function pushbutton2_Callback(hObject, eventdata, handles)
% hObject handle to pushbutton2 (see GCBO)
% eventdata reserved - to be defined in a future version of MATLAB
% handles structure with handles and user data (see GUIDATA)
input=get(handles.edit1,'string');
no=str2num(input);
if no==1
S11_1=importdata('H:\project_oct31\wall_900.mat');
S11_2=importdata('H:\project_oct31\metal_900.mat');
kk=importdata('H:\project_oct31\reflection\brick\metal\metal_900.mat');

```

```

for j=1:no
invF2 = ifft(S11_2{j},201);
    abm{j}(:,1) = abs(invF2);

```



```

    % ab1 = normalize(ab1);
    handles.metal{j}(:,1) = abm{j}(1:64);
[m_pos(j)]=first_ref(handles.metal{j});
end
%kk=handles.metal;
%save('H:\projct_oct31\reflection\brick\metal_1125','kk');
%mm=handles.metal;
%
for j=1:no
    handles.metal{j}(:,1)=kk{j}(1:64);
[m_pos(j)]=first_ref(handles.metal{j});
%m_pos(j);
end

for i=1:no
    invF1 = ifft(S11_1{i},201);
    ab1{i}(:,1) = abs(invF1);
    % ab1 = normalize(ab1);
    handles.wall{i}(:,1) = ab1{i}(1:64);

    % v(i)=max(target1);
end
for m=1:no
    mag1=max(handles.wall{m}((m_pos(m)+1):64));
    for l=(m_pos(m)+1):64
        if mag1==handles.wall{m}(l);
            pos=l;
        end
    end
    test= handles.wall{m}(m_pos(m)+4);
    handles.wall{m}(m_pos(m)+4)=mag1;
    handles.wall{m}(pos)=test;
end
%mm=handles.metal;
%save('H:\pendrive_23\New Folder\metal_invf_data\metal_900','mm');
handles.ref1=handles.metal{no}-handles.wall{no};
pos=first_ref(handles.metal{no});
a=handles.wall{no}(pos)/max(handles.metal{no}(8:64));
handles.h2=handles.wall{no}-a.*handles.metal{no};
guidata(hObject, handles);
% --- Executes on button press in pushbutton3.
function pushbutton3_Callback(hObject, eventdata, handles)
% hObject    handle to pushbutton3 (see GCBO)
% eventdata  reserved - to be defined in a future version of MATLAB
% handles    structure with handles and user data (see GUIDATA)
input=get(handles.edit1,'string');
no=str2num(input);
axes(handles.axes1);

```

```

[m_pos]=first_ref(handles.metal{no});
dist=cal_dist();
for i=1:m_pos
    handles.h2(i)=0;
end
if handles.count>4
    handles.count=1;
end
if handles.count==1
    plot(dist,handles.wall{no},':ob','linewidth',2);
    title(' Range profile target');
elseif handles.count==2
    plot(dist,handles.metal{no},':ob','linewidth',2);
    title(' Range profile metal');
elseif handles.count==3
    plot(dist,handles.ref1,':ob','linewidth',2);
    title(' air wall reflection');
elseif handles.count==4
    plot(dist,handles.h2,':ob','linewidth',2);
    title('wall air reflection');
end
%title(' Range profile target');
ylabel('Absolute value of S11');
xlabel('Downrange in metres');
handles.count=handles.count+1;
guidata(hObject, handles);
% --- Executes on button press in pushbutton4.
function pushbutton5_Callback(hObject, eventdata, handles)
% hObject    handle to pushbutton5 (see GCBO)
% eventdata  reserved - to be defined in a future version of MATLAB
% handles    structure with handles and user data (see GUIDATA)
sum=0;
input=get(handles.edit1,'string');
no=str2num(input);
%for k=1:no
k=no;
[m_pos]=first_ref(handles.metal{k});
ref_coff=(handles.wall{k}(m_pos))/max(handles.metal{k}(8:64));
er=(1+ref_coff)^2/(1-ref_coff)^2;
sum=sum+er;
%end
%er=sum/no;
er=sum;
[m_pos1]=first_ref(handles.metal{no});
str=sprintf('dielectric constant:%f',er);
set(handles.text3,'string',str);
[m2_pos]=second_ref(handles.h2,m_pos1);
dist=cal_dist();

```

```

D1=dist(m_pos1);
D2=dist(m2_pos);
Diff=(D2-D1);
%D_wall=Diff*100;
D_wall=(Diff/sqrt(er))*100;
st=sprintf('wall width:%f cm',D_wall);
set(handles.text4,'string',st);
guidata(hObject, handles);

```

```

% --- Executes on button press in pushbutton6.
function pushbutton6_Callback(hObject, eventdata, handles)
% hObject handle to pushbutton6 (see GCBO)
% eventdata reserved - to be defined in a future version of MATLAB
% handles structure with handles and user data (see GUIDATA)
cla(handles.axes1,'reset');
set(handles.text2,'string','');
set(handles.text3,'string','');
set(handles.text4,'string','');
guidata(hObject, handles);

```

// Imaging: Beam forming

```

Er = 4.9;
t = 0.110;
% for cw=1:8
  for cd=1:21
    v=0;
%clear all;
close all;
clc;
tic
BW = 2.0*10^9; %% Bandwidth of The System
c = 3*10^8; %% Speed of light in [m/s]
time_difference = (2*t/c)*(sqrt(Er)-1); %%delay calculation due to the wall
appdist =c*time_difference/2;
za = 1:201;
time = (za-1)/BW;
dist = time*c/2;
index =int16( (2)/(dist(2)-dist(1)));
indexvc=round(appdist/dist(2));
indexpc = round(.48/dist(2)); %%check phase delay due to antenna air first reflection
scanp =30;

filename= 'D:\focusing\beamforming\12.mat'; %%path for target data
maxm_iter=10000;
check=0;
xold=0.4;
count=0;
r=0.41;

```

```

d=0.50;
theta0=0;
xupdated=0;
Ymax = 2;
Xmax = 0.05*scanp;
h = 0.05; % element spacing [m]
ux = 0:h:Xmax-h; % radar platform positions [m]
N = 30; % dimension for image map x-coordinates
M = 20; % dimension for image map y-coordinates
%% ----- end user-specified parameters -----
%%
%% compute "look" positions for radar platform
uy=0:0.075:0.75*20;
del_x = Xmax/(N); % grid spacing [m] - to correspond to
del_y = Ymax/(M); % physical dimensions of the object space
n = 1:N;
x_grid(n) = del_x.*(n-1);
m = 1:M;
y_grid(m) = del_y.*(m-1);
% allocate memory (N - crossrange coordinates; M - downrange coordinates)
% Etotal1 = zeros(N,M);
% Etotal2 = zeros(N,M);
Etotal3 = zeros(N,M);
Etemp3 = zeros(N,M);
delR = zeros(N,M);
indx = zeros(N,1);
Dtotal = zeros(N,M);
delayRoundTrip=zeros(N,M);
% delTF = tRange/(nT-1); % ns/division for PSR data. This is used to
% interpolate data from PSRs to the image space.

for l = 1:30 % loop over each position of Tx/RX platform
for k = 1:20
    for n=1:30
delZsq = ( t+d+r)^2;
h=0.05;
s=1:30;
    ux = 0:h:Xmax-h;
    x_grid(s) = del_x.*(s-1);
    delYsq=(uy(k));
delXsq = ( ux(l) - x_grid(n) )^2;
R(n,k) = sqrt( delXsq+delYsq );
theta0(n,k)= acos((uy(k))/R(n,k));
check=0;
xold=0.4;
count=0;
while( check==0)

```

```

xupdated= xold -f(Er, theta0(n,k), xold, d, t,r, R(n,k))/df(Er, theta0(n,k), xold, d, t,r);
if(abs(xupdated-xold)< diff)
    check=1;
    %display('we have converged');
end
if(count>maxm_iter)
    check=1;
    %display('too many iterations');
end
xold=xupdated;
count=count+1;
end
thetatwo(n,k)=xupdated;
thetaone(n,k)= asin(sqrt(Er)*sin(xupdated));
Dtotal(n,k) = (R(n,k)*cos(theta0(n,k))-t-
d)/cos(thetaone(n,k))+sqrt(Er)*t/cos(thetatwo(n,k))+d/cos(thetaone(n,k))+0.225; % total round-trip distance
delayRoundTrip(n,k) = Dtotal(n,k)/c; % round-trip delay without considering wall
for u=1:201
Etemp3(n,k) = Etemp3(n,k)+(array(1,u))*exp(-4*pi*iota*delayRoundTrip(n,k)*fq(u));
end
end
end
Etotal3 = Etotal3+ Etemp3;
end
toc
for i=1:30
    for j=1:20
        image(i,j)= abs(Etotal3(i,j));
    end
end
image=image';
figure ,imagesc(x_grid,y_grid,image);
title('DS beamforming');
xlabel('Crossrange (m)');
ylabel('Downrange (m)');
set(gca,'YDir','normal');
colorbar;
% Er=Er+0.1;
t=t+0.001;
for ln=1:20
    v=v+1;
    image1{cd}(v,:)=image(ln,:);
end
% image2{cw,cd}=image1;
clear image;
end

```

```
// Function used in beamfoming
```

```
function dx= df( Er, theta0, theta2, d, t,r)  
dx=(r+d)*(1+(tan(asin(sqrt(Er)*sin(theta2)))^2))*sqrt(Er)*cos(theta2)*1/(sqrt(1-  
Er*(sin((theta2)^2))))+t*(1+(tan(theta2))^2);  
end
```

```
function x=f(Er, theta0, theta2, d, t,r, R)  
x=(r+d)*tan(asin(sqrt(Er)*sin(theta2)))+t*tan(theta2)-R*sin(theta0);  
end
```

```
// Image quality indices value calculation
```

```
clear all;  
clc;  
M=importdata('D:\focusing\WALL N DIE ERROR BOTH\125wall.mat');  
for k=1:11  
a1=0;  
b1=0;  
a2=0;  
b2=0;  
a3=0;  
b3=0;  
c3=0;  
b4=0;  
I=M{k};  
for j=1:13  
for i=1:30  
a1=a1+(I(j,i))^2;  
b1=b1+I(j,i);  
end  
end  
c1(k)=a1/b1^2;  
  
% m1=c1;  
for j=1:11  
for i=1:30  
a2=a2+(I(j,i))^4;  
b2=b2+I(j,i);  
end  
end  
c2(k)=a2/b1^4;  
for j=1:13  
for i=1:30  
% a3=a3+I(j,i);  
b3(j,i)=I(j,i)^2/b1;  
c3=c3+b3(j,i)*log(b3(j,i));  
end  
end
```

```

c4(k)=c3;
for j=1:13
for i=1:30
b4=b4+(I(j,i)-(1/30)*b1)^2;
% c4=sqrt(b4)/b1;
end
end
c5(k)=sqrt(b4)/b1;
end
die=-1:0.2:1;
k=max(c1);
c1=c1./k;
l=max(c5);
c5=c5./l;
c2=c2*10^7;
figure(1),plot(die,c1(1:11),'-k','linewidth',2);
title('Normalize sum of image intensity at thickness 12.5 cm ');
ylabel('magnitude');
xlabel('change in dielectric');
figure(2),plot(die,c2(1:11),'-k','linewidth',2);
title('Negative of image entropy at thickness 12.5 cm');
ylabel('magnitude');
xlabel('change in dielectric');
figure(3),plot(die,c5(1:11),'-k','linewidth',2);
title('Ratio of Standard deviation to mean at thickness 12.5 cm');
ylabel('magnitude');
xlabel('change in dielectric');
figure(4), plot(die,c4(1:11));

```

// Calculation of higher order matrix by using means and variance of the image

```

clear all;
clc
for pp=1:N
% pp=1;
clc;
n=input('enter the value of n:');
M=importdata('D:\focusing\WALL N DIE ERROR BOTH\125wall.mat');
for k=1:11
a1=0;
a2=0;
a3=0;
I=M{k};
for j=1:13
for i=1:30
a1=a1+I(j,i);
end
end
end

```

```

mw=a1/(i+j-2);
for j=1:13
    for i=1:30
        a2=a2+(I(j,i)-mw)^2;
    end
end
sgma=sqrt((1/(i+j-2-1))*a2);
for j=1:13
    for i=1:30
        a3=a3+(I(j,i)-mw)^n;
    end
end
gamma(k)=(a3/((i+j-2-1)*sgma^n));
end
gamma=abs(gamma);
k=max(gamma);
gamma=gamma./k;
% for l=1:18
% gamma(l)=(mx-abs(gamma(l)))/mx;
% end
die=-1:.2:1;
if pp==1
    plot(die,gamma,'-k','linewidth',2);
end
if pp==2
    plot(die,gamma,'--k','linewidth',2);
end
if pp==3
    plot(die,gamma,':k','linewidth',2);
end
if pp==4
    plot(die,gamma,'-.k','linewidth',2);
end
if pp==5
    plot(die,gamma,'-k*','linewidth',2);
end

hold on;
% pp=pp+1;
end
title('nth standarized moment ');
ylabel('magnitude');
xlabel(' change in dielectric ');

```